

# International Association for Gondwana Research



## 2022 Annual Convention & 19th International Symposium on Gondwana to Asia

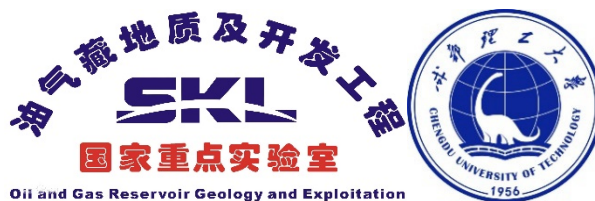
### Abstract Volume

#### *Editors*

Mingcai Hou<sup>1</sup>, Zhiwu Li<sup>1</sup>, Hao Zou<sup>1</sup> and M. Santosh<sup>2</sup>

<sup>1</sup> State Key Laboratory of Oil and Gas Reservoir Geology and Exploitation  
Chengdu University of Technology, Chengdu 610059, China

<sup>2</sup> School of Earth Sciences and Resources, China University of Geosciences Beijing, 29  
Xueyuan Road, Beijing 100083, China



#### *Organized by*

- State Key Laboratory of Oil and Gas Reservoir Geology and Exploitation
- Key Laboratory of Reconstruction and Application of Deep-time Geographic Environment, Ministry of Natural Resources
- Key Laboratory of Tectonic Controls on Mineralization and Hydrocarbon Accumulation of Ministry of Natural Resources
- Applied Nuclear Technology in Geosciences Key Laboratory of Sichuan Province
- College of Earth Sciences, Chengdu University of Technology
- College of Energy, Chengdu University of Technology

November 4-7, 2022, Chengdu

International Association for Gondwana Research

2022 Annual Convention & 19th International Symposium on Gondwana to Asia

Abstract Volume

*Editors*

Mingcai Hou, Zhiwu Li, Hao Zou and M. Santosh

Published by the International Association for Gondwana Research

Headquarters: Division of Interdisciplinary Science,  
Kochi University, Akebono-cho 2-5-1, Kochi 780-8520, Japan  
Pages: 79

© 2022, International Association for Gondwana Research

---

# Contents

|   |    |
|---|----|
| Neoproterozoic-Paleoproterozoic crustal evolution of the Wutai Complex, North China Craton<br><i>Pin Gao, M. Santosh</i> .....  | 1  |
| Study on Process Mineralogy and Leachability of Qianjiadian Sandstone-Type Uranium Ore<br><i>Yuanqing Fan, Hao Song, Qi Li, Mei Li, Qianmin Du, Zexin Wang</i> .....  | 2  |
| Activity analysis of the Longxian-Baoji fault zone in the northeastern margin of the Tibetan Plateau<br>based on geomorphological parameters<br><i>Qi Huang</i> .....   | 4  |
| Metallogenic characteristics and ore controlling factors of Hong Hai Gou coal rock type uranium deposit<br><i>Beining Hu, Hao Song, Qianmin Du, Mei Li, Zexin Wang</i> .....  | 5  |
| Relationship between uranium mineralization, pyrite and carbonaceous debris in the Honghaigou uranium<br>deposit, Yili basin, Xinjiang<br><i>Qianmin Du, Hao Song, Mei Li, Qi Li, Zexin Wang, Yan Liang, Yuanqing Fan, Meiling Duan</i> .....   | 8  |
| The activity analysis of the middle segment of Haiyuan fault zone based on DEM terrain feature factor<br><i>Lushan Liu</i> .....  | 10 |
| Magmatic response of oroclinal bending: insights from the Monglian Orocline, Central Asia<br><i>Jiaqi Ling, Pengfei Li</i> .....  | 11 |
| Paleo-peatlands as organic carbon pools in geological history<br><i>Longyi Shao, He Wen, Xiangyu Gao, Baruch Spiro, Xuetian Wang, Zhiming Yan and David J Large</i> .....   | 12 |
| Structural control on the 2021 M7.4 Maduo earthquake in NE Tibet: Crustal flow and fluids<br><i>Ziqiang Yang</i> .....  | 15 |
| Geochemical and uranium isotope variations in the Mengqiguer Sandstone-Type Uranium Deposit,<br>Yili Basin, China<br><i>Mei Li, Hao Song, Qianmin Du, Meiling Duan, Zexin Wang, Yan Liang, Yuanqing Fan</i> .....   | 16 |
| Element geochemical characteristics of the Hanchiatien Formation black shale during weathering in<br>Northern Sichuan, Southwestern China<br><i>Meiling Duan, Hao Song, Wei Hu, Xin Liao</i> .....  | 18 |
| Multiple timings of garnet-forming high-grade metamorphism and Cl-rich mineral formation in the<br>Neoproterozoic continental collision zone revealed by petrochronology in the Sør Rondane Mountains,<br>East Antarctica<br><i>Fumiko Higashino, Tetsuo Kawakami, Shuhei Sakata, Takafumi Hirata</i> ..... | 20 |
| Forming Proterozoic basement within eastern Central Asian Orogenic Belt: Evidence from zircon<br>U-Pb-Hf-O isotopes<br><i>Zhiwei Wang, Taichang Zhu, Jingwen Yu, Lingling Yuan</i> .....  | 22 |
| Identification and origin of late Paleoproterozoic Gaositai hornblendite in northern North China Craton:<br>Evidence from zircon U-Pb isotopes and amphibole trace elements<br><i>Taichang Zhu, Yuxin Sun, Zhenyu Liu, Yin Xu, Jingwen Yu, Zhiwei Wang</i> .....  | 23 |
| Relationship between early Paleozoic magmatic events and uranium mineralization in the northern China<br><i>Zexin Wang, Hao Song, Qianmin Du, Yan Liang, Huijie Yu</i> .....  | 24 |
| Pressure-Temperature-time paths of pelitic gneisses indicating long-lived metamorphism in central<br>Sør Rondane Mountains, East Antarctica<br><i>Tetsuo Kawakami, Sota Niki, Masayasu Suzuki, Shuhei Sakata, Tatsuro Adachi, Fumiko Higashino,<br/>Masaoki Uno, and Takafumi Hirata</i> .....              | 26 |
| Local MORB Mantle Heterogeneity Beneath the Southwest Indian Ridge: Implications for Mantle<br>Processes during Gondwana break-up<br><i>Wei Wang, Yunpeng Dong, Katherine A. Kelley, Zhenggang Li, Fengyou Chu</i> .....  | 29 |
| Integrated software for EPMA dating about uranium minerals<br><i>Tao Xiao, Hao Song</i> .....   | 30 |
| Geochemical constraints on metacarbonates from the Cauvery Suture Zone, Southern Granulite Terrane, India.<br><i>Thoti. Yellappa</i> .....  | 32 |

|  |    |
|--|----|
| A summary of the occurrence states of the sandstone type uranium deposits in Erlian Basin<br><i>Huijie Yu, Hao Song, Peng Qiao, Zexin Wang, Qianmin Du, Mei Li, Yan Liang,<br/>Yuanqing Fan, Meiling Duan</i> .....  | 34 |
| Latest Cambrian stage of metamorphism in the Aktyuz high-pressure Complex (North Tien Shan;<br>western part of the Central Asian Orogenic Belt): evidence from migmatized garnet-mica gneisses<br><i>Anfisa V. Skoblenko (Pilitsyna), Nadezhda A. Kanygina</i> ..... | 36 |
| Key factors affecting hydrocarbon accumulation in ancient dolomite gas reservoirs of Xixiangchi<br>Formation (southern Sichuan Basin, China)<br><i>Wei Luo, Zejin Shi, Xiuquan Hu, Dianguang Zang, Wenzhi Wang</i> .....   | 38 |
| Trondhjemites and their Implications for Neoarchean crustal growth in the Qianxi Complex, North China Craton<br><i>Ming-Xian Wang, M. Santosh, Cheng-Xue Yang, Yirang Jang, Bing Yu, Pin Gao</i> .....   | 39 |
| Carbon in orogenic belts: Sink or source for atmospheric CO <sub>2</sub> fluctuations?<br><i>M. Satish-Kumar</i> .....   | 40 |
| Ultrahigh-temperature granulites from southern India: multi-stage metamorphism during Gondwana assembly<br><i>Bing Yu, M. Santosh, Toshiaki Tsunogae, Cheng-Xue Yang, Sung Won Kim</i> .....   | 43 |
| Generation of crystal-rich erupted products by fluid-driven crystal-mush remobilization: Perspective<br>from the Nageng (sub-)volcanic complex, East Kunlun Orogen, NW China<br><i>Xiao-Dong Chen, Bin Li</i> .....  | 44 |
| Reconstructing the Lancang Terrane (SW Yunnan) and implications for early Paleozoic Proto-Tethys<br>evolution at the northern margin of Gondwana<br><i>Yuehua Wei, Jian-Wei Zi, Guichun Liu</i> .....  | 45 |
| Origin of fertile lithospheric mantle beneath eastern North China Craton: Combined effects from<br>melt impregnation and asthenospheric cooling<br><i>Lei-Tao Cao, Jian-Ping Zheng, Hong-Kun Dai</i> .....   | 46 |
| Long-lived Paleoproterozoic collision process over 150 Myr in the Trans-North China Orogen:<br>insights from metamorphic records in the Fuping Complex<br><i>Li Tang, M. Santosh, Richard M. Palin, Li-Hui Jia, Yuan-Ming Sheng</i> .....                            | 47 |
| Geochronology and geochemistry of the Algoma-type banded iron formation in the Fuping Complex,<br>North China Craton: Implications for Paleoproterozoic metallogeny and tectonic setting<br><i>Tao Zeng, Li Tang, M. Santosh</i> .....                               | 48 |
| Distal gold mineralization associated with porphyry system: The case of Hongzhuang and Yuanling<br>deposits, East Qinling, China<br><i>Yuan-Ming Sheng, Li Tang, Shou-Ting Zhang, Yu Zhao, M. Santosh</i> .....  | 50 |
| Origin and evolution of magma and tectonic implication of mafic dykes: The Permian diabases<br>in Santanghu Basin, NW China<br><i>Minru Zhao, Xin Jiao, Yiqun Liu, Dingwu Zhou, Ziyuan Meng, Yiyao Yang</i> .....  | 52 |
| Neoarchean Vertical Tectonism in eastern North China: Structure, Metamorphism and Numerical Modeling<br><i>Jian Zhang, Chen Zhao, Chenying Yu, Ting Yang, Guochun Zhao, Peter A. Cawood,<br/>Changqing Yin, Jiahui Qian, Peng Gao</i> .....                          | 53 |
| The Triassic lower crust in West Qinling and the strict dichotomy of the Qinling–Dabie Orogen<br><i>Thomas Bader, Lifei Zhang, Xiaowei Li</i> .....  | 54 |
| Geological control of the eastern Great Wall: Mountain-basin relationships in the eastern North China Craton<br><i>Boran Liu, Sanzhong Li, Franz Neubauer, Junlai Liu</i> .....  | 56 |
| Orocline in the Eastern Central Asian Orogenic Belt<br><i>Yongjiang Liu, Qingbin Guan, Sanzhong Li, Zhaoxu Chen, Tong Zhou</i> .....   | 57 |
| Traversing the Himalayan Orogen 2022-Report of the 10 <sup>th</sup> Student Himalayan Field Exercise Tour<br><i>M. Yoshida, K. Arita, T. Sakai, B.N. Upreti</i> .....  | 58 |
| Geochemical characteristics and tectonic significance of the Marzheng diorites on the southern margin of<br>the East Kunlun Orogenic Belt<br><i>Bin Zhang, Yunpeng Dong, Shengsi Sun, Dengfeng He, Bo Hui, Yuangang Yue, Xiang Ren, Weidong He</i> .....             | 59 |
| Calc-alkaline plutons in intra-oceanic arc of Proto-Tethys Ocean (Qilian Orogen, NW China) and<br>construction of arc upper crust<br><i>Chao Wang, Shuguang Song, Guochun Zhao, Mark B. Allen, Li Su, Tianyu Gao, Tao Wen, Di Feng</i> .....                         | 60 |

|   |    |
|---|----|
| Quantifying the extent of the Paleo-Asian Ocean during the Late Carboniferous to Early Permian<br><i>Donghai Zhang, Baochun Huang, Guochun Zhao, Joseph G. Meert</i> .....  | 61 |
| A Tarim-North India connection in northern Gondwana associated with final closure of the Proto-Tethys Ocean:<br>Constraints from provenance of early Paleozoic sedimentary rocks in the Altyn Tagh orogen<br><i>Qian Liu, Guochun Zhao, Jianhua Li, Jinlong Yao, Yigui Han, Peng Wang, Toshiaki Tsunogae</i> .....                        | 62 |
| New Carboniferous paleomagnetic data from Mongolia and their implications for the paleogeographic evolution of the<br>Central Asian Orogenic Belt<br><i>Qiang Ren</i> .....   | 65 |
| Online databases of the geologic formations of the Indian Plate, China and Indochina, with<br>display onto plate reconstructions of East Asia<br><i>OGG, James, DU, Wen, CHANG, Sabrina, MISHRA, Suyash, ZAHIROVIC, Sabin, AULT, Aaron,<br/>HOU, Hongfei, MAMALLAPALLI, O'Neil, LI, Haipeng, HOU, Mingcai, DONG, Bui, OGG, Gabi</i> ..... | 66 |
| Doushantuo Formation phosphorite succession (SW China) records the Ediacaran Phosphogenesis Event: New evidence<br>from Danzhai phosphorite deposit<br><i>Li-Ming Yu, Hao Zou, Bin Xiao, Jiang-Han Wu, Jin-Xiang Sheng, Hui-Dong Yu, Hai-Feng Cheng, Chang-Cheng<br/>Huang</i> .....  | 68 |
| The last Neoproterozoic rift magmatism on the margin of western Yangtze<br><i>Chang-Cheng Huang, Hao Zou, Hai-Feng Chen, Hui-Dong Yu, Bin Xiao, Chun-Mei Liu</i> .....  | 69 |
| Study on the origin and enrichment of sedimentary rare earth elements: A case of REE deposits in the adjacent areas of<br>Yunnan and Guizhou<br><i>Bin Xiao, Hao Zou, Enyuan Tian, Liming Yu, Changcheng Huang, Chenghui Hu, Daxing Gong</i> .....  | 71 |
| Geochemical and Hf-O isotopic evidence from the Mopanshan complex in the western margin of the Yangtze, South<br>China: Implications for breakup of Rodinia Supercontinent<br><i>Hui-Dong Yu, Hao Zou, Hai-Feng Chen, Chang-Cheng Huang, Chun-Mei Liu, Cheng-Hui Hu</i> .....   | 72 |
| Metallogenic characteristics and ore-controlling factors of clay-type lithium deposit in Guizhou<br><i>Daxing Gong, Bin Xiao</i> .....  | 74 |
| Cenozoic tectonic activity characteristics of Qingshuihe Basin based on fluvial geomorphology And tectonic analysis<br><i>Yang Wang</i> .....   | 75 |
| Subduction-related mafic to felsic magmatism in the Xiangpishan concentric calc-alkaline arc complex, NE Tibetan<br>Plateau<br><i>Feng-Hui Zou, Cai-Lai Wu, Li-Huan Deng, Dong Gao, Yuan-Hong Gao</i> .....   | 77 |
| Tracing archives of intra-oceanic arcs and tracking periods of subduction erosion: evidence from greywacke sandstones<br>of central and eastern Kazakhstan<br><i>Inna Safonova, Alina Perfilova</i> .....   | 79 |

# Neoproterozoic-Paleoproterozoic crustal evolution of the Wutai Complex, North China Craton

Pin Gao<sup>1,2\*</sup>, M. Santosh<sup>1,2\*</sup>

<sup>1</sup> School of Earth Sciences and Resources, China University of Geosciences Beijing, 29 Xueyuan Road, Beijing 100083, P. R. China

<sup>2</sup> Department of Earth Sciences, University of Adelaide, Adelaide SA 5005, Australia

\* Corresponding author e-mail: santosh@cugb.edu.cn

The early history of the Earth including the formation of continents and cratons is of wide interest in understanding the evolution of our planet. Compared with the short-lived oceanic crust, the continental crust which is mainly composed of the granitoids is the more stable archive for investigating the early Earth. Here we present an overview of the lithology, geochemistry, zircon U-Pb, and Hf isotopic geochronology of the Neoproterozoic and Paleoproterozoic granitoids from the Wutai Complex located within the central part of the North China Craton (NCC). The Neoproterozoic and Paleoproterozoic granitoids in the Wutai Complex can be divided into two groups: 1) Neoproterozoic TTG [the major mineral assemblage is plagioclase, biotite, and quartz with very few K-feldspar; age peaks at ca. 2530 Ma; peraluminous, calc-alkaline, K-poor, magnesian, lower contents of the Rare Earth Element (REE), Light Rare Earth Element (LREE) and Heavy Rare Earth Element (HREE) stronger differentiation, show the features of the 'S-type' granite] and 2) Paleoproterozoic granitoids [mainly composed of plagioclase, K-feldspar, quartz, biotite, and muscovite; age peaks at ca. 2130 Ga; metaluminous, calc-alkaline, K-rich, ferroan, higher contents of the REE, LREE, and HREE weaker differentiation, show the features of the 'I-type' granite]. Zircon Hf isotopic data indicate that the Neoproterozoic TTGs were sourced from the partial melting of juvenile mafic/basaltic proto crust, and the Paleoproterozoic granitoids were generated from the juvenile materials together with the partial melting of the Neoproterozoic magmatic (TTG) basement. Our study indicates that the Neoproterozoic and Paleoproterozoic mark major continent growth periods in the Wutai Complex. The Neoproterozoic

continent growth might be related to the shallow subduction-related arc magmatism, whereas the Paleoproterozoic continent growth occurred through rift-related magmatism. Our study also confirms the role of active plate tectonics and associated geodynamic processes during the Neoproterozoic and Paleoproterozoic.

**Keywords:** Neoproterozoic TTG; Paleoproterozoic granitoids; Early crustal evolution; Wutai Complex; North China Craton.

# Study on Process Mineralogy and Leachability of Qianjiadian Sandstone-Type Uranium Ore

Yuanqing Fan <sup>a</sup>, Hao Song <sup>a, b, \*</sup>, Qi Li <sup>a</sup>, Mei Li <sup>a</sup>, Qianmin Du <sup>a</sup>, Zexin Wang <sup>a</sup>

<sup>a</sup> Chengdu University of Technology, Chengdu, Sichuan 610059, China.

<sup>b</sup> Applied Nuclear Technology in Geosciences Key Laboratory of Sichuan Province, Chengdu, Sichuan 610059, China.

\* Corresponding author at: Chengdu University of Technology, Chengdu 610059, China.

The development of clean energy, including nuclear power, must be accelerated to achieve the goals of carbon peaking and carbon neutrality (Xie et al., 2021). Uranium mining and utilization have become increasingly important in recent decades. However, sandstone-type uranium deposits in China often have low-grade uranium ore and complex geological-hydrogeological conditions, which have always restricted the exploitation and utilization of uranium (Que et al., 2008; Su et al., 2012). Therefore, how to extract uranium ore greenly and efficiently is the key problem to realize the sustainable and stable development of nuclear energy, and the leaching performance of uranium ore is one of the key indicators of the efficiency of the in-situ leaching uranium mining process.

In this study, based on the guidance of theoretical knowledge of process mineralogy and the technical support of pressure agitation leaching, X-ray fluorescence analyzer (XRF), X-ray diffraction (XRD), Inductively coupled plasma mass spectrometer (ICP-MS), TIMA automatic mineral analyzer and other measurement methods were used to compare and analyze the uranium-bearing minerals of different lithology in the Qianjiadian sandstone-type uranium deposit before and after leaching.

The results are as follows: 1) Sandstone-type uranium deposits of different lithology are mainly composed of quartz, feldspar, and other minerals. The uranium content of medium-fine siltstone, fine sandstone-coarse siltstone, and fine-fine sandstone are 3374  $\mu\text{g/g}$ , 131  $\mu\text{g/g}$ , and 1737  $\mu\text{g/g}$ , respectively. The leaching rates of slag were 76 %, 60 %, and 41 %, respectively. 2) The main elements such as Si, Fe, Ca, and Mg in the ore have no obvious correlation with the uranium leaching rate, while Al has a negative correlation with the uranium leaching rate. Under neutral leaching conditions,

the contents of stable minerals such as quartz and feldspar are positively correlated with uranium leaching rate, while clay minerals (kaolinite and chlorite) with a large specific surface area are significantly negatively correlated with uranium leaching rate. 3) Uranium minerals are mainly pitchblende and coffinite (Fig.1), and the dissociation degree of uranium minerals is poor. There is a significant positive correlation between completely dissociated mineral content and leaching amount. By comparison, it is found that pitchblende is generally more likely to be associated or symbiotic with other gangue minerals than coffinite, resulting in worse dissociation.

The conclusions are as follows: 1) The particle size of rock-type uranium ore has an important influence on the stirring leaching of uranium. The smaller the particle size, the greater the leaching rate. The main reason is that the diffusion path of leaching solution in gangue minerals decreases. 2) Quartz and feldspar are not easily dissolved in the leaching process, which will help to reduce the salinity in the leaching solution, reduce oxygen consumption, and relatively reduce the adverse effects of non-uranium elements and minerals on the uranium leaching process. There is a significant negative correlation between clay minerals and uranium leaching. The reason may be that clay minerals have a high specific surface area, which can adsorb water molecules and replace cations, so the swelling phenomenon is more obvious. Therefore, before in-situ leaching of uranium ore, attention should be paid to the content of clay minerals and other minerals with high specific surface area and their spatial distribution relationship with uranium ore. 3) The dissociation degree of uranium minerals has an important influence on uranium leaching. The smaller the particle size of uranium ore, the greater the proportion of completely dissociated uranium ore, and it is suitable for

uranium leaching by pressure stirring. Therefore, before the leaching of sandstone-type uranium ore, it is necessary to study the process mineralogy and performance of the ore, and it has important guiding significance for the selection of the uranium mining process.

E-mail address: songh hao@163.com (H. Song).

**References:**

Xie W., 2021. The "14th Five-Year Plan" nuclear power development welcomes a new window. *China Economic Weekly*. 68-70

Que W., Wang H F., Niu Y Q, Zhang F F., Gu W C., 2008. Development and Prospect of Uranium Mining and Metallurgy Technology in China. *China Engineering Science*. 4-53

Su X B., Du Z M., 2012. Development and prospect of China Uranium in-situ leaching technology. *China Mining*. 21, 79-83

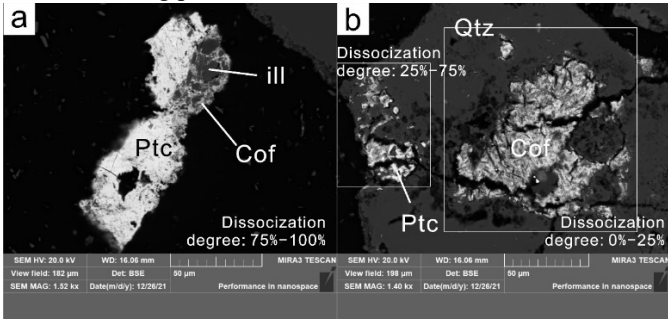


Fig.1 BSE diagram of dissociation degree of uranium minerals in Qianjiadian

**Keywords:** Nuclear power; Sandstone-type uranium deposits; In-situ leaching uranium; TIMA; Qianjiadian.

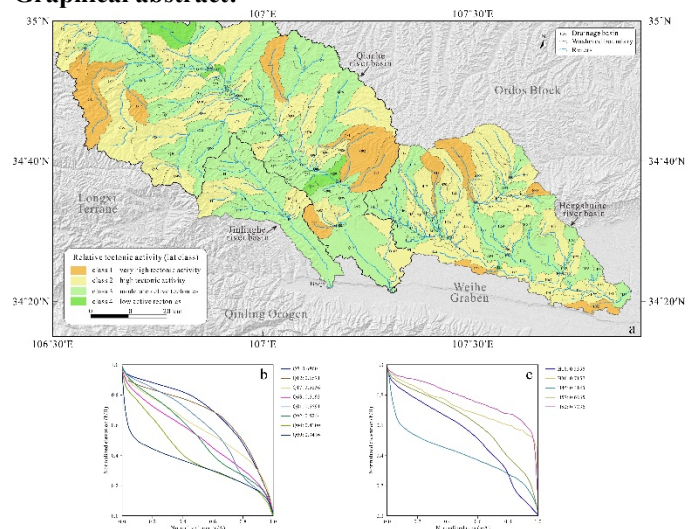
# Activity analysis of the Longxian-Baoji fault zone in the northeastern margin of the Tibetan Plateau based on geomorphological parameters

Reporter: Huang Qi

The Longxian-Baoji fault zone is located at the intersection of the southwestern margin of the Ordos block, the northeastern margin of the Tibet Plateau and the Qinling orogenic belt. The tectonic deformation activity has been intense since the Late Cenozoic. Based on the SRTM DEM data, this paper extracted three watersheds (Qianhe River Basin, Hengshuihe River Basin, Jinlinghe River Basin) in the study area. Through the analysis of several geomorphological parameters such as hypometric integral (HI), standardized stream length-gradient index (SL/K) and Hack profile, elongation ratio (Re), Drainage Basin Asymmetry Factor (AF) and Valley floor width-to-height ratio (VF), the relative tectonic activity class is finally used to evaluate the strength of tectonic activity in the study area. Comprehensive analysis found that the study area has experienced relatively strong tectonic activity, the areas with strong activity show the characteristics of distribution along faults, in the eastern part of Longxi Terrane and the southwestern part of Ordos Block have strong structural tilting, and their tilting directions are mainly in the east and northwest directions respectively. At the same time, the activity of the Longxian-Qishan fault (LQF) is the strongest, its northwest side is weak, and its southeast side is strong which is most prominent in the section from Zhangjiayuan Town in Qianyang County to Yaojiagou Town in Fengxiang; The tectonic activity of the Taoyuan-Guichuansi fault (TGF) is strong in the north and weak in the south; the Guguan-Guozhen fault (GGF) has strong tectonic activity in the periphery of Longxian County and the area of Xiangong

Town; the tectonic activity of Qianyang-Biaojiao fault (QBF) is the weakest, but it shows high tectonic activity in the area of Biaojiao Town.

### Graphical abstract:



(a): Relative tectonic activity classes map of the study area; (b) and (c): Hypsometric curves in basins with the highest relative tectonic activity classes, where (b) is the Hypsometric curve in the Qianhe River Basin, (c) is the Hypsometric curve in the Hengshuihe River Basin.

# Metallogenic characteristics and ore controlling factors of Hong Hai Gou coal rock type uranium deposit

Beining Hu<sup>a</sup>, Hao Song<sup>a,b,\*</sup>, Qianmin Du<sup>a</sup>, Mei Li<sup>a</sup>, Zexin Wang<sup>a</sup>

<sup>a</sup> Chengdu University of Technology, Chengdu 610059, China

<sup>b</sup> Kay Laboratory of Earth Exploration and Information Techniques, Ministry of Education, Chengdu 610059, China

\* Corresponding author at: Chengdu University of Technology, Chengdu 610059, China. E-mail address: songh hao@163.com (H. Song).

Coal is one of the important energy resources in China, accounting for about 60% of China's primary energy structure, which is an important non-renewable resource. In the process of coal mining, a variety of key metals associated with the coal mine were found. The coal itself is mainly composed of organic matter, which makes it have strong adsorption and reduction. After a series of geological processes, the coal mine can enrich a variety of key metals, forming a "coal type key metal deposit". The more common key metal deposits associated with coal are formed by coal and aluminum, magnesium, scandium, titanium, niobium, tantalum, uranium, gold, silver, rare earth elements, etc. (Dai et al., 2020). This paper mainly introduces the coal-type uranium deposits, studies and summarizes the characteristics and formation process of coal measure uranium deposits in Ili basin.

## 1. Introduction

The research of uranium plays an important role in the field of nuclear industry. Therefore, uranium ore, as the main source of uranium resources, is one of the main types of ore deposits developed in China. Coal-rock uranium can further meet our needs for uranium resources, so it is one of the most important types of uranium ore. Among them, the Ili Basin is a good producer of kerosene. The Hong Hai Gou is a large coal-rock-type uranium deposit discovered in the Ili Basin in recent years. Because of its unique climate and topographical and structural conditions, uranium is easy to be enriched and integrated here, which has important research significance.

## 2. General characteristics and research contents

Uranium deposit of Hong Hai Gou coal-rock type in Ili basin is characterized by high grade, thin thickness and continuous and stable ore body. According to previous studies, the following summarizes the formation process and characteristics of coal-type uranium deposits in this area. Its

ore body is mainly endowed with the upper section of the Middle Jurassic Xi Shan Kiln Formation No. 12<sup>#</sup> coal seam (Wang et al., 2015). The thickness of coal-type uranium ore body in this area is relatively stable, with an average thickness of about 1.02 meters and an average grade of about 0.0992%, which is at the medium level (general grade), and the grade change is also relatively stable. The uranium ore body is single in shape, mainly plate-shaped and lenticular, sloping along the coal seam and extending along the coal seam to the interior of the basin.

This article looked at the relevant information and found out it could reveal the ore control factors of the coal-rock uranium ore in the region by studying its structural characteristics, the thickness and degree of metamorphism of the uranium coal seam, and its spatial position relationship with the oxidation zone between the overburden. By sampling to test and analysis comparatively, we studied sedimentary facies and oxidation zones, and the status of uranium in coal, as well as the characteristics of sediment equivalence and mineralization factors in the region are summarized.

The results of the study show that the occurrence state of uranium in coal includes inorganic state and organic state. The researchers found that the carrier coal reservoir of coal type uranium is mainly low rank coal and long flame coal, and only a small amount of high rank bituminous coal has uranium mineralization. The combination of riverbed sedimentary subphase and swamp sedimentary facies is beneficial to coal-rock type uranium mineralization. The movement of groundwater and its solubility also have a certain impact on the enrichment of uranium. In addition, the sand body characteristics of the coal-rock uranium type uranium ore covered with sandstone are also closely related to the formation of uranium mineralization. Below I will analyze and

summarize the willingness to produce the above results one by one.

### 3. Analysis of ore forming

#### 3.1. Causes of uranium enrichment

The process of enrichment of uranium in the research area is that uranium-rich fluids flow underground under external forces such as gravity and pressure (Wang et al., 2015), and when the fluid penetrates downwards in contact with the coal seam, uranium began to precipitate and enrich because of the strong reducing effect of coal. The chemical composition of coal is carbon, hydrogen, sulfur and other elements, which are low valence. Therefore, when coal seams are in contact with high valence uranium containing ions, they tend to lose electrons and show strong reducibility. The solubility of uranium in water after reduction becomes low, coupled with the adsorption of organic matter in coal, which leads to uranium enrichment and mineralization.

#### 3.2. Relationship between coal maturity and uranium mineralization

Coal rank is a parameter that affects the saturation state of coal seams. It represents the level of maturity that can be achieved in coalification.

The rank of coal is related to the degree of metamorphism, i.e. maturity of coal. Low rank coal belongs to low rank coal, and the lower the degree of metamorphism, the less humic acid is decomposed, the higher the content. The higher the content of humic acid, the more kinds of organic matter, so more uranium is adsorbed and enriched, so low-grade coal is more prone to uranium mineralization than high-grade coal. The loose and porous structure of long bituminous coal can provide more enrichment space for uranium elements, so obvious uranium mineralization can also occur.

#### 3.3. Relationship with sedimentary facies

Most of the industrial uranium mineralization enriched in coal rock type deposits in Ili basin belongs to epigenetic uranium (uranium ions are transported to coal seams through fluid to reduce and precipitate). Because the coal seam has poor permeability, almost the coal seam can only have a certain vertical permeability, while the overlying sand body can provide a channel for the movement and migration of elements because of its good permeability. Therefore, the formation of coal lithology uranium deposit is closely related to sedimentary facies. Sedimentary facies, i.e. sedimentary environment, will affect the type, nature, scale and distribution range of sand bodies. When thick and large sand bodies developed in favorable facies zones are formed, they provide a seepage channel for ore bearing fluids. If the sedimentary sand bodies are overlaid on the coal seams, the ore bearing fluids can flow downward in the process of migration and the coal seams can be reduced to enrich the mineralization (Wang et al., 2015). These sedimentary facies are favorable for the formation of coal rock type uranium mineralization.

#### 3.4. Relationship with groundwater

Uranium element and sulfur element have quite good affinity. Groundwater in the study area has quite good solubility for uranium. During the transportation process, uranium migrates in the sand body in the form of uranyl sulfate ion. After a large amount of oxygen is consumed, it is reduced by strong reducing substances in the coal seam, and uranium element is enriched in the coal seam. Groundwater is the carrier of Uranium Migration and the driving force of uranium enrichment and mineralization at a certain location.

### 4. Analysis of ore controlling factors

#### 4.1. Relationship with interlayer oxidation zone

Interlayer oxidation zone refers to the oxidation zone formed by the oxygen-containing groundwater percolating to the deep along the permeable rock layer sandwiched between the impermeable rock layers, so that the permeable rock layer is oxidized. The interlayer oxidation zone is zonal and can be divided into oxidation zone (including strong oxidation zone and weak oxidation zone), oxidation-reduction transition zone and reduction zone.

Enrichment of coal rock type uranium ore bodies between the weak oxidation zone and transition zone. Compared with the strong oxidation zone and reduction zone, the weak oxidation zone has less uranium dissolution and leaching. In addition,  $^{234}\text{U}$  is easily absorbed by iron and clay minerals in the oxidation zone, so uranium mineralization is obvious. As the most complex position of water rock reaction, the transition zone is the main enrichment area of uranium elements (Sun et al., 2004).

#### 4.2. The thickness of the coal seams and the lithology of the roof

The thickness of the coal seams and the lithology of the roof in the study area have a certain impact on uranium mineralization, that is, they determine the enrichment status of uranium deposits, forming a total of four output states: the top of the coal seam, between the overlying gray sand body and the coal seam, between the mudstone and the coal seam, and in the thin mudstone; The relationship between uranium mineralization and interlayer oxidation zone is that uranium is enriched in the transition zone of weak oxidation zone and occurs in plate and lens shape; The tectonic movement in the coal accumulation period also had a significant impact on the enrichment of uranium deposits. Under the influence of the Karamay movement in Indosinian-middle Yan Shan period, the tectonic stress in the southern margin of Ili basin changed from expansion depression to compression convergence, and the evolution of the basin changed from fault subsidence to uplift and denudation. After a series of tectonic activities, more fractures were finally developed in the coal seams, providing sufficient space for uranium enrichment, which can be fully reduced and precipitated (Jia et al., 2020).

### 5. Summary

① Coal is a strong reducing substance with uranium element precipitation and enrichment. The enriched uranium in coal

seams is organically combined, and the sulfur element in coal in the study area is positively correlated with uranium element. It is speculated that uranium element may form complex ions with sulfate ion in groundwater. With the migration of groundwater, it will reduce with the underlying coal seams under the infiltration of coarse sand body, so that uranium element can be precipitated and enriched.

② The occurrence state of uranium in coal includes inorganic state and organic state. The researchers found that the carrier coal reservoir of coal type uranium is mainly low rank coal and long flame coal, and only a small amount of high rank bituminous coal has uranium mineralization. This may be because the low rank coal and long flame coal have low metamorphism and retain more original organic matter, resulting in stronger adsorption, and more loose and porous structure, which is conducive to the enrichment of uranium (Zhou et al., 2019). Therefore, we can pay more attention to the study of uranium mineralization in low rank coal in this area.

③ The coal rock type uranium deposit in the study area belongs to epigenetic uranium, that is, uranium ions are transported to coal seams with fluid migration, reduced and precipitated, and enriched and mineralized. If the uranium element is to better contact with the coal seam, the overlying sand body needs to have good permeability, which can provide a channel for uranium element migration. Sedimentary facies affect the permeability of sand body by affecting its characteristics, such as the grain size, type and distribution range, thus becoming one of the metallogenic factors of uranium deposit.

④ The groundwater in the study area has a strong ability to dissolve uranium elements, resulting in the complexation between uranium and sulfate in the water to generate uranyl sulfate ions.

⑤ Enrichment of coal rock type uranium ore bodies in weak oxidation zone transition zone, obviously controlled by interlayer oxidation zone

The lithology and thickness of coal seam roof, and the lithology and thickness of coal seam roof have a significant impact on the enrichment position of uranium deposit.

This research was sponsored by the National Natural Science Foundation Program of China (42173072, U1967207), and Everest Scientific Research Program (CDUT).

**Keywords:** Hong Hai Gou deposit, coal-rock-type uranium deposits, uranium enrichment, ore controlling factors, metallogenic factors.

#### References:

- Shifeng Dai, Lei Zhao, Qiang Wei, et al, 2020. Key metal resources in coal measures in China: enrichment types and distribution [J]. Science Bulletin, 65 (33), 3715-3729. DOI:10.1360/TB-2020-0112.
- Xianqing Zhou, Yong Qin, Lu Lu, 2019. Land deer Advances in geological and geochemical studies of coal type uranium in China [J]. Coal field geology and exploration, 47(04), 45-53.
- Maomao Wang, Li Hua, Yubo Qiu, 2015. Analysis of coal rock type uranium mineralization in honghaigou area, Yili basin, Xinjiang [J]. China coal geology, 27(12), 12-16
- Zhanxue Sun, Jinhui Liu, Yonggang Zhu, Zhang Wen, 2004. Metallogenic process and Redox Zoning of sandstone uranium deposits: evidence of uranium series imbalance [J] Geoscience, (02), 224-230.
- Zhiyong Jia, Hujun Zhang, Wenzheng Chen, Lei Zhang, Yubo Qiu, 2020. Study on ore controlling factors of honghaigou coal rock type uranium deposit in the southern margin of Yili basin, Xinjiang [J]. Mineral exploration, 11(11), 2417-2423

# Relationship between uranium mineralization, pyrite and carbonaceous debris in the Honghaigou uranium deposit, Yili basin, Xinjiang

Qianmin Du <sup>a</sup>, Hao Song <sup>a,b,\*</sup>, Mei Li <sup>a</sup>, Qi Li <sup>a</sup>, Zexin Wang <sup>a</sup>, Yan Liang <sup>a</sup>, Yuanqing Fan <sup>a</sup>, Meiling Duan <sup>a</sup>

<sup>a</sup> Chengdu University of Technology, Chengdu 610059, China

<sup>b</sup> Kay Laboratory of Earth Exploration and Information Techniques, Ministry of Education, Chengdu 610059, China

\* Corresponding author at: Chengdu University of Technology, Chengdu 610059, China. E-mail address: songh hao@163.com (H. Song).

Sandstone-hosted uranium deposits, dominated by epigenetic oxidation of the uranium-bearing oxygenated groundwater (Wright, 1955), are currently one of the most significant geological discoveries and the most economically beneficial uranium-type both in China and abroad, owing to the lower cost of in situ leaching technology (Cuney, 2009; Bonnetti et al., 2020). The Meso-Cenozoic Yili Basin in northwestern China hosts important uranium and coal resources (Song et al., 2019). The Honghaigou uranium deposit is a recently discovered large-scale uranium deposit in the southwestern Yili Basin, China. The uranium mineralization in the Yili Basin is mainly distributed in the dark coal-bearing clastic rock formations of the Middle and Lower Jurassic Shuixigou Group.

This study aims to ascertain the characteristics of mineral assemblages associated with uranium mineralization to reveal the synergy of the carbonaceous debris, pyrite, and microorganisms that have created the diversity of occurrence state of uranium minerals and the mineral symbiosis by using energy spectral analysis, backscattering detection, and electron probe microanalysis. The results show that the uranium minerals are mainly pitchblende, with a small amount of coffinite and uranium-bearing titanium minerals. The main type of uranium minerals are mostly disseminated, clustered, or veinlet, being distributed along the edges and in the pores between detrital grains, and pitchblende are usually closely symbiotic with pyrite and carbonaceous debris. It is found that components of carbonaceous debris are mainly composed of

vitrinite and inertinite, the fabric of some plant cells is well preserved, and a large number of pyrites can be found in the cell cavities. According to the occurrences of pyrite, morphologies of pyrite are orderly evolved from microcrystalline. Large quantities of Pyrites have been discovered in ore-bearing rocks, with complex morphologies, which can be divided into framboidal, euhedral, and cement pyrite. A large number of framboidal pyrites and uranium are distributed in carbonaceous debris, and the energy spectrum scan also shows that there is a significant positive correlation between uranium minerals and the P element in the carbonaceous debris which indicates that there is microbial uranium mineralization in the uranium reservoir.

Carbonaceous debris not only plays a direct role in the process of uranium mineralization through adsorption, complexation, and reduction, but also plays an indirect role in the reduction and enrichment of uranium through microbial community (Zhang et al., 2019). Overall, during the ore stage, the large amount of pyrite has impelled the reduction and precipitation of uranium minerals, with the catalysis and acceleration of microbes (Peng et al., 2022). The synergy of pyrite, carbonaceous debris, and microorganisms has created the diversity of occurrence state of uranium minerals.

**Keywords:** Occurrence, Pyrite, Carbonaceous debris, Uranium mineralization, Honghaigou deposit

This research was sponsored by the National Natural Science Foundation Program of China (42173072, U1967207), and Everest Scientific Research Program (CDUT).

## References:

- Bonnetti, C., Zhou, L., Riegler, T., Brugger, J., Fairclough, M., 2020. Large S isotope and trace element fractionations in pyrite of uranium roll front systems result from internally-driven biogeochemical cycle. *Geochimica et Cosmochimica Acta* 282, 113–132. <https://doi.org/10.1016/j.gca.2020.05.019>
- Cuney, M., 2009. The extreme diversity of uranium deposits. *Miner Deposita* 44, 3–9. <https://doi.org/10.1007/s00126-008-0223-1>
- Peng, H., Jiao, Y., Dong, F., Guo, X., 2022. Relationships between uranium occurrence, pyrite and carbonaceous debris in Fuxin Formation in the Songliao Basin: Evidenced by mineralogy and sulfur isotopes. *Ore Geology Reviews* 140, 104580. <https://doi.org/10.1016/j.oregeorev.2021.104580>
- Song, H., Ni, S., Chi, G., Zhang, C., Hou, M., Liu, H., Wang, G., Yan, W., 2019. Systematic variations of H-O-C isotopes in different alteration zones of sandstone-hosted uranium deposits in the southern margin of the Yili Basin (Xinjiang, China): A review and implications for the ore-forming mechanisms. *Ore Geol. Rev.* 107, 615–628. <https://doi.org/10/gppkcf>
- Wright, R.J., 1955. Ore controls in sandstone uranium deposits of the Colorado Plateau. *Economic Geology* 50, 135–155. <https://doi.org/10.2113/gsecongeo.50.2.135>
- Zhang, F., Jiao, Y., Wu, L., Rong, H., Wang, L., 2019. Relations of Uranium Enrichment and Carbonaceous Debris within the Daying Uranium Deposit, Northern Ordos Basin. *J. Earth Sci.* 30, 142–157. <https://doi.org/10.1007/s12583-017-0952-0>

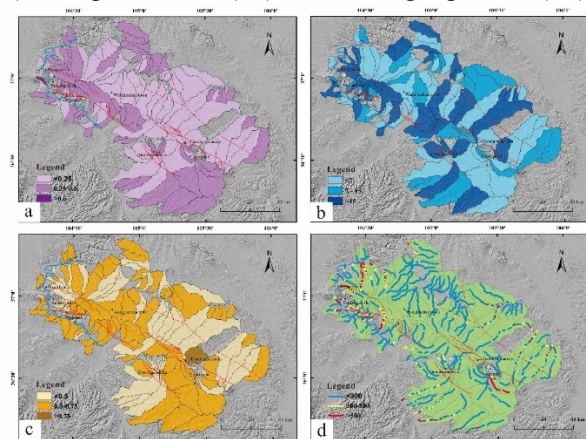
# The activity analysis of the middle segment of Haiyuan fault zone based on DEM terrain feature factor

Lushan Liu

Haiyuan Fault Zone as an Important Part of the Northeastern Tibetan Plateau Boundary, is a large fault zone characterized by sinistral strike-slip movement, It is of great significance to the study of structural pattern and Quaternary tectonic geomorphology in the northeastern margin of the Qinghai-Tibet Plateau. In this paper, through the analysis of digital elevation model (DEM) by arcgis and other software, a variety of geomorphic parameters are calculated to analyze the activity of the middle segment of Haiyuan fault zone. The results of data analysis show that Hypsometric integral (HI) is generally distributed in the study area with small north side and large south side of the fault zone, the average HI value of the basin on the fault zone is 0.39, and the geomorphic evolution of the basin is in the middle age. The results of Asymmetric factor (AF) show that  $|AF-50| < 7$  of 46 basins is the first level, and the tectonic activity is general,  $7 < |af-50| < 15$  of the 27 watersheds are of secondary level, with strong tectonic activity, the  $|af-50| > 15$  of 46 watersheds is of grade III, with strong tectonic activity. The calculated value of Elongation Ratio (Re) is between 0.3 and 0.8, of which 50 are less than 0.5, with strong activity, there are 63 of them with 0.5-0.75, and their activity is general, and 1 of them with more than 0.75 is weak. The results of Stream length gradient (SL) show that the area near the Yellow River and the Yanchi-Haiyuan section are greatly affected by lithology and structure. The activity analysis shows that the tectonic activity of the

fault and the basin on the southern side of the fault is strong, and the activity of the northern side of the fault is weak. The activity of Wangtan-Wangjiashan section and Yanchi-Haiyuan section in the middle part of the Haiyuan fault zone is significantly stronger than that of Dangjiagou-Yanchi section.

**Keywords:** Hypsometric integral (HI); Asymmetric factor (AF); Elongation Ratio (Re); Stream length gradient (SL)



a. Colored spatial distribution of the hypsometric integral (HI) of the catchments; b. Colored spatial distribution of the asymmetric factor (AF) of the catchments; c. Colored spatial distribution of the Elongation Ratio (Re) of the catchments; d. Colored spatial distribution of the Stream length gradient (SL) of the catchments.

## Magmatic response of oroclinal bending: insights from the Mongolian Orocline, Central Asia

Jiaqi Ling, Pengfei Li

State Key Laboratory of Isotope Geochemistry, Guangzhou Institute of Geochemistry, Chinese Academy of Sciences, Guangzhou, 510460, China

Email: [lingjiaqi18@mails.ucas.ac.cn](mailto:lingjiaqi18@mails.ucas.ac.cn); [pengfeili@gig.ac.cn](mailto:pengfeili@gig.ac.cn)

---

The orocline, which was formed by bending of a relatively linear orogen, widely occurs in global orogens. Previous studies mainly focus on geodynamic mechanisms of oroclinal bending, but how large-scale oroclinal bending affects the arc magmatism remains poorly understood. Here we concentrate on magmatic evolution in the inner hinge zone of the Mongolian Orocline with an aim to investigate magmatic response of oroclinal bending. Our results show that Permian-Triassic magmatic rocks in the research area show

geochemical characteristics of typical arc magmatism, which could result from the subduction of the Mongol-Okhotsk oceanic plate. Trace elements of these rocks demonstrate the crustal thickening in the research area, which we interpret to result from large scale of oroclinal bending. Our results highlight the crucial impact of oroclinal bending on the arc magmatism along the convergent plate boundary.

# Paleo-peatlands as organic carbon pools in geological history

Longyi Shao<sup>1</sup>, He Wen<sup>1</sup>, Xiangyu Gao<sup>1</sup>, Baruch Spiro<sup>2</sup>, Xuetian Wang<sup>1</sup>, Zhiming Yan<sup>3</sup>  
and David J Large<sup>4</sup>

<sup>1</sup> College of Geoscience and Surveying Engineering, China University of Mining and Technology (Beijing), Beijing 100083, China;

<sup>2</sup> Department of Earth Sciences, Natural History Museum, London SW7 5BD, UK

<sup>3</sup> Institute of Architectural Engineering, Weifang University, Weifang 261061, China

<sup>4</sup> Faculty of Engineering, University of Nottingham, Nottingham NG7 2RD, UK

## Introduction

Peatlands, as one of the important ecosystems, has the ability of long-term carbon sequestration, is an extremely important carbon pool, and plays a vital role in the global carbon cycle. Paleo-peatlands generated fuels such as coal through subsequent compaction and coalification, in other words, coal is the product of paleo-peatlands (Stach et al., 1982). Paleo-peatlands are the main storage places for terrestrial carbon, and they are also important records of paleoclimate (Shao et al., 2020). Net primary productivity (NPP) of the paleo-peatland refers to the fixed carbon of peatland in the primary production process, and studying the NPP in paleo-peatlands is of great significance for understanding the generation, development, and evolution of paleo-peatlands.

In this paper, based on the discussion of the identification of Milankovitch cycles in coal seams using geophysical logs, we present a procedure for the analysis of the productivity of paleo-peatlands.

## 2. Using Geophysical Logs to Identify Milankovitch Cycles

Geologists read the stratigraphic cycles using paleoclimate proxy records and link the recognized sedimentary oscillations to the Milankovitch cycles (Hinnov and Hilgen, 2012). Information recorded by the geophysical logs can be an ideal paleoclimate proxy which has been commonly used in the study of cyclostratigraphy in recent years (Wu et al. 2011). The logging response of gamma-ray, density, and resistivity can reflect the variation in ash yield and the V/I (vitrinite to inertinite) ratio in a coal seam. The results of spectral analysis include three main groups of frequencies in descending order, labeled as  $f_1$ ,  $f_2$ , and  $f_3$ , respectively. Then the cycle lengths, including L1, L2, and L3, could be estimated based on these

frequencies. When  $L_3$ ,  $L_2$ , and  $L_1$  proportion ( $L_3 : L_2 : L_1$ ) obtained for the target coal seam is similar to the orbital periodicity proportion (eccentricity : obliquity : precession) cited from Berger et al. (1992) in a certain geological period, it can be considered that the formation of the coal seam was affected by Milankovitch cycles.

In addition, the sedimentary sections have to possess the following characteristics in order to ensure the study of the Milankovitch cycles: 1) the thickness of the strata should be sufficiently large to ensure the period of coal deposition includes several eccentricity cycles; 2) the strata are continuous to ensure the continuity of the Milankovitch cycles; 3) the depositional strata are strongly driven by the orbital climate and preferably have clear sedimentological cyclicity (Boulila et al., 2010).

## 3. Calculation of Net Primary Productivity of Paleo-peatlands

After extracting the frequencies from the coal seams, the net peatland productivity (NPP) can be calculated. Fig. 3 shows the procedures of the peatland productivity analysis.

### 1) Calculate the average rate of coal deposition

The average rate of coal deposition refers to the deposition thickness of target seam per thousand years, which represents the rate of coal seam deposition, with the unit of  $m/ka^{-1}$ . The average rate of coal deposition,  $R_{coal}$ , can be calculated based on the cycle length ( $m$ ) of  $L_1$ ,  $L_2$ , and  $L_3$  and the orbital periodicity ( $ka$ ) cited from Berger et al. (1992), with  $t_1$  (eccentricity),  $t_2$  (obliquity), and  $t_3$  (precession), respectively.

### 2) Calculate the period of coal deposition

The period of coal deposition,  $T_{coal}$ , with unit of  $ka$ , can be calculated based on the thickness of coal ( $m$ ) and  $R_{coal}$ .

### 3) Calculate the long-term average carbon accumulation rate of the coal

The long-term average carbon accumulation rate of the coal,  $R_c$ , refers to the amount of carbon (g) accumulated per square meter and per year, with the unit of  $gC\ m^{-2}\ a^{-1}$ , and can be calculated based on the measured carbon concentration of the coal (%), the apparent density of the coal ( $g\ cm^{-3}$ ), and  $R_{coal}$ .

#### 4) Estimate the carbon loss during coalification

Certain amounts of carbon have been lost during coalification. The higher the degree of coalification, the more carbon will be lost in the process of coal formation. The carbon loss during coalification can be estimated by the van Krevelen diagram (Diessel, 1992).

#### 5) Calculate the long-term average carbon accumulation rate for the initial peatland

The long-term average carbon accumulation rate for the initial peatland,  $R_p$ , refers to the amount of carbon accumulated in paleo-peatland per square meter and per year, with the unit of  $gC\ m^{-2}\ a^{-1}$ . It can be calculated based on the carbon loss percentage during coalification and  $R_c$ .

#### 6) Calculate the net primary productivity (NPP) of the paleo-peatland

NPP of the paleo-peatland refers to the fixed carbon of peatland in the primary production process, with unit of  $gC\ m^{-2}\ a^{-1}$ .

The ratio of Holocene NPP of the paleo-peatland to long-term average carbon accumulation rate for the initial peatland can be used at different latitudinal settings of different geological ages. According to this quantitative ratio, the NPP of the paleo-peatlands can be calculated by the  $R_p$  multiplied by this ratio

#### 4. NPP of paleo-peatlands as possible proxy of global atmospheric CO<sub>2</sub>

For a specific latitude and under stable hydrologic conditions, the main factors controlling the NPP of paleo-peatlands could be the atmospheric CO<sub>2</sub> and O<sub>2</sub> levels (Beerling and Woodward, 2001). The source of carbon in vegetation including paleo-peatlands is atmospheric CO<sub>2</sub>, fixed through photosynthesis. Therefore, the difference of NPP values of different ages could be influenced, among other factors, also by variations in atmospheric CO<sub>2</sub> levels in different geological ages. The oxygen required by plant respiration is sourced from atmospheric O<sub>2</sub>, which could reduce the fixed carbon content of paleo-peatlands (Beerling and Woodward, 2001; Large and Marshall, 2015). Beerling and Woodward (2001) conducted a numerical simulation between O<sub>2</sub> content and NPP, and they have found that the NPP of the continental biosphere decreased by 10% when the atmospheric O<sub>2</sub> content increased by 11%. Therefore, the increased atmospheric O<sub>2</sub> level could slow down the increase in the NPP of paleo-peatlands to some extent. Despite the negative effect of atmospheric O<sub>2</sub>, the atmospheric CO<sub>2</sub> still have a positive effect on the NPP of paleo-peatlands, and the different atmospheric CO<sub>2</sub> levels in different geological ages

should result in different NPP values of paleo-peatlands.

Several case studies for the Late Permian, Middle Jurassic, Early Cretaceous and Holocene showed that the NPPs of paleo-peatlands are mainly controlled by the atmospheric CO<sub>2</sub> contents. The higher NPP values are associated with the higher atmospheric CO<sub>2</sub> contents, although excessive O<sub>2</sub> level might decrease the NPP of paleo-peatlands to some extent (Shao et al., 2022). Therefore, it can be suggested that NPP values could be a possible proxy of global atmospheric CO<sub>2</sub> during geological periods.

#### 5. Conclusions

1) The method of calculating NPP of paleo-peatlands give the essence in this review paper. The high-precision period of coal deposition could be obtained by identifying Milankovitch cycles from geophysical logs in coal seams. Based on the obtained coal deposition period, the NPP values of paleo-peatlands could be calculated.

2) The NPP value is an important proxy for the paleoclimate. The atmospheric CO<sub>2</sub> levels play a key role in controlling the NPP of paleo-peatlands. The variation trend of the NPP values of different ages should be compatible with the variation of atmospheric CO<sub>2</sub> levels in different geological ages.

#### Acknowledgments

This study is supported by the Fundamental Research Funds for the Central Universities (Grant No. 2022YJSDC05).

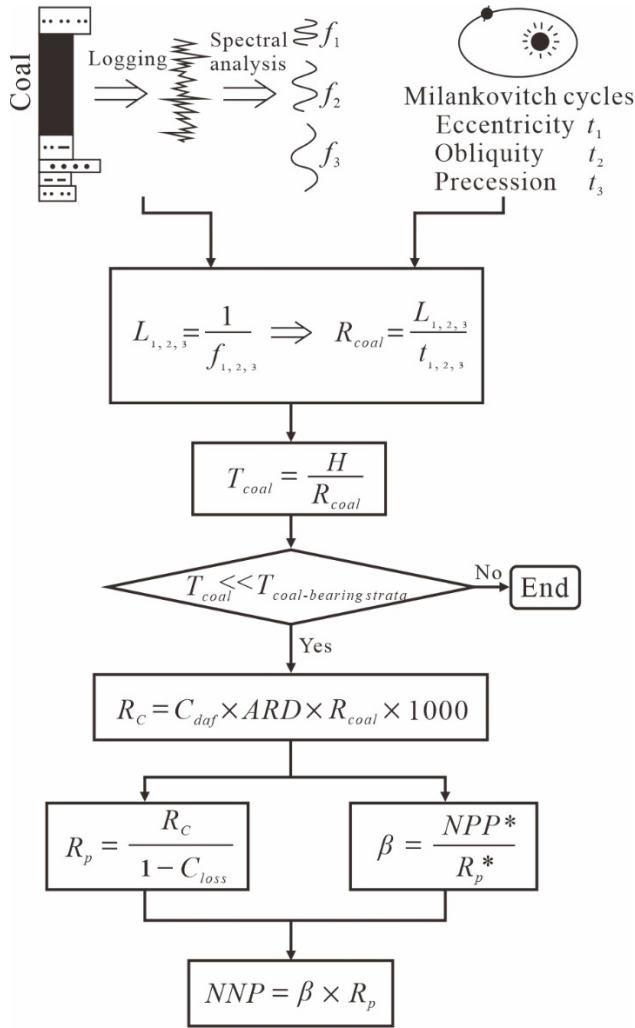


Fig. 1. Sketch showing procedures of the paleo-peatland productivity analysis.

$f_1, f_2, f_3$  represent the main average frequencies ( $\text{cycle } m^{-1}$ ) of the spectral analysis;  $t_1, t_2, t_3$  represent Milankovitch periodicities (eccentricity, obliquity, precession);  $L_1, L_2, L_3$  represent different cycle length ( $m$ );  $R_{coal}$  represents rate of coal deposition ( $m \text{ ka}^{-1}$ );  $H$  represents thickness of coal seam ( $m$ );  $T_{coal}$  represents period of coal deposition ( $ka$ );  $T_{coal-bearing strata}$  represents period of coal-bearing strata deposition ( $ka$ );  $ARD$  is the apparent density of coal ( $g \text{ cm}^{-3}$ );  $C_{daf}$  is the measured average carbon concentration of the coal (dry-ash-free basis, %);  $C_{loss}$  is carbon loss percentage during

the coalification (%);  $R_c$  represents the long-term average carbon accumulation rate for the coal ( $g \text{ C } m^{-2} a^{-1}$ );  $R_p$  represents the long-term average carbon accumulation rate for the paleo-peatlands ( $g \text{ C } m^{-2} a^{-1}$ );  $NPP^*$  represents the Holocene net primary productivity of the paleo-peatland ( $g \text{ C } m^{-2} a^{-1}$ );  $R_p^*$  represents the Holocene long-term average carbon accumulation rate for the peatland ( $g \text{ C } m^{-2} a^{-1}$ );  $\beta$  is the quantitative ratio between the Holocene net primary productivity level and the long-term average carbon accumulation rate for the peatland;  $NPP$  is the net primary productivity of the paleo-peatlands ( $g \text{ C } m^{-2} a^{-1}$ ).

### References:

- Beerling, D.J. and Woodward, F.I., 2001. Vegetation and the terrestrial carbon cycle: Modeling the first 400 million years. Cambridge: Cambridge University Press, 405.
- Berger, A., Loutre, M.F. and Laskar, J., 1992. Stability of the astronomical frequencies over the earth's history for paleoclimate studies. *Science*, 255(5044): 560–566.
- Diessel, C., 1992. Coal-bearing depositional system. New York: Springer-Verlag, 721.
- Hinnov, L., Hilgen, F.J., 2012. Cyclostratigraphy and astrochronology. In: Gradstein, F., Ogg, J., Schmitz, M., Ogg, G. (Eds.), *The Geologic Time Scale 2012*. Elsevier, 63–83.
- Large, D.J. and Marshall, C., 2015. Use of carbon accumulation rates to estimate the duration of coal seams and the influence of atmospheric dust deposition on coal composition. *Geological Society London Special Publications*, 404(1): 1–9.
- Shao, L.Y., Wang, X.T., Gao, X.Y. and Cheng, A.G., 2020. DDE-based coal resource potential assessment and coal geology knowledge innovation. *Coal Geology of China*, 32(09): 47–53 (in Chinese with English abstract).
- Shao, L., Wen, H., Gao, X., Spiro, B., Wang, X., Yan, Z. and Large, D.J., 2022. Identification of Milankovitch Cycles and Calculation of Net Primary Productivity of Paleo-peatlands using Geophysical Logs of Coal Seams. *Acta Geologica Sinica - English Edition*. Accepted.
- Stach, E., Mackowsky, M.-T., Teichmüller, M., Taylor, G.H., Chandra, D., Techmüller, R., 1982. *Stach's Textbook of Coal Petrology*, 3rd edn. Borntraeger, Stuttgart, 535 pp.

---

## Structural control on the 2021 M7.4 Maduo earthquake in NE Tibet: Crustal flow and fluids

Ziqiang Yang\*

\*E-mail: 201710252@stumail.nwu.edu.cn

---

Tomographic images of P and S wave velocity ( $V_p$ ,  $V_s$ ) and Poisson's ratio ( $\nu$ ) show that the 21 May 2021 Maduo earthquake (M 7.4) in NE Tibet occurred in a low- $V_s$  and high- $\nu$  anomaly, probably reflecting crustal fluids that affected the rupture nucleation. Our  $V_p$  anisotropy results show that at 40 km depth under the southern part of the study region, the fast-velocity direction (FVD) is NW-SE, which is mainly controlled by the Indo-Eurasia collision. At 60 km depth under the study Tomographic images of P and S wave velocity ( $V_p$ ,  $V_s$ ) and Poisson's ratio ( $\nu$ ) show that the 21 May 2021 Maduo earthquake (M 7.4) in NE Tibet occurred in a low- $V_s$  and

high- $\nu$  anomaly, probably reflecting crustal fluids that affected the rupture nucleation. Our  $V_p$  anisotropy results show that at 40 km depth under the southern part of the study region, the fast-velocity direction (FVD) is NW-SE, which is mainly controlled by the Indo-Eurasia collision. At 60 km depth under the study region and at 40 km depth under the northern part of the region, the FVDs are NE-SW to N-S, reflecting lower crustal flow. The E-W FVDs at 60 km depth beneath the Qilian Mountain range reflects the lower crustal flow that is blocked by the adjacent rigid terrain. The lower crustal flow may lead to intra-crustal and crust-mantle decoupling in the study region.

## Geochemical and uranium isotope variations in the Mengqiguer Sandstone-Type Uranium Deposit, Yili Basin, China

Mei Li <sup>a</sup>, Hao Song <sup>a,b,\*</sup>, Qianmin Du <sup>a</sup>, Meiling Duan <sup>a</sup>, Zexin Wang <sup>a</sup>, Yan Liang <sup>a</sup>, Yuanqing Fan <sup>a</sup>

<sup>a</sup> Chengdu University of Technology, Chengdu 610059, China

<sup>b</sup> Kay Laboratory of Earth Exploration and Information Techniques, Ministry of Education, Chengdu 610059, China

\* Corresponding author at: Chengdu University of Technology, Chengdu 610059, China. E-mail address: songhao@163.com (H. Song).

Sandstone-type uranium deposits, of which the worldwide resources total approximately 31%, are of greater economic significance compared with all the other known types (Zhang et al., 2018). In China, it is mainly distributed in sedimentary basins in the north, such as Yili Basin. The Southern Yili uranium district is located within the Yili Basin of NW China and is presently the largest U-producing district in China (Zhang and Liu, 2019). The uranium mineralization in the basin is mainly distributed in the sandstone layer of Xishanyao Formation in Middle-Lower Jurassic. We conducted petrographic, geochemical, and uranium isotope analysis in the sandstone samples from the important Mengqiguer sandstone-type uranium deposit located in the Yili basin of the Xishanyao Formation. This study aims to preliminarily identify the position of interlayer oxidation zones in uranium deposits through the petrographic and geochemical characteristics, and further to jointly indicate uranium mineralization combined with uranium isotope results.

Our petrographic results suggested that the interlayer oxidation zone can be divided into four zones: strong oxidation zone, weak oxidation zone, transition zone (mineralized zone) and reduction zone. From oxidation zone to reduction zone, the color gradually fades from red to gray. At the same time, due to the different sensitivity of U, Th and Ra elements in the interlayer oxidation zone, the Th/U ratio and U-Ra equilibrium coefficient can be calculated according to the element content to indicate the geochemical characteristics of different zones. The result showed that: In the oxidation zone, due to the loss of U, Ra is adsorbed by Fe and Mn oxides, the Th/U ratio is close to 1, and the U-Ra equilibrium coefficient is greater than 1; In the mineralization area of the transition zone, due to the

enrichment of U, the Th/U ratio significantly decrease, and the U-Ra equilibrium coefficient is below than 1.

Finally, the samples were analyzed by uranium isotope. Natural U consists of primordial-formed <sup>238</sup>U and <sup>235</sup>U, which are the two parent isotopes of the <sup>238</sup>U- and <sup>235</sup>U-series chains. In the <sup>238</sup>U-series decay chain, the <sup>234</sup>U nuclide is continuously formed and is the longest-lived daughter of all of the intermediate nuclides of the U-series decay chains (Andersen et al., 2017). In sandstone-type uranium deposits, the largest fractionation occurs during the reduction of U(VI) to U(IV). Uranium reduction is generally associated with the preferential enrichment of <sup>238</sup>U over <sup>235</sup>U, leading to high sedimentary  $\delta^{238}\text{U}$  values that are diagnostic of reducing environments (Clarkson et al., 2021).  $\delta^{238}\text{U}$  help evaluating the direction and timing of uranium migration in ore bodies (Golubev et al., 2022). At the same time, in the open system, the imbalance between <sup>234</sup>U and <sup>238</sup>U also indicates the different stages of mineralization and redox conditions. Variations in the <sup>238</sup>U/<sup>235</sup>U isotope ratio at sandstone-type uranium deposits showed that changing in the redox conditions during the advance of the uranium deposition front resulted in considerable fractionation of uranium isotopes in uranium ores. The fact that the  $\delta^{238}\text{U}$  and <sup>234</sup>U/<sup>238</sup>U values are correlated indicates that the transfer of the <sup>234</sup>U isotope into the aqueous phase could be coupled with isotope fractionation in the <sup>238</sup>U-<sup>235</sup>U system during the formation migration of uranium in the orebody.

**Keywords:** Sandstone-type uranium deposit, interlayer oxidation zone, uranium isotope

This research was sponsored by the National Natural Science Foundation Program of China (42173072, U1967207),

---

and Everest Scientific Research Program (CDUT).

**References:**

- Andersen, M.B., Stirling, C.H., Weyer, S., 2017. Uranium Isotope Fractionation. *Reviews in Mineralogy and Geochemistry* 82, 799–850. <https://doi.org/10/gfx6hj>
- Clarkson, M.O., Hennekam, R., Sweere, T.C., Andersen, M.B., Reichart, G.-J., Vance, D., 2021. Carbonate associated uranium isotopes as a novel local redox indicator in oxidatively disturbed reducing sediments. *Geochimica et Cosmochimica Acta* 311, 12–28. <https://doi.org/10/gmhqkm>
- Golubev, V.N., Chernyshev, I.V., Kochkin, B.T., Tarasov, N.N., Ochirova, G.V., Chugaev, A.V., 2022. Uranium Isotope Variations ( $^{234}\text{U}/^{238}\text{U}$  and  $^{238}\text{U}/^{235}\text{U}$ ) and Behavior of U–Pb Isotope System in the Vershinnoe Sandstone-Type Uranium Deposit, Vitim Uranium Ore District, Russia. *J. Earth Sci.* 33, 317–324. <https://doi.org/10/gqb2k8>
- Zhang, C., Liu, H., 2019. A growing sandstone type uranium district in South Yili Basin, NW China as a result of extension of Tien Shan Orogen: Evidences from geochronology and hydrology. *Gondwana Research* 76, 146–172. <https://doi.org/10.1016/j.gr.2019.06.006>
- Zhang, X., Nie, F.-J., Xia, F., Zhang, C.-Y., Feng, Z.-B., Ullah, R., Zhang, P.-F., 2018. Provenance constraints on the Xishanyao Formation, southern Yili Basin, northwest China: evidence from petrology, geochemistry, and detrital zircon U–Pb geochronology. *Can. J. Earth Sci.* 55, 1020–1035. <https://doi.org/10/gd68vx>

# Element geochemical characteristics of the Hanchiatien Formation black shale during weathering in Northern Sichuan, Southwestern China

Meiling Duan<sup>1</sup>, Hao Song<sup>\*1,2</sup>, Wei Hu<sup>2</sup>, Xin Liao<sup>3</sup>

<sup>1</sup> College of Earth Sciences, Chengdu University of Technology, Chengdu 610059, China;

<sup>2</sup> State Key Laboratory of Geo-Hazard Prevention and Geo-Environment Protection (Chengdu University of Technology), Chengdu 610059, China;

<sup>3</sup> Faculty of Geosciences and Environmental Engineering, Southwest Jiaotong University, Chengdu 611756, China

Continental weathering plays an essential role in global material cycling, nutrient supply of ecosystem, topographic and geomorphic evolution, and supergene mineralization (Brantly et al., 2007; Percival et al., 2016), thereby impacting water/soil quality, ecosystem sustainability and human health. As an important surface process, weathering can cause disintegration or decomposition of rocks that differ from unweathered rocks in structure or composition (Li et al., 2007). Black shale tends to suffer from chemical weathering in nature due to its high content of organic matter, sulfide minerals (e.g. pyrite) and Partial trace element (e.g. U, Mo, V). The unique environmental and petrophysical impact of black shale weathering has paid attention over the past decades (Ling et al., 2016; Gu et al., 2020). The migration of elements in weathering of black shale mainly focuses on the environmental effects of heavy metal pollution (Peng et al., 2004) or speculate weathered provenance and sedimentary environment (Pi et al., 2013) or link their responses to climate change (Aaron et al., 2021). Therefore, it's of great significance to study activity of elements for comprehending black shale weathering mechanism.

Silurian Hanchiatien black shale is widely exposed in southwest China, and its bedding structure developed (Ernst et al., 2021). The sampling area is located at the contact edge of The Sichuan Basin and the Longmenshan tectonic belt, where faults and fissures are well developed and geological hazard such as landslides and collapses caused by earthquakes frequently occur, which is of role significance for the study of supergene geochemistry.

In order to study the variation of elements in the weathering

process of black shale, taking a field weathering profile of the Silurian Hanchiatien Formation black shale in Sichuan, Southwestern China as an example, observation under microscope, whole rock X-ray fluorescence spectroscopy (XRF), Inductively Coupled Plasma Mass Spectrometry (ICP-MS) and other methods were used. The major and trace elements of different degrees of weathering rock samples were studied.

The results show that, 1) the content of SiO<sub>2</sub> in the profile ranges from 57.73% to 74.08%. The contents of Al<sub>2</sub>O<sub>3</sub>, K<sub>2</sub>O, TiO<sub>2</sub>, MgO, <sup>T</sup>Fe<sub>2</sub>O<sub>3</sub>, Na<sub>2</sub>O, CaO, MnO and P<sub>2</sub>O<sub>5</sub> in the profile range from 10.51%~17.59%, 1.81%~4.52%, 0.55%~0.78%, 1.35%~2.94%, 5.06%~6.59%, 0.33%~1.15%, 0.23%~5.41%, 0.03%~0.21% and 0.10%~0.30%. 2) In the bedrock and above layers, Rb, Cs, Th, Sc, Cr, Co and Ni are enriched in shale samples with respect to the Upper Continent Crust; On the contrary, Sr, Ba, Zr, Nb, Hf and Ta are depleted with respect to the Upper Continent Crust. 3) The contents of  $\sum$ REE,  $\sum$ LREE and  $\sum$ HREE ranged from 185.18 $\mu$ g/g~261.62 $\mu$ g/g, 131.56 $\mu$ g/g~202.60 $\mu$ g/g and 7.22 $\mu$ g/g~9.32 $\mu$ g/g, respectively.

The conclusions are as follows: 1) The activity laws of elements in the weathering profile are different. Al, K and Fe elements'  $\tau_{Nb,j}$  are close to 0, and their migration is not obvious. Mg and Ca elements have significant migration in weathering process. In the surface regolith, trace elements are generally enriched, indicating the influence of external input. Sr, Mn and U were severely depleted and migrated significantly during weathering, showing strong activity. Pb, Zn, Cu, Rb and Cs elements are extremely enriched on the whole. 2)  $\sum$ REE is 182.23  $\mu$ g/g in the bedrock and 215  $\mu$ g/g in the regolith. The

content of rare earth elements increases in the regolith, which are resulted from the absorption by the clay minerals that are formed during the weathering process. 3) According to the chemical alteration index (CIA=69.51~76.21), it can be judged that the weathering profile belongs to the moderate weathering degree. The weathering index from bedrock to regolith gradually increases with the degree of weathering strengthened. 4) A-CN-K diagram shows that the black shale weathering trend line is basically parallel to the A-CN edge, indicating that CaO and Na<sub>2</sub>O contents decrease during the weathering process from the bedrock to the weathering layer, and Ca, Na and Mg elements are obviously run away from minerals. Thereby, the profile has reached the weak to moderate chemical weathering stage and being initial stage of Ca and Na removal. Above all, the study on the element activity in weathering profile is of great significance to reveal the weathering process and mechanism of shale. This research was sponsored by the National Natural Science Foundation Program of China (42090051, 42173072), and Everest Scientific Research Program (CDUT).

**Keywords:** Blackshale; Weathering; Elemental geochemistry; Southwestern China.

**\*Corresponding author at:** College of Earth Sciences, Chengdu University of Technology, No.1, Erxianqiao East three road, Chenghua district, Chengdu, 610059, China.

**E-mail address:** songhao2014@cdut.edu.cn (H. Song)

## References:

- Aaron B, Niels H, Robert E, et al. 2021. Co-variation of silicate, carbonate and sulfide weathering drives CO<sub>2</sub> release with erosion[J]. *Nature Geoscience*, 14(4): 211-216.
- Brantley S L, Goldhaber M B and Ragnarsdottir K V. 2007. Crossing disciplines and scales to understand the critical zone[J]. *Elements*, 3(5): 307-314.
- Ernst A, Li Q J, Zhang M, et al. 2021. Bryozoans from the lower Silurian (Telychian) Hanchiatien Formation from southern Chongqing, South China[J]. *Journal of Paleontology*, 95(2): 252-267.
- Gu X, Rempe D M, Dietrich W E, et al. 2020. Chemical reactions, porosity, and microfracturing in shale during weathering: the effect of erosion rate[J]. *Geochimica et Cosmochimica Acta*, 269: 63-100.
- Li X S, Han Z Y, Yang S Y, et al. 2007. Chemical weathering intensity and element migration features of the Xiashu loess profile in Zhenjiang[J]. *Acta Geographica Sinica*, 62(11): 1174-1184.
- Ling S X, Wu X Y, Sun C W , et al. 2016. Mineralogy and geochemistry of three weathered Lower Cambrian black shale profiles in Northeast Chongqing, China[J]. *Geosciences Journal*, 20(6): 793-812.
- Peng B, Song Z L, Tu X L, et al. 2004. Release of Heavy Metals During Weathering of the Lower Cambrian Black Shales in Western Hunan, China[J]. *Environmental Geology*, 45(8): 1137-1147.
- Percival L, Cohen A S, Davies M, et al. 2016. Osmium isotope evidence for two pulses of increased continental weathering linked to Early Jurassic volcanism and climate change[J]. *Geology*, 44(9): 759-762.

# Multiple timings of garnet-forming high-grade metamorphism and Cl-rich mineral formation in the Neoproterozoic continental collision zone revealed by petrochronology in the Sør Rondane Mountains, East Antarctica

Fumiko Higashino\*, Tetsuo Kawakami, Shuhei Sakata\*\*, Takafumi Hirata\*\*

Department of Geology and Mineralogy, Graduate School of Science, Kyoto University, Kitashirakawa-Oiwake-cho, Sakyo-ku, Kyoto 606-8502, Japan

\*Corresponding author.

TEL: +81 75 753 4150

E-mail: higashino.fumiko.2m@kyoto-u.ac.jp

\*\* Present address: University of Tokyo, Japan

The Sør Rondane Mountains (SRM), East Antarctica is located in a key area of Gondwana formation where the East African-Antarctic Orogen and Kuunga Orogen cross (e.g., Satish-Kumar et al., 2013 and references therein). The East African-Antarctic Orogen (EAAO) and the Kuunga Orogen is respectively considered to be a collision of east-west Gondwana at ca. 750-620 Ma and north-south Gondwana at ca. 570-530 Ma (Meert, 2003). In contrast, there are previous studies suggesting that the younger event is also included in the EAAO (e.g., Jacobs and Thomas, 2004; Jacobs et al., 2015; Fitzsimons, 2016).

The SRM is divided into the Northeastern-terrane (NE-terrane) and the Southwestern-terrane (SW-terrane) by a mylonite zone termed the Main Tectonic Boundary (MTB) that dips gently to the north and the northeast (Osanai et al., 2013). Osanai et al. (2013) interpreted that the timing of peak metamorphism (650-600 Ma) and retrograde metamorphism under andalusite-stability field (590-530 Ma) are the same in the NE- and SW-terranes. Most of the previous U-Pb zircon dating to determine the timing of metamorphism in the SRM used separated zircon grains, and *in situ* U-Pb zircon dating that takes microstructural context into account has been limited (e.g., Higashino et al., 2013, 2015; Kawakami et al., 2017). Additionally, a petrochronological approach that takes

into account the distribution of rare earth elements (REE) between zircon and garnet has been limited in the SRM (e.g., Hokada et al., 2013).

In order to evaluate equilibrium between multiple generations of zircon and garnet, the distribution coefficient of REE between zircon and garnet [ $D_{\text{REE}(Zm/Grt)}$ ] is one of the best tools to check equilibrium between these minerals, because it can be used combining with microstructural constraints (e.g., Rubatto, 2002; Taylor et al., 2017; Kawakami et al., 2019). In this study, therefore, linkage between garnet-forming metamorphism and *in situ* U-Pb dating of zircon is made by petrochronological approach; microstructural constraints and evaluation of zircon-garnet equilibrium, utilizing  $D_{\text{REE}(Zm/Grt)}$  on array plot and REE pattern of zircon.

We investigate seven pelitic and mafic gneisses from the SRM. Since the outermost domain of the zircon enclosed in garnet is a possible equilibrium counterpart with the host garnet, the outermost domain of zircon is paired with garnet in order to calculate  $D_{\text{REE}(Zm/Grt)}$  and plotted in the array plots. As the result, several different periods of garnet-forming metamorphism at >600 Ma and <580 Ma both in the NE- and SW-terranes are recognized. In addition, flat HREE pattern of zircon mantle and core with the date of ca. 650-600 Ma is obtained in two samples, presumed to represent equilibrium

with garnet (cf. Rubatto, 2017). These observations suggest multiple timings of garnet-zircon equilibrium within a single sample. In contrast to previous simple tectonic interpretation, polymetamorphism (>600 Ma metamorphism overprinted by <580 Ma metamorphism) is recognized in the SRM. It is noted that there is a possibility of continuous zircon growth, because clear time interval between the garnet growths is not recognized. In order to correlate each timing with large-scale orogeny, *P-T-t-D-fluid* path in each sample is required.

On the other hand, matrix minerals tend to change their compositions by the effect of fluid infiltration (e.g., Uno et al., 2017). This means that the existence of Cl-rich biotite and amphibole in the matrix may imply the effect of igneous intrusions including hidden plutonic bodies. Multiple timings of Cl-rich mineral formation are also revealed in the SRM. In addition to constraining the timing of garnet formation, therefore, Cl-rich biotite present in the matrix helps detecting heat advection from granitic intrusion by hydrothermal Cl-bearing fluids.

**Keywords:** rare earth element, zircon, garnet, distribution coefficient, continental collision zone.

## Reference:

- Fitzsimons, I. C., 2016. Pan–African granulites of Madagascar and southern India: Gondwana assembly and parallels with modern Tibet. *Journal of Mineralogical and Petrological Sciences*, 111(2), 73-88.
- Higashino, F., Kawakami, T., M. Satish-Kumar, Ishikawa, M., Maki, K., Tsuchiya, N., Grantham, G.H., Hirata, T., 2013. Chlorine-rich fluid or melt activity during granulite facies metamorphism in the Late Proterozoic to Cambrian continental collision zone- An example from the Sør Rondane Mountains, East Antarctica. *Precambrian Research* 234, 229-246.
- Higashino, F., Kawakami, T., Tsuchiya, N., Satish-Kumar, M., Ishikawa, M., Grantham, G.H., Sakata, S., Hattori, K., Hirata, T., 2015. Geochemical behavior of zirconium during Cl-rich fluid or melt infiltration under upper amphibolite facies metamorphism – A case study from Brattnipene, Sør Rondane Mountains, East Antarctica. *Journal of Mineralogical and Petrological Sciences* 110, 166-178.
- Hokada, T., Horie, K., Adachi, T., Osanai, Y., Nakano, N., Baba, S., Toyoshima, T., 2013. Unraveling the metamorphic history at the crossing of Neoproterozoic orogens, Sør Rondane Mountains, East Antarctica: Constraints from U-Th-Pb geochronology, petrography, and REE geochemistry. *Precambrian Research* 234, 183-209.
- Jacobs, J., Thomas, R. J., 2004. Himalayan-type indenter-escape tectonics model for the southern part of the late Neoproterozoic–early Paleozoic East African–Antarctic orogen. *Geology*, 32(8), 721-724.
- Jacobs, J., Elburg, M., Läufer, A., Kleinhanns, I. C., Henjes-Kunst, F., Estrada, S., Ruppel, A. S., Damaske, D., Montero, P., Bea, F., 2015. Two distinct late Mesoproterozoic/early Neoproterozoic basement provinces in central/eastern Dronning Maud Land, East Antarctica: The missing link, 15–21 E. *Precambrian Research*, 265, 249-272.
- Kawakami, T., Higashino, F., Skrzypek, E., Satish-Kumar, M., Grantham, G., Tsuchiya, N., Ishikawa, M., Sakata, S., Hirata, T., 2017. Prograde infiltration of Cl-rich fluid into the granulitic continental crust from a collision zone in East Antarctica (Perlebandet, Sør Rondane Mountains). *Lithos* 274-275, 73-92.
- Kawakami, T., Horie, K., Hokada, T., Hattori, K., Hirata, T., 2019. Disequilibrium REE compositions of garnet and zircon in migmatites reflecting different growth timings during single metamorphism (Aoyama area, Ryoke belt, Japan). *Lithos*, 338–339, 189–203.
- Meert, J., 2003. A synopsis of events related to the assembly of eastern Gondwana. *Tectonophysics*, 362, 1-40.
- Osanai, Y., Nogi, Y., Baba, S., Nakano, N., Adachi, T., Hokada, T., Toyoshima, T., Owada, M., Satish-Kumar, M., Kamei, A., Kitano, I., 2013. Geologic evolution of the Sør Rondane Mountains, East Antarctica: Collision tectonics proposed based on metamorphic processes and magnetic anomalies. *Precambrian Research*, 234, 8-29.
- Rubatto, D., 2002. Zircon trace element geochemistry: partitioning with garnet and the link between U-Pb ages and metamorphism. *Chemical Geology* 184, 123-138.
- Rubatto, D., 2017. Zircon: the metamorphic mineral. *Reviews in mineralogy and geochemistry*, 83(1), 261-295.
- Satish-Kumar, M., Hokada, T., Owada, M., Osanai, Y., Shiraishi, K., 2013. Neoproterozoic orogens amalgamating East Gondwana: Did they cross each other?. *Precambrian Research* 234, 1-7.
- Taylor, R. J. M., Clark, C., Harley, S. L., Kylander-Clark, A. R. C., Hacker, B. R., Kinny, P. D., 2017. Interpreting granulite facies events through rare earth element partitioning arrays. *Journal of Metamorphic Geology*, 35(7), 759-775.
- Uno, M., Okamoto, A., Tsuchiya, N., 2017. Excess water generation during reaction-inducing intrusion of granitic melts into ultramafic rocks at crustal P–T conditions in the Sør Rondane Mountains of East Antarctica. *Lithos*, 284, 625-641.

# Forming Proterozoic basement within eastern Central Asian Orogenic Belt: Evidence from zircon U-Pb-Hf-O isotopes

Zhiwei Wang<sup>a, b\*</sup>, Taichang Zhu<sup>a, b</sup>, Jingwen Yu<sup>a, b</sup>, Lingling Yuan<sup>c</sup>

<sup>a</sup> Hebei Key Laboratory of Strategic Critical Mineral Resources, Hebei GEO University, Shijiazhuang 050031, China

<sup>b</sup> College of Earth Sciences, Hebei GEO University, Shijiazhuang, 050031, China

<sup>c</sup> Key Laboratory of Metallogenic Prediction of Nonferrous Metals and Geological Environment Monitoring, Ministry of Education, School of Geoscience and Info-Physics, Central South University, Changsha 410083, China

Corresponding author: wangzw14@mails.jlu.edu.cn (Z.W. Wang)

Postal address: 136 Huai'an Road, College of Earth Sciences, Hebei GEO University, Shijiazhuang, 050031, China

The Xing'an-Airgin Sum Block (XAB), a micro-continent within the Central Asian Orogenic Belt (CAOB), contains increasingly-recognized Meso-Neoproterozoic geological records. The origin, spatial-temporal distribution of ancient materials, and their role in the crustal evolution, however, remain controversial. In this study, Mesoproterozoic and Paleozoic granites from the Erenhot region of central Inner Mongolia, eastern CAOB, are studied incorporating both zircon U-Pb dates and Hf-O isotopes. The presence of 1.4 Ga calc-alkaline granite-rhyolite association indicates that the Precambrian basement of the XAB extends from Sonid Zuoqi to Erenhot in the west (Yang et al., 2021; Wang et al., 2022a, b). The 384, 317 and 281 Ma monzogranites that include Mesoproterozoic xenocrystic zircons have Proterozoic two-stage Hf model ages, further indicating the widespread presence of Proterozoic crust under the western XAB (Wang et al., 2022b). The cyclic growth and reworking of the Proterozoic crust appear to be intimately linked with orogenesis during the relevant supercontinent cycles. The 1450–1360 Ma juvenile crustal growth at Erenhot and synchronous ancient crust reworking at Sonid Zuoqi and Abagaqi were likely caused by the retreating subduction involved in Columbia breakup (Wang et al., 2022a). While the 1.2–1.0 Ga reworking and 0.9–0.7 Ga growth events within the Erenhot basement may have been a response to the assembly and breakup of Rodinia (Wang et al., 2022a). Our research also supports the suggestion that the reworking of the Neoproterozoic crust played an important role during the Paleozoic multi-stage accretion of CAOB (Wang et al., 2016, 2017, 2022b; Yuan et al., 2022).

## References:

- Wang, Z.W., Xu W.L., Pei, F.P., Wang, F., Guo, P., 2016. Geochronology and geochemistry of early Paleozoic igneous rocks of the Lesser Xing'an Range, NE China: Implications for the tectonic evolution of the eastern Central Asian Orogenic Belt. *Lithos*, 2016, 261: 144-163.
- Wang, Z.W., Xu W.L., Pei, F.P., Guo, P., Wang, F., Li, Y., 2017. Geochronology and geochemistry of early Paleozoic igneous rocks from the Zhangguangcai Range, northeastern China: Constraints on tectonic evolution of the eastern Central Asian Orogenic Belt. *Lithosphere*, 2017, 9(5): 803-827.
- Wang, Z.W., Wang, Z.H., Zhang, Y.J., et al., 2022a. Linking ~1.4-0.8 Ga Volcanic-Sedimentary Records in Eastern Central Asian Orogenic Belt with Southern Laurentia in Supercontinent Cycles. *Gondwana Research*, 105: 416-431.
- Wang, Z.W., Peng, J., Yu, J.W., Zhu, T.C., Zhang, Y.J., Tian, Y.J., Xu, B., Shi, J.T., 2022b. Meso- to Neoproterozoic zircon xenocrysts in late Carboniferous granite from the western Xing'an Block: Records of the supercontinent evolution[J]. *Geological Bulletin of China*, 41(2-3): 486-497 (in Chinese with English abstract).
- Yang, Z.N., Wang, Z.W., Zhang, L.Y., et al., 2021 Building the Proterozoic basement of the western Xing'an-Airgin Sum Block in the eastern Central Asian Orogenic Belt and its implications for the Nuna breakup and Rodinia assembly. *Precambrian Research*, 366: 106420.
- Yuan, L.L., Zhang, X.H., Yang, Z.L., 2022. The Timeline of Prolonged Accretionary Processes in Eastern Central Asian Orogenic Belt: Insights from Episodic Paleozoic Intrusions in Central Inner Mongolia, North China. *GSA Bulletin*, 134(3/4): 629–657.

# Identification and origin of late Paleoproterozoic Gaositai hornblende in northern North China Craton: Evidence from zircon U-Pb isotopes and amphibole trace elements

Taichang Zhu<sup>a, b</sup>, Yuxin Sun<sup>a, b</sup>, Zhenyu Liu<sup>a, b</sup>, Yin Xu<sup>a, b</sup>, Jingwen Yu<sup>a, b</sup>, Zhiwei Wang<sup>a, b\*</sup>

<sup>a</sup> Hebei Key Laboratory of Strategic Critical Mineral Resources, Hebei GEO University, Shijiazhuang 050031, China

<sup>b</sup> College of Earth Sciences, Hebei GEO University, Shijiazhuang, 050031, China

Corresponding author: wangzw14@mails.jlu.edu.cn (Z.W. Wang)

Postal address: 136 Huai'an Road, College of Earth Sciences, Hebei GEO University, Shijiazhuang, 050031, China

The Paleoproterozoic tectonic evolution of the northern North China Craton has been a hot research topic. Previous studies mostly focused on the formation and metamorphic ages of the Neoarchean metamorphic complex, ~2.5 and 1.8 Ga metamorphic volcanic rocks and granitic rocks, revealing the Neoarchean subduction and Paleoproterozoic collision to extension processes, but the latter still lack constraints from the mafic to ultramafic rocks. We first identified a suite of 1.85 Ga hornblende from the Gaositai mafic-ultramafic complex. In this study, systematic studies of petrology, zircon U-Pb geochronology, *in situ* major and trace elements of amphibolite are the key to revealing the genesis of the Paleoproterozoic ultramafic rocks and the geodynamic mechanism in the northern North China Craton.

LA-ICP-MS zircon U-Pb dating suggests the primary magmatic zircons with oscillatory zoning and high Th/U ratios formed at  $1851 \pm 44$  Ma, and the older captured zircons recorded the 2.2, 2.4, 2.5 Ga tectonic-thermal events. Hence, we confirm the existence of late Paleoproterozoic ultramafic rocks in Gaositai area, northern Hebei Province. Together with Paleoproterozoic post-collisional granites, it formed a bimodal igneous assemblage.

The olivine, clinopyroxene, and coarse hornblende were the early-crystallizing minerals because the fine-grained olivine and clinopyroxene inclusions formed in the core of coarse hornblende crystal. This suggests that the hornblende was likely in equilibrium with the parental magma. Hence, we attempt to qualitatively estimate the composition of

equilibrium magma using the trace element composition and  $A_{m/L}D$  values of hornblende. Both hornblende and its equilibrium melt compositions show relative enrichment in LREEs and LILEs (e.g., Rb, Ba, K, Pb), and depletion in HREEs and HSFES (e.g., Nb, Ta, Zr, Hf, Ti), which is geochemically similar to those of the amphiboles and their host basaltic rocks in subduction zones. The presence of phlogopite, strongly fractionated HREE patterns of hornblende and equilibrium melt imply that the hornblende magma originated from a hydrous garnet-facies mantle source metasomatized by K-rich silicate melt. Furthermore, the variations of major and trace elements in hornblende from core to rim also reveal the mineral fractional crystallization and magmatic recharge.

Amphibole-rich rocks were mostly produced at oceanic ridge subduction or post-collision extension settings. Zircon trace elements (high U/Yb), melt compositions equilibrium with hornblendes (low Lu/Hf and high Th/Yb), and bimodal igneous assemblage, are more in favor of a post-collision origin. The 1.9-1.8 Ga magmatic and metamorphic events in northern North China Craton documented the continent-continent collision and post-collision extension between eastern and western North China blocks. The extension process led to the underplating of basaltic magma and the cumulate origin of hornblende beneath the lower crust.

# Relationship between early Paleozoic magmatic events and uranium mineralization in the northern China

Zexin Wang <sup>a</sup>, Hao Song <sup>a,b</sup>, Qianmin Du <sup>a</sup>, Yan Liang <sup>a</sup>, Huijie Yu <sup>a</sup>

<sup>a</sup> Chengdu University of Technology, Chengdu 610059, China

<sup>b</sup> Kay Laboratory of Earth Exploration and Information Techniques, Ministry of Education, Chengdu 610059, China

\* Corresponding author at: Chengdu University of Technology, Chengdu 610059, China. E-mail address: songhao@163.com (H. Song).

As a strongly incompatible element, uranium usually tends to crystallize at the end of magmatic differentiation or enter other minerals in the form of isomorphism. However, because the distribution coefficient of  $U^{4+}$  between melt and hydrothermal solution is very low, even the rock formed by highly differentiated magma still has low uranium content, which leads to the fact that some granitic rocks with relatively high uranium content are often ignored in prospecting and exploration activities, but the uranium in these rocks may be activated and migrated by later geological events and eventually enriched to form deposits. Therefore, this paper focus on the uranium deposits around Qaidam block in order to provide guidance for the research of the distribution law and the prospecting work of uranium deposits. Around the early Paleozoic, the Qaidam block and the adjacent Altyn block and Alxa block began the process of subduction and collision, and triggered a series of magmatic events. A large number of U-rich A-type or highly differentiated granitoids, such as Mangya granite (Xu et al., 2020), Jiling granite (Wang et al., 2019), HaideWula granite (Lei et al., 2021), were formed in the Altyn Mountain, Longshou Mountain, Kunlun Mountains and other areas around the Qaidam block. These U-rich granites provide the material basis for the subsequent uranium metallogenic events. There are various types of uranium deposits developed in and around the Qaidam block, including volcanic-related type, metasomatite type, sandstone type and granite-related type. Although the metallogenic age of some deposits has nothing to do with the age of host rocks, the uranium source is provided by these uranium rich granitic rocks. The uranium in these rocks migrated and finally enriched under various geological processes in the later stage, such as Jiling Na-metasomatic type uranium deposit (Zhong et al., 2020) and sandstone type uranium deposit in Qaidam Basin

(Abudukeyumu et al., 2022; Yan, 2020). The diagenetic ages of these U-rich granitoids are mostly concentrated in 400~440 Ma, which is related to the reassembly of the block after the breakup of Gondwana continent. Therefore, the distribution of uranium deposits and points in and around the Qaidam block is controlled by these early Paleozoic uranium rich granitoids, and the supercontinent cycle provides a driving force for the emergence of these uranium deposits and points.

This research was sponsored by the National Natural Science Foundation Program of China (42173072, U1967207), and Everest Scientific Research Program (CDUT).

**Keywords:** Magma-structural evolution, U-rich granite, Uranium deposits

## References:

- Abudukeyumu, A., Song, H., Chi, G., Li, Q., Zhang, C., 2022. Quaternary uranium mineralization in the Qaidam Basin, northern Tibetan Plateau: Insights from petrographic and C-O isotopic evidences. *Ore Geology Reviews* 140, 104628. <https://doi.org/10.1016/j.oregeorev.2021.104628>
- Wang, K.-X., Yu, C.-D., Yan, J., Liu, X.-D., Liu, W.-H., Pan, J.-Y., 2019. Petrogenesis of Early Silurian granitoids in the Longshoushan area and their implications for the extensional environment of the North Qilian Orogenic Belt, China. *Lithos* 342–343, 152–174. <https://doi.org/10.1016/j.lithos.2019.05.029>
- Xu, N., Wu, C., Gao, Y.-H., Lei, M., Zheng, K., Gao, D., 2020. Tectonic evolution of the South Altyn, NW China: constraints by geochemical, zircon U–Pb and Lu–Hf isotopic analysis of the Palaeozoic granitic plutons in the Mangya area. *Geol. Mag.* 157, 1121–1143. <https://doi.org/10.1017/S0016756820000126>
- Zhong, J., Wang, S.-Y., Gu, D.-Z., Cai, Y.-Q., Fan, H.-H., Shi, C.-H., Hu, C.-N., 2020. Geology and fluid geochemistry of the Na-metasomatism U deposits in the Longshoushan

uranium metallogenic belt, NW China: Constraints on the ore-forming process. *Ore Geology Reviews* 116, 103214. <https://doi.org/10.1016/j.oregeorev.2019.103214>

Yan, W.-Q., 2020. Sedimentary environment and provenance analysis of Neogene-Quaternary in Yuejin-Qigequan area, western Qaidam Basin. Chengdu University of Technology.

Lei, Y.-L., Dai, J.-W., Bai, Q., Wang, K.-X., Sun L.-Q., Liu, X.-D., Yu, C.-D., He, S.-W., 2021. Genesis and implications of peraluminous A-type rhyolite in the Haidewula area, East Kunlun Orogen. *Acta Petrologica Sinica*, 37 (7) :1964–1982. <https://doi:10.18654/1000-0569/2021.07.02>

# Pressure-Temperature-time paths of pelitic gneisses indicating long-lived metamorphism in central Sør Rondane Mountains, East Antarctica

Tetsuo Kawakami<sup>1\*</sup>, Sota Niki<sup>2</sup>, Masayasu Suzuki<sup>1</sup>, Shuhei Sakata<sup>3</sup>, Tatsuro Adachi<sup>4</sup>, Fumiko Higashino<sup>1</sup>, Masaoki Uno<sup>5</sup>, and Takafumi Hirata<sup>2</sup>

<sup>1</sup> Department of Geology and Mineralogy, Graduate School of Science, Kyoto University, Japan

<sup>2</sup> Geochemical Research Center, Graduate School of Science, The University of Tokyo, Japan

<sup>3</sup> Earthquake Research Institute, The University of Tokyo, Japan

<sup>4</sup> Advanced Asian Archaeological Research Center, Kyushu University, Japan

<sup>5</sup> Graduate School of Environmental Studies, Tohoku University, Japan

\*Corresponding author: [t-kawakami@kueps.kyoto-u.ac.jp](mailto:t-kawakami@kueps.kyoto-u.ac.jp)

The Sør Rondane Mountains (SRM) in East Antarctica is located at the crossing point of the East African Orogen (EAO) and the Kuunga Orogen and, therefore, is a paleogeographically important area in understanding the formation and evolution of the Gondwana (e.g., Satish-Kumar et al., 2013). Several tectonic models are proposed to explain the formation of the SRM. Grantham et al. (2013) propose that overthrusting of the Namuno Terrane (part of the EAO with African affinity) onto the Nampula Terrane (Antarctic affinity) occurred at ca. 580-540 Ma, and the SRM is part of the hanging wall of the meganappe. Osanai et al. (2013) divide the SRM into the NE terrane and the SW terrane bounded by the Main Tectonic Boundary (MTB), based on the difference in inherited zircon ages and in metamorphic pressure-temperature-time (*P-T-t*) paths between the terranes: the granulite-facies gneisses in the NE terrane records clockwise *P-T-t* path whereas those in the SW terrane records counterclockwise *P-T-t* path. They considered that ca. 650-600 Ma is a timing of decompression in the NE terrane and decompression in the SW terrane, and that ca. 590-530 Ma is a timing of retrograde metamorphism under the andalusite stability field. Based on these pieces of observation, Osanai et al. (2013) proposed that the NE terrane overthrusts onto the SW terrane

at ca. 650-600 Ma. Recent studies reported *P-T-t* paths not consistent with the tectonic model of Osanai et al. (2013) (Kawakami et al., 2017; Tsubokawa et al., 2017). In order to understand the tectonic evolution of the SRM, it is important to determine detailed *P-T-t* paths from unstudied areas of the SRM.

We used a Sil-Bt-Grt gneiss from central SRM (Menipa) to construct a *P-T-t* path. The gneiss contains abundant garnet of ~4-5 mm diameter. The garnet [ $\text{Mg}/(\text{Mg}+\text{Fe}_{\text{total}}) = 0.34\text{-}0.44$ ] is often texturally sector-zoned. The core/rim boundary of garnet is defined by the discontinuous phosphorus zoning, and the rim is further divided into the inner and outer rims bounded by low-phosphorus annulus. The core is enriched relatively in Ca and Y compared to the rim. The core includes calcic (~An33-51) plagioclase inclusions. Rare kyanite, rare Mg-rich staurolite [ $\text{Mg}/(\text{Mg}+\text{Fe}_{\text{total}}) = 0.44$ , ZnO = 1.6-1.9 wt%] and sillimanite are included in the inner rim, whereas sillimanite is included in the outer rim. Rutile inclusions are ubiquitous in garnet.

We constrained the *P-T* conditions of the peak metamorphic stage (~1.0 GPa, ~800 °C) was estimated using the coexistence of sillimanite and kyanite combined with temperature estimate by the Zr-in-rutile geothermometer (Tomkins et al., 2007)

applied to the rutile enclosed in the inner rim of garnet. The retrograde re-equilibrium  $P$ - $T$  conditions of  $\sim 0.38$  GPa and  $\sim 610$  °C was estimated by applying the GASP geobarometer and garnet-biotite geothermometer (Holdaway et al., 1998; Holdaway, 2001) to biotite and plagioclase in contact with garnet rim. Finer-grained kyanite-biotite intergrowth compared to above-mentioned retrograde assemblage locally replaces rim of garnet. Application of the same geothermobarometry (Holdaway et al., 1998; Holdaway, 2001) gave  $P$ - $T$  conditions of  $\sim 0.29$  GPa and  $\sim 540$  °C.

Zircon is present in the matrix and included in garnet, biotite and quartz. Zircon is commonly  $\sim 60$   $\mu\text{m}$  in diameter and has inherited cores overgrown by CL-dark to CL-moderate mantle and thin CL-bright rim. The *in situ* LA-ICP-MS U-Pb zircon dating under thin section revealed that metamorphic dates from ca. 615 Ma to 559 Ma, characterized by low Th/U, are preserved both in the matrix zircon and in zircon enclosed in garnet rim. The ca. 559 Ma zircon is included in the outer rim of garnet together with sillimanite, and ca. 562 Ma zircon domain showed  $\text{Yb}_n/\text{Gd}_n \sim 0.9$ . This suggest that ca. 560 Ma zircon grew in equilibrium with garnet. Taking into account that kyanite and sillimanite is included in the inner rim of garnet, Ky-grade metamorphism took place before ca. 560 Ma. Ubiquitous sillimanite in the matrix and sillimanite inclusions in the outer rim of garnet suggest that sillimanite-grade metamorphism started at ca. 560 Ma. On the other hand, the ca. 601 Ma zircon domain showed  $\text{Yb}_n/\text{Gd}_n \sim 1.2$ , suggesting equilibrium growth of zircon with garnet. Since zircon domains showing  $\text{Yb}_n/\text{Gd}_n \sim 0.7$ - $1.2$  are common from ca. 600 to ca. 560 Ma, we interpret that the garnet growth started at ca. 600 Ma and continued until ca. 560 Ma. Duration of zircon growth at high- $T$  is supported by the temperature estimate by Ti-in-zircon geothermometer (Ferry and Watson, 2007) which gave  $T > 700$  °C for all the ca. 600 to ca. 560 Ma zircon domains.

A V-bearing, grossular-rich green garnet surrounded by kelyphite occurs in a calcareous metapelite in the same area, Menipa (Osanaï et al., 1990). The green garnet has a chemically homogeneous core with kelyphitic rims. This garnet was dated by *in situ* LA-ICP-MS U-Pb method (Niki et al., 2022). The rim of the green garnet yielded U-Pb garnet age of  $593 \pm 8$  Ma and  $586 \pm 9$  Ma. Titanite in the kelyphitic rim gave concordant U-Pb age ranging from ca. 550 to ca. 500 Ma from one sample and  $548 \pm 7$  Ma from another sample. Outer zone of the kelyphite rim contains apatite, which gave U-Pb age of  $496 \pm 9$  Ma. From these data, we consider that green garnet growth took place at ca. 590 Ma, followed by kelyphite formation starting from ca. 550 Ma and continued until ca. 500 Ma.

Coincidence of ca. 600 Ma metamorphic age obtained from the Sil-Bt-Grt gneiss with ca. 593-586 Ma green-garnet growth age within uncertainty suggests that the ca. 600-586 Ma was the timing of prograde metamorphism in Menipa. On the other

hand, ca. 550-500 Ma U-Pb titanite age from kelyphite is consistent with the ca. 560 Ma U-Pb zircon age obtained from the Sil-Bt-Grt gneiss, because high closure temperature of titanite (Holder et al., 2019) means that it records the timing of kelyphite formation. Continuous zircon growth between these timings and high- $T$  ( $T > 700$  °C) recorded as Ti content of zircon suggests long-lived high- $T$  metamorphism for  $\sim 40$  Myr. Therefore, based on petrochronological data presented above, we propose that high- $T$  metamorphism continued from ca. 600 Ma to ca. 560 Ma, and decompression started at ca. 550 Ma. Average exhumation rate to the upper crustal levels during the period of ca. 550-500 Ma was estimated to be 0.46 mm/yr.

The  $P$ - $T$ - $t$  path constrained by this study, especially the timing of exhumation, is consistent with the tectonic model by Grantham et al. (2013), while it is not consistent with the Osanaï et al. (2013) model. It is likely that the studied sample from the central SRM experienced collision at ca. 600 Ma, and was hot (700-800 °C) until ca. 560 Ma when the exhumation started. Therefore, the metamorphic evolution is likely continuous and polymetamorphism (i.e., EAO overprinted by Kuunga Orogeny) is not required to explain the  $P$ - $T$ - $t$  path of this study. More petrochronologically constrained  $P$ - $T$ - $t$  paths from unstudied areas of the SRM are required to understand the formation mechanism of the SRM.

**Keywords:** Collision zone; Granulite; P-T-t path; U-Pb zircon dating; U-Pb garnet dating

## References:

- Ferry, J. M., Watson, E. B. (2007). New thermodynamic models and revised calibrations for the Ti-in-zircon and Zr-in-rutile thermometers. *Contributions to Mineralogy and Petrology*, 154, 429–437.
- Grantham, G. H., Macey, P. H., Horie, K., Kawakami, T., Ishikawa, M., Satish-Kumar, M., Tsuchiya, N., Graser, P., Azevedo, S. (2013). Comparison of the metamorphic history of the Monapo Complex, northern Mozambique and Balchenfjella and Austhameren areas, Sør Rondane, Antarctica: Implications for the Kuunga Orogeny and the amalgamation of N and S. Gondwana. *Precambrian Research*, 234, 85–135.
- Holdaway, M. J. (2001). Recalibration of the GASP geobarometer in light of recent garnet and plagioclase activity models and versions of the garnet-biotite geothermometer. *American Mineralogist*, 86, 1117–1129.
- Holdaway, M. J., Mukhopadhyay, B., Dyar, M. D., Guidotti, C. V., Dutrow, B. L. (1997). Garnet-biotite geothermometry revised: New Margules parameters and a natural specimen data set from Maine. *American Mineralogist*, 82, 582–595.
- Holder, R. M., Hacker, B. R., Seward, G. G. E., Kylander-Clark, A. R. C. (2019). Interpreting titanite U-Pb dates and Zr thermobarometry in high-grade rocks: empirical constraints on elemental diffusivities of Pb, Al, Fe, Zr, Nb, and Ce. *Contributions to Mineralogy and Petrology*, 174, 1–19.
- Kawakami, T., Higashino, F., Skrzypek, E., Satish-Kumar, M., Grantham, G., Tsuchiya, N., Ishikawa, M., Sakata, S., Hirata, T. (2017). Prograde infiltration of Cl-rich fluid into the

- 
- granulitic continental crust from a collision zone in East Antarctica (Perlebandet, Sør Rondane Mountains). *Lithos*, 274–275, 73–92.
- Niki, S., Kawakami, T., Adachi, T., Uno, M., Higashino, F., Hirata, T. (2022). Triple dating of a metapelite from Menipa, Sør Rondane Mountains, East Antarctica based on U–Pb isotopic systems of garnet, titanite, and apatite. JpGU annual meeting 2022 abstract.
- Osanai, Y. (1990). Finding of Vanadium-Bearing Garnet from the Sør Rondane Mountains, East Antarctica Yasuhito. *Antarctic Record*, 34, 279–291.
- Osanai, Y., Nogi, Y., Baba, S., Nakano, N., Adachi, T., Hokada, T., Toyoshima, T., Owada, M., Satish-Kumar, M., Kamei, A., Kitano, I. (2013). Geologic evolution of the Sør Rondane Mountains, East Antarctica: Collision tectonics proposed based on metamorphic processes and magnetic anomalies. *Precambrian Research*, 234, 8–29.
- Satish-Kumar, M., Hokada, T., Owada, M., Osanai, Y., Shiraishi, K. (2013). Neoproterozoic orogens amalgamating East Gondwana: Did they cross each other? *Precambrian Research*, 234, 1–7.
- Tomkins, H. S., Powell, R., & Ellis, D. J. (2007). The pressure dependence of the zirconium-in-rutile thermometer. *Journal of Metamorphic Geology*, 25, 703–713.
- Tsubokawa, Y., Ishikawa, M., Kawakami, T., Hokada, T., Satish-Kumar, M., Tsuchiya, N., Grantham, G. H. (2017). Pressure-temperature-time path of a metapelite from Meffjell, Sør Rondane Mountains, East Antarctica. *Journal of Mineralogical and Petrological Sciences*, 112, 77–87.
- Wu, C. M., Zhang, J., Ren, L. D. (2004). Empirical garnet-biotite-plagioclase-quartz (GBPQ) geobarometry in medium- to high-grade metapelites. *Journal of Petrology*, 45, 1907–1921.

# Local MORB Mantle Heterogeneity Beneath the Southwest Indian Ridge: Implications for Mantle Processes during Gondwana break-up

Wei Wang<sup>a,b,c</sup>, Yunpeng Dong<sup>a</sup>, Katherine A. Kelley<sup>b</sup>, Zhenggang Li<sup>c</sup>, Fengyou Chu<sup>c</sup>

<sup>a</sup>State Key Laboratory of Continental Dynamics, Department of Geology, Northwest University, Xi'an, China.

<sup>b</sup>Graduate School of Oceanography, University of Rhode Island, Narragansett Bay Campus, Narragansett, RI, USA.

<sup>c</sup>Key Laboratory of Submarine Geosciences, Second Institute of Oceanography, MNR, Hangzhou, China.

The Southwest Indian Ridge formed during the break up of the Gondwana supercontinent 100 Ma ago, separating the African and Antarctic plates. Understanding the formation and evolution history of SWIR is of great importance for revealing the break-up process of the Gondwana supercontinent. The heterogeneity of the mantle source is a direct manifestation of continental break-up and ridge evolution. Due to the ultra-slow spreading rate of SWIR, its mantle convection cannot effectively homogenize the mantle source composition. Therefore, the mantle sources beneath the SWIR exhibit extremely heterogeneous. Studying the origin of such mantle heterogeneity will significantly contribute to understanding the mantle processes during the Gondwana break-up.

Trace elements and radiogenic isotope ratios of mid-ocean ridge basalts are often used to reveal the origins of mantle heterogeneity, but in the SWIR 48°–51°E region, the origins of heterogeneity remain controversial. Magmatic volatile contents are vital tracers of mantle heterogeneities, which may fractionate otherwise constant volatile/non-volatile elemental ratios, such as the H<sub>2</sub>O/Ce ratio. Volatile element constraints can provide a valuable test of models for the origins of mantle heterogeneities in this region.

Here, we present new data for nine rare basaltic glass samples from the 48-51°E region of SWIR, which enable careful assessment of the effects of primary vs. secondary

processes on the glass volatile contents. These samples are strongly affected by variable extents of carbon degassing, and shallow assimilation of Cl-rich fluid, but also reveal consistently high H<sub>2</sub>O/Ce ratios (458.8±14.9), among the highest in MORBs, that cannot be explained by late-stage secondary processes, crustal assimilation, or simple melting of peridotite mantle at variable depths. Instead, the high H<sub>2</sub>O/Ce ratios are features of the mantle source composition. The 48-51°E region is notably more depleted in highly incompatible trace elements relative to other regions of the SWIR, although this depletion is not apparent in H<sub>2</sub>O, which is similarly abundant throughout the SWIR. We link the high H<sub>2</sub>O/Ce ratios in these glasses with other trace element characteristics diagnostic of subduction and fluid addition (Nb/Nb\* < 1, low Ce/Pb, Th/U, Zr/Sm, and high La/Nb ratio), suggesting that the mantle source reflects signatures of a refractory mantle residue that previously melted within a subduction zone.

We conclude that recycled residual sub-arc mantle was formed from the subduction or arc magmatism during the break-up of the Gondwana supercontinent and migrated with the asthenosphere to replace part of the upper mantle beneath the SWIR.

## Integrated software for EPMA dating about uranium minerals

Tao Xiao <sup>a</sup>, Hao Song <sup>a, b, \*</sup>

<sup>a</sup> Chengdu University of Technology, Chengdu, Sichuan 610059, China.

<sup>b</sup> Applied Nuclear Technology in Geosciences Key Laboratory of Sichuan Province, Chengdu, Sichuan 610059, China.

The electron probe chemical dating method was first proposed by Suzuki (1991) of Nagoya University in Japan. Based on the decay theory of radionuclides, he accurately measured the content of U-Th-Pb in the paragneiss and monazite in a geological body in Southeast Japan through electron probe, successfully calculated the "chemical age" and plotted the isochron through the obtained data. In the nearly 30-year development history, this method has been fully studied. The significance of this study is not only that it can be applied to in-situ microzoning dating of uranium minerals such as monazite and zircon, but also that it has made progress and breakthrough in other uranium minerals. Now, as one of the in-situ micro dating methods, the electron probe dating method is widely used in the dating of U-bearing accessory minerals. Although there are more new testing methods have been applied such as ion probe and LA-ICP-MS nowadays, due to various factors such as cost and memory effect, the electron probe dating method still has a place in various dating methods.

In view of the poor sealing of the minerals to be tested, which are prone to the loss of radiogenic Pb and include multiple age domains, geologists have proposed a variety of treatment schemes for single point apparent ages (Suzuki and Adachi, 1991a, 1994; Montle et al., 1996; Cocherie, 1998). The classical isochron age calculation method requires that the variation range of U-Th-Pb is large, and the data points are scattered enough to obtain reasonable age results. When the conditions are not met, the isochron age error obtained is very large, and Sometimes the calculated age is negative, which is obviously unreasonable. The premise of calculating U-Pb age and the Pb age is that Th/Pb and U/Pb have a large range of variation. When this condition is not met, the results will not be ideal. The weighted average age algorithm has no requirements for the above conditions. A reasonable age value can be obtained by calculating the weighted average of the apparent ages of each single point, which belong to the same age domain within the error range. Each data processing scheme for calculating U-Pb age has its applicability,

advantages and disadvantages. Using different data processing methods, the results may be very different. In order to make better use of electron probe to determine the contents of U, Th and Pb in samples and improve the accuracy of age calculation results, the selection of data processing methods is particularly effective.

At present, the main processing method for the chemical dating of electron probe U-Th-Pb is to calculate the apparent age of a single measuring point by using the empirical formula, Bowles (1990) iterative method or the age calculation program compiled by Guo et al. (2012). After setting the error of a single point artificially, the weighted average value of the apparent age is calculated by Isoplot software (Ludwig et al., 1991). However, there is no special data processing software for uranium bearing minerals' electron probe dating data. Based on the decay theory of radionuclides, a software for calculating the chemical ages of uranium minerals has been developed from two aspects: single point chemical age calculation and data processing. In the graphical user interface, users can set errors, import files (Excel files) and other operations. The functions that can be realized include:

- (1) Generation of age histogram, weighted average age map and age estimation map.
- (2) K-means clustering, dividing the age domain.
- (3) Eliminating the abnormal measuring points in the same age domain by using the Dixon test method.
- (4) Calculating the uncertainty of the age of a single point by using the error transfer formula.
- (5) Judging the closeness of the U-Th-Pb system by using the correlation between elements.
- (6) Calculating the weighted average age, error and MSWD.

In order to verify the correctness and effectiveness of our calculation formula and design software, we selected the EPMA data of ten points (XS-7-1 and XS-7-10) to test our calculation method and error in Panzihua Datian area (Pei et al., 2021). Run the program, one point are removed from the data, and the age is 97.58 Ma. The age about remaining nine

points are given by procedure. Since the reliability of age measured depends largely on Pb content, 5% of Pb content is set as a single point of age error (Bowles, 1990). The weighted mean age is  $79.3 \pm 3.0 \text{ Ma}$  ( $2\sigma$ ) and  $\text{MSWD} = 3.7$ . The weighted average age given in the original article is  $84.1 \pm 3.2 \text{ Ma}$  ( $2\sigma$ ) and  $\text{MSWD} = 3.7$ . The results show that the two ages are consistent within the error range, indicating the reliability of the program designed in this study. The application of this software is of great help to improve the accuracy and efficiency of U-Th-Pb chemical dating.

**Keywords:** EPMA, Geological age, Uranium mineral, Python program

**\*Corresponding author at:** College of Earth Sciences, Chengdu University of Technology, No.1, Erxianqiao East three road, Chenghua district, Chengdu, 610059, China.

**E-mail address:** songhao2014@cdut.edu.cn (H. Song)

**References:**

- Bowles JFW. 1990. Age dating of individual grains of uraninite in rocks from electron microprobe analyses. *Chemical Geology*, 83(1-2):47-53.
- Guo G L, Zhang Z S, Liu X D, Feng Z S, Lai D R, Zhou W T., 2012, Crystallographic dating study of uranium electron probe from uranium deposits in the photic channel [J] *Donghua University of technology, Beijing, China*, 35 (04): 309-314.
- Ludwig K R., 1999, Users Manual for ISOPLOT/EX, Version 2.0: A geochronological toolkit for Microsoft Excel [CP/OL]. Berkeley Geochronology, Spec Publa. 1a.
- Montel J, Foret S, Veschambre M, et al., 1996, Electron microprobe dating of monazite. *Chemical Geology*, 131:37~53.
- Kazuhiro Suzuki, Mamoru Adachi., 1991. Precambrian provenance and Silurian metamorphism of the Tsubonosawa paragneiss in the South Kitakami terrane, Northeast Japan, revealed by the chemical Th-U-total Pb isochron ages of monazite, zircon and xenotime [J]. *Geochemical Society Of Japan*, 25(5) : 357~376.

## Geochemical constraints on metacarbonates from the Cauvery Suture Zone, Southern Granulite Terrane, India.

Thoti. Yellappa\*

CSIR-National Geophysical Research Institute, Uppal Road, Hyderabad, India

\*Email: yellappa\_thoti@yahoo.co.uk

Calcsilicate rocks are chemically precipitated sediments generally formed by the deposition of calcareous sediments or from volcanic rocks, hydrothermal veins, or by the intrusions of igneous plutons where cross-cutting carbonate rocks. These are widely occurring within the Neoproterozoic-Cambrian collisional belts of the Gondwana supercontinent. In southern granulite terrane (SGT), India, there are several occurrences of calcsilicate rocks/metacarbonate rocks in various parts of terrane, especially in the central part of Cauvery Suture Zone (CSZ) around Neoproterozoic Manamedu Ophiolite Complex and south of Karur-Kadvur gabbro-anorthosite complex. Field observations show that these calcsilicates occur in the form of elongated thick bands as well as massive to layered forms in association with the garnet sillimanite gneiss, hornblende gneiss, and two pyroxene granulites. The lithologies are dominant with calcite, mangano-calcite, and quartz with well foliated and displaying several shear kinematic indicators like small-scale displacements, boudin structures, and rotated porphyroblasts. Petrological studies reveal that these lithologies dominantly consist of 60-80% calcite-bearing minerals like calcite, scapolite, wollastonite, diopside, grossularite, and minor quartz with feldspars including some accessory minerals like magnetite and sulphides. Their whole-rock chemistry represents lower contents of SiO<sub>2</sub> (16 to 33 wt%), Al<sub>2</sub>O<sub>3</sub> (0.1 to 5.6 wt%), and higher concentrations of CaO (33-44.5 wt%) with varied MgO (0.5 to 12 wt%). The important trace elements include Rb varies from 1.5 to 85 ppm, Sr is from 58 to 462 ppm and Ba is 11 to 3653 ppm with total REE varying from 18 to 63 ppm. The Carbon-Oxygen isotope measurements of these calcsilicates represent  $\delta^{13}\text{C}$  ratios in the range of 0.01-3.03‰ and  $\delta^{18}\text{O}$  ratios are in the range of 12.91 to 24.83. On various tectonic discrimination plots of the geochemistry, results reveal that these have been derived from various sources of felsic rocks as well as sedimentary recycling and have been

evolved under open-ocean to continental margin settings in the form of inland sediments and are coeval to the Neoproterozoic metacarbonates of East Antarctica, Highland complex-Sri Lanka, Madagascar and Mozambique belt of East Gondwana.

### References:

- Collins, A.S, Clark, C., Plavsa, D., 2014. Peninsular India in Gondwana: the tectonothermal evolution of the southern granulite terrane and its Gondwana counter parts. *Gondwana Research* 25, 190-203.
- Otsuji, N., Satish Kumar, M., Kamei, A., Tsuchiya, N., Kawakami, T., Ishikawa, T., Grantham, G.H., 2013. Late Tonian to early Cryogenian apparent depositional ages from metacarbonate rocks from the Sor Rondane Mountains, East Antarctica. *Precambrian Research* 234, 257-273.
- Piper, J.D.A., 2000. The Neoproterozoic Supercontinent: Rodinia or Palaeopangaea? *Earth and Planetary Science letters* 176,131-146
- Satish Kumar M., Shirakawa, M., Imura, A., Otsuji, N.M., Imanaka Nohara, R., Malaviarachch, S.P.K., Fitzsimons I.C.W., Sajeev, K., Grantham, G.H., Windley, B.F., Hokada, T., Takahashi T., Shimoda, G., Goto, K.T., 2021. A geochemical and isotopic perspective on tectonic setting and depositional environment of Precambrian meta-carbonate rocks in collisional orogenic belts. *Gondwana Research* 96, 163-204.
- Yellappa, T., Chetty, T.R.K., Tsunogae, T., Santosh, M., 2010. Manamedu complex: Geochemical constraints on Neoproterozoic suprasubduction zone ophiolite formation within Gondwana suture in southern India. *Journal Geodynamics* 50, 268-285.

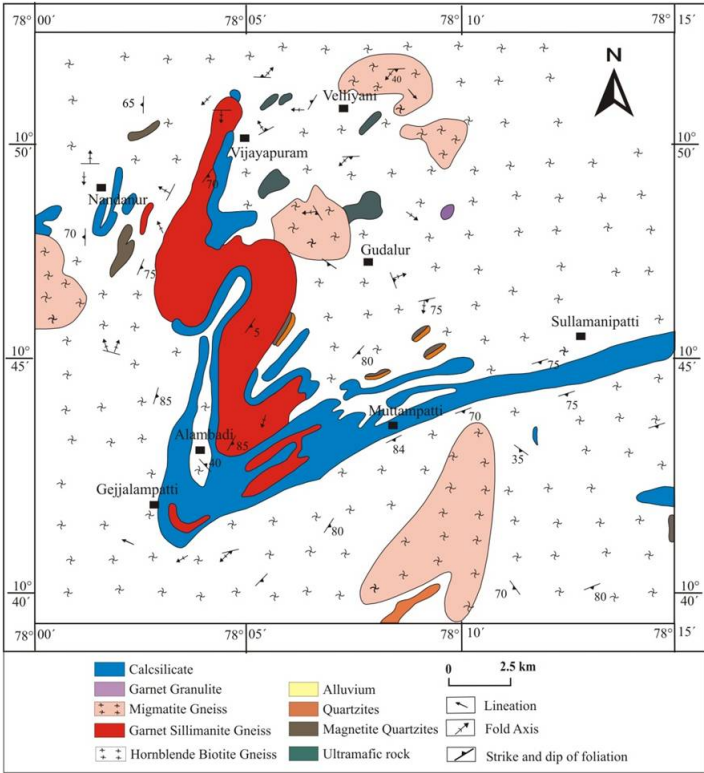


Fig.1: Geological map showing distributions of calcsilicate /metacarbonate rocks in south of Karur area, Southern Granulite Terrane, India (modified after GSI)

## A summary of the occurrence states of the sandstone type uranium deposits in Erlian Basin

Huijie Yu<sup>a</sup>, Hao Song<sup>a\*</sup>, Peng Qiao<sup>a,b</sup>, Zexin Wang<sup>a</sup>, Qianmin Du<sup>a</sup>, Mei Li<sup>a</sup>, Yan Liang<sup>a</sup>, Yuanqing Fan<sup>a</sup>, Meiling Duan<sup>a</sup>

<sup>a</sup> Chengdu University of Technology, Chengdu, Sichuan 610059, China

<sup>b</sup> Geologic Party No. 208, CNNC, Baotou 014010, China

Corresponding author *E-mail addresses*: songhhao@163.com (H. Song)

Uranium resource is an important energy mineral and an important guarantee for the sustainable development of nuclear energy in China. Erlian Basin, located in the central part of Inner Mongolia, is a rift basin formed by Jurassic-Cretaceous extension. The progress of uranium exploration over the years have made Erlian Basin one of the three major uranium-producing basins in northern China, and its uranium resources have increasingly become prominent in the whole basin (Nie, 2015). Bayan Wula, Hadatu, Saihan Gaobi, Manglai and other uranium deposits are located in Erlian Basin from northeast to southeast. These deposits are generally distributed in NE-SW direction and are located on the same NE trending structural belt. The ore bodies are mainly stratiform and tabular, and mainly occur in the 3rd and 4th sub members of Saihan formation of Lower Cretaceous.

The study on the occurrence state of uranium is to analyze the occurrence form, association type and relationship with other landmark minerals of uranium minerals in rocks. It is of great significance to trace the metallogenic process, establish prospecting indicators and develop and utilize the deposit. The research on the occurrence state of uranium in sandstone type uranium deposits is not only of theoretical significance but also of practical value. In addition to understanding the formation mechanism of uranium minerals and the formation environment of the deposit, it can also provide important basis for future uranium mining (Yang, 2021). In the study of the occurrence of uranium, the methods of alpha track etching, electron probe and scanning electron microscope are often used. Alpha track etching can be used to study the distribution and existing forms of uranium in ores. Electron probe (EPMA)

and scanning electron microscope (SEM) can further determine the types of uranium minerals and the occurrence characteristics of uranium (Yang, 2021).

Taking the occurrence state of uranium in several uranium deposits in Erlian Basin as the research object, this paper analyzes and discusses the occurrence state of uranium minerals, the spatial location of uranium deposits, the shape of ore bodies and the provenance of uranium deposits in Erlian Basin. Based on the analysis and summary of uranium minerals in the Bayanwula deposit, it is shown that the deposit has three types of uranium minerals: adsorbed uranium, independent uranium minerals and uranium bearing minerals. Among them, the adsorbents of uranium are mainly clay minerals, organic carbon and colloidal pyrite. The main types of independent uranium minerals are pitchblende, coffinite and uranothorite. Uranium-bearing minerals are mainly uranium-bearing ilmenite, uranium-bearing anatase and uranium-bearing rare earth minerals (Guo, 2014). In addition, the uranium mineral types of Hadatu deposit, Saihan Gaobi uranium deposit and Manglai uranium deposit are mainly pitchblende, coffinite and ningyoite (Yu, 2019. Hu et al., 2011. Yang, 2021). According to the uranium mineral types and spatial location of the above four deposits, the following conclusions can be drawn:

(1) Pitchblende and coffinite are the main forms of uranium mineral occurrence in several uranium deposits in Erlian Basin. In addition, there are also a small amount of ningyoite and uranothorite.

(2) The spatial positions of different uranium minerals are different: pitchblende mainly occurs near pyrite and

organic matter, which is formed by the multi-stage reduction superposition of pyrite and organic matter. Coffinite is mostly found in quartz crevices and around semi idiomorphic granular pyrite, which is related to the dissolution of quartz under alkaline conditions. Ningyoite is a kind of secondary uranium mineral, which fills pyrite fissures in the form of stockwork and fiber, and is the result of later fluid transformation; Uranothorite mostly occurs along the edge of pyrite, and also occurs in quartz or feldspar.

(3) Uranium minerals are mostly found in the vicinity and fissure of pyrite. The main mineral associated with uranium minerals in each deposit is pyrite.

**Keywords:** Erlian Basin; Uranium deposits; Occurrence form of uranium minerals; Pitchblende; Coffinite

This research was sponsored by the National Natural Science Foundation Program of China (42173072, U1967207), and Everest Scientific Research Program (CDUT).

## References:

- Guo, H W., 2014. Study on metallogenic characteristics and metallogenic regularity of Bayanwula uranium deposit, Inner Mongolia. China University of Geosciences (Beijing).
- Hu, J J., Fengjun Nie, et al., 2011. Study on occurrence state of sandstone type uranium deposit in Saihan Gaobi area, Erlian Basin. *Mining Technology*. 11(2): 35-37.
- Nie, F J., 2015. Segmentation and uranium mineralization of Saihan formation of sandstone type uranium deposit in Erlian Basin, Inner Mongolia. *Geological Bulletin*. 34(10): 1952-1963.
- Yang, C G., 2021. Petrogeochemical characteristics and genesis of Manglai uranium deposit in Erlian Basin. Donghua University of Technology.
- Yu, Y C., 2019. Characteristics and mineralization of sandstone type uranium deposit in Hadatau area, Erlian Basin. Donghua University of Technology.

# Latest Cambrian stage of metamorphism in the Aktyuz high-pressure Complex (North Tien Shan; western part of the Central Asian Orogenic Belt): evidence from migmatized garnet-mica gneisses

Anfisa V. Skoblenko (Pilitsyna), Nadezhda A. Kanygina

Geological Institute, Russian Academy of Sciences, Pyzhevsky lane, 7a, Moscow, Russia

In the structure of the western part of the Central Asian Orogenic Belt (CAOB), which encompasses Kazakhstan, Tien Shan and NW China, numerous large blocks with Precambrian crustal complexes are distributed among the Early Palaeozoic accretionary wedge and island arc formations along with the different parts of ophiolitic suites (Degtyarev et al., 2017). The blocks are referred to the Precambrian terranes, which represent varisized tectonic blocks up to 2600 km long, comprised by mostly Mesoproterozoic and Neoproterozoic metamagmatic and metasedimentary formations, in some cases Early Precambrian complexes are exposed. Thus, in the SW part of the west CAOB Precambrian crustal metamorphic formations represented by mostly orthogneisses and metarhyolites, are recognized within the Chu-Kendykta, Zheltau and Issyk-Kul (North Tien Shan) terranes, and make up the basement of the indicated terranes (Skoblenko et al., 2022). The Precambrian formations are overlain by weakly metamorphosed sedimentary cover, an accumulation of which occurred in the Ediacaran-Cambrian. Moreover, the presence of high- and ultrahigh-pressure metamorphic formations, namely, eclogites associated with garnet-bearing gneisses and schists, are discriminative for the studied area. The rocks are believed to have been formed through the subduction of different slices of Precambrian crust of the terranes up to depths exceeding 60 km in the Early Palaeozoic (Cambrian-to-Early Ordovician), and following exhumation of the high-pressure varieties to the upper horizons of the crust. In the SW part of west CAOB such complexes are distinguished within the Zheltau (Anrakhai Block), Issyk-Kul (Makbal Block) and Chu-Kendykta (Aktyuz Block) terranes.

The eclogites of the Aktyuz Block are known from the

cognominal Aktyuz Complex, where these are thought to represent strongly metamorphosed and ductilely deformed gabbroic dyke swarm emplaced within the continental crust prior to metamorphism (Kröner et al., 2012). In turn, the Sm-Nd and Lu-Hf garnet isochron age estimate of 474 Ma obtained for the eclogites, is considered to constrain the timing of the high-pressure metamorphism occurrence in the rocks (Rojas-Agramonte et al., 2013). However, the age estimate, characterizing the timing of metamorphic transformations in the widespread garnet-bearing gneisses enclosing the eclogites, has remained unknown so far. This significantly complicated a conduction of regional correlations for the studied area, especially with respect to the Early Paleozoic evolution of the Chu-Kendykta and adjacent terranes.

Among the metamorphic crustal formations of the Aktyuz Block in the SE part of the Chu-Kendykta terrane crustal formations including garnet-bearing orthogneisses and gneissic granites of the Aktyuz Complex, garnet-bearing ortho- and paragneisses of the Kemin Complex and paragneisses with schists of the Kokdzhon Complex, are distinguished. The gneisses of the Aktyuz and Kemin Complexes associated with intensively retrogressed eclogites, are referred to felsic granulites, which likely experienced the high-pressure metamorphism and partial melting under eclogite facies conditions (Orozbaev et al., 2010). The garnet-mica gneisses of the Aktyuz Complex contain two populations of zircons, which constrain two age clusters of ca. 844 Ma and ca. 490 Ma, respectively, which likely characterize two stages of the rocks' evolution in the late Neoproterozoic (emplacement of the gneisses' protoliths) and in the latest Cambrian (high-pressure metamorphism of the gneisses' protoliths). The protoliths of

the eclogite-bearing gneisses apparently comprised the basement of the Chu-Kendyktas terrane and then underwent metamorphic transformations in the Early Palaeozoic. Within the frames of the conducted investigations the latest Cambrian (ca. 490 Ma) stage of metamorphic evolution of the high-pressure complexes in the Aktyuz Block has been first ascertained.

Detrital zircons from the metasedimentary formations of the Kokdzhon and Kemin Complexes of the Aktyuz Block display the main age peaks at 600, 800, 1000 Ma and weaker peaks at ~1.5 and 2.5 Ga. Protoliths of the rocks were represented by terrigenous lithologies formed after eroded felsic complexes of mostly Ediacaran, late Neoproterozoic, Mesoproterozoic and Palaeoproterozoic-to-Neoproterozoic ages, accumulated during the Cambrian. The rocks likely made up sedimentary cover of the Chu-Kendyktas terrane and constituted the sand-siltstone-shale series. The presence of varisized rims of 495–471 Ma in detrital zircons of the metasedimentary formations is interpreted to have been related to the near-peak-to-retrograde stages of the latest Cambrian-Middle Ordovician metamorphic evolution of the rocks. The obtained age estimates for the

crustal complexes of the Aktyuz block correlate well with those of the similar complexes known from the adjacent Issyk-Kul (North Tien Shan) terrane (Makbal Complex) and Zheltau terrane (Southern Kazakhstan) in the SW part of the CAOB.

The study was supported by RSF (Grant 21-77-00055).

#### References:

- Degtyarev, K., Yakubchuk, A., Tretyakov, A., Kotov, A., Kovach, V., 2017. Precambrian geology of the Kazakh Uplands and Tien Shan: an overview. *Gondwana Res.* 47, 44–75.
- Orozbaev R.T., Takasu A., Bakirov A.B. Sakiev K.S., 2010. Metamorphic history of eclogites and country rock gneisses in the Aktyuz area, Northern Tien-Shan, Kyrgyzstan: a record from initiation of subduction through to oceanic closure by continent-continent collision. *Journal of Metamorphic Geology.* 28, 317–339.
- Skoblenko, A.V., Degtyarev, K.E., Kanygina, N.A., Pang, K.-N., Lee, H.-Y., 2022. Precambrian and Early Palaeozoic metamorphic complexes in the SW part of the Central Asian Orogenic Belt: Ages, compositions, regional correlations and tectonic affinities. *Gondwana Research.* 105, 117-142.

## Key factors affecting hydrocarbon accumulation in ancient dolomite gas reservoirs of Xixiangchi Formation (southern Sichuan Basin, China)

Wei Luo<sup>1,2\*</sup>, Zejin Shi<sup>1,2</sup>, Xiuquan Hu<sup>1,2</sup>, Dianguang Zang<sup>3</sup>, Wenzhi Wang<sup>4</sup>

<sup>1</sup>College of Energy, Chengdu University of Technology, Chengdu 610059, China

<sup>2</sup>State Key Laboratory of Oil and Gas Reservoir Geology and Exploitation, Chengdu University of Technology, Chengdu 610059, China

<sup>3</sup>BGP Southwest Geophysical Research Institute, CNPC, Chengdu 610051, China

<sup>4</sup>Exploration and Development Research Institute, PetroChina Southwest Oil and Gas Field Company, Chengdu 610096, China

\*Corresponding author; Email: [weelo515@163.com](mailto:weelo515@163.com)

The Upper Cambrian Xixiangchi Formation in the southern Sichuan Basin, China, has favorable hydrocarbon accumulation conditions. The accumulation factors and enrichment conditions of this formation were key considerations in this study. By analyzing core, thin section, seismic, and geochemical data, we demonstrate that the granular and crystalline dolomite in the Xixiangchi Formation are characterized by vertical, overlapping development and low single-reservoir thickness. During the transformation of karst and tectonism, dissolution pores and fractures developed to form an ideal reservoir space. The reservoir of the Xixiangchi Formation is connected to the Lower Cambrian source rock through a fault system. The high-energy shoal facies of the Xixiangchi Formation are located on the oil and

gas migration path, providing an appropriate reservoir space for forming the source reservoir configuration relationship between the lower generation and upper reservoir. The key factors affecting hydrocarbon accumulation in the Xixiangchi Formation are sufficient oil and gas supply, development of inherited paleo-uplift, effective transportation system, and favorable reservoir-forming combination. The inherited paleo-uplift controls the distribution of gas reservoirs. Owing to the short migration distance of oil and gas, they are found near source hydrocarbon accumulation, and the paleo-uplift slope area should be targeted for exploration in future studies.

**Keywords:** Xixiangchi Formation; Sichuan Basin; Hydrocarbon accumulation; Dolomite gas reservoir; Paleo-uplift.

# Trondhjemites and their Implications for Neoproterozoic crustal growth in the Qianxi Complex, North China Craton

Ming-Xian Wang<sup>1</sup>, M. Santosh<sup>1,2</sup>, Cheng-Xue Yang<sup>1,3</sup>, Yirang Jang<sup>4</sup>, Bing Yu<sup>1</sup>, Pin Gao<sup>1</sup>

<sup>1</sup> School of Earth Sciences and Resources, China University of Geosciences Beijing, Beijing, China

<sup>2</sup> Department of Earth Science, University of Adelaide, Adelaide, South Australia, Australia

<sup>3</sup> Institute of Earth Sciences, China University of Geosciences Beijing, Beijing, China

<sup>4</sup> Department of Earth and Environmental Science, Chonnam National University, Gwangju, Republic of Korea

\*Corresponding author e-mail: [santosh@cugb.edu.cn](mailto:santosh@cugb.edu.cn)

Tonalite-trondhjemite-granodiorite (TTG) rock suites form a major component of Archean continental crust. It is important to do detailed research about their timing of formation and petrogenetic evolution to understand the growth of continents in the Early Earth. Here we investigate trondhjemites with the associated amphibolite from the Qianxi Complex in the North China Craton and present petrological, geochemical and zircon U-Pb, REE and Lu-Hf data to understand the timing of their formation and petrogenetic history. The trondhjemites in our study show typical Na-rich features as other Archean TTG rocks and high Al content. According to the geochemical characteristics of these rocks, trondhjemites in this study are derived from a subduction-related hydrous basalt. The zircon grains from the trondhjemite samples together with the associated amphibolite show a peak  $^{207}\text{Pb}/^{206}\text{Pb}$  age around 2515 Ma representing the timing of the protolith formation with a followed metamorphic

age of 2451-2490 Ma suggesting the assembly of the microblocks in the NCC. On the basis of the geochemical characteristics and zircon age data presented in this study, in conjunction with those in previous studies from the Qianxi Complex, the subduction-related arc building occurred dominantly during 2.6-2.5 Ga. The Lu-Hf isotope data from zircon grains in the trondhjemite and amphibolite samples of this study display dominantly positive  $\epsilon_{\text{Hf}}(t)$  values, indicating juvenile components feature. Concluded from our new results together with the data reported in earlier researches, a major crust-building event through multiple magmatism during Neoproterozoic existed and active subduction might have initiated in the late Mesoproterozoic, with the peak of magmatism during 2.6-2.5 Ga, followed by metamorphism at ca. 2.45-2.49 Ga.

**Keywords:** Neoproterozoic TTG; Early crustal growth; Qianxi Complex; North China Craton.

# Carbon in orogenic belts: Sink or source for atmospheric CO<sub>2</sub> fluctuations?

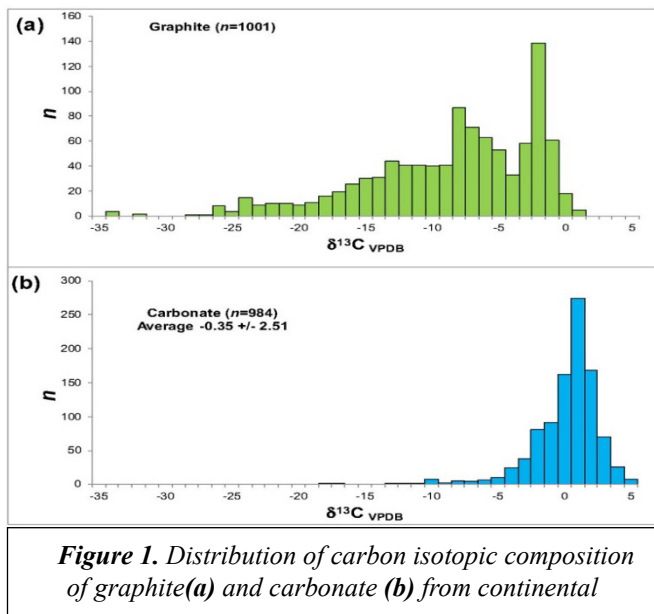
M. Satish-Kumar

(Department of Geology, Faculty of Science, Niigata University, 2-8050 Ikarashi, Nishi-ku, Niigata 950-2181, Niigata Japan)

Global warming and climate fluctuations, largely controlled by greenhouse gases such as CO<sub>2</sub> and CH<sub>4</sub> in the atmosphere, are subjects of prime importance to human beings. Carbon and its geodynamic cycle not only in the surface, but also in the tectonically active convergent margins play significant roles in controlling the Earth's carbon budget, ever since the biological process became active in the surface. Organic carbon and carbonate carbon are two key reservoirs that can act as a source or sink for carbon at convergent margins during plate subduction, arc magmatism and continent building processes. Therefore, it is important to understand the movement of carbon through different reservoirs in the Earth, in particular relating to the global tectonic activities at convergent margins. A recent study on Earth's tectonic carbon conveyor belt quantified the fluxes into and out of all reservoirs in the deep oceanic carbon cycle over past 250 million years and provided boundary conditions for future carbon cycle models (Muller et al., 2022). However, a quantitative evaluation of carbon at continental collision zone is still not clear yet. Here I present a comprehensive synthesis on the forms of carbon, its movement among various reservoirs in the East African Antarctic Orogen (EAAO) by utilizing the carbon isotopic composition as a proxy. The results suggest that large volumes of carbon can be stored in the middle to lower continental crust in the form of graphitic carbon and carbonate carbon, as long-term sinks. Examples from metasedimentary rocks from Antarctica, Sri Lanka, India and Madagascar are used to demonstrate that continental collision zones across the globe can, in fact, act as carbon sinks for hundreds of millions of years or even for billions of years, if the continental crust remain tectonically stable.

Carbonate carbon is an important reservoir in the continental crust. It has attained specific attention and significance in recent decades and research focusing on carbon

sequestration of various crustal rocks has gained momentum. Natural examples of carbonation of crustal rocks show how carbonation progress in various environments such as during serpentinization of mantle rocks (e.g., Okamoto et al., 2021). However, pure sedimentary carbonate rocks trapped in orogenic belts are also of key importance, since they remain stable as metacarbonate rocks for longer time scales, even after subjected to moderate to ultra-high temperature metamorphism (e.g., Satish-Kumar et al., 2001, 2002, 2011a, 2021). Decarbonation reactions can release a portion of carbon as CO<sub>2</sub>, however the volume is limited, depending on the silicate impurities, especially hydrous minerals as detrital components. A comprehensive compilation of carbon and oxygen isotopic composition of orogenic metacarbonate rocks in EAAO, as illustrated in Figure 1a, served as prima-facie evidence on the minimal effect of decarbonation and CO<sub>2</sub> release from carbonate rocks during orogenesis. Thus, pure carbonate rocks in orogenic belts act as long-term sinks.



Graphite, the purest form of carbon in collisional orogenic belts, is an important reservoir of carbon in continental crust. Extensive studies on graphite occurrence were carried out in a variety of rock types in the continental collision zones. Based on the mode of occurrence, they were classified into three types, disseminate flakes, coarse aggregates and as veins. In addition, formation of graphite and its concentration is also observed along the contact zones between different lithologies (e.g., Satish-Kumar and Santosh, 1998). To understand the source and movement of carbon, the carbon isotope fractionation between carbonate minerals, graphite and carbon-bearing fluids ( $\text{CO}_2$  or  $\text{CH}_4$ ) during metamorphism need to be quantified (Farquhar and Chacko, 1991, Satish-Kumar et al., 1998, 2002; Santosh et al., 2003; Satish-Kumar, 2000, 2005). For example, various carbon-bearing phases at the Skallvikshalsen locality in the Lützow Holm Complex, East Antarctica all forms of carbon are observed in a single outcrop scale and thereby movement of carbon within the crust could be traced clearly. Carbon isotopic composition of graphite and associated metacarbonate rocks suggest that they are consistent with graphite precipitation from  $\text{CO}_2$  fluids locally released through decarbonation reactions.

Vein-type graphite, such as those extensively studied in Sri Lanka, can also act as a reservoir of carbon. They form thick, extensive and huge deposits of highly crystalline graphite precipitated from fluids, supposed to have released from mantle derived magma (Touret et al., 2019). The  $\text{CO}_2$ -rich fluids, observed in quartz pods within the graphite veins, record compositional characteristics of fluids that deposited graphite veins. Carbon isotopic composition of graphite even in meter thick veins, remain constant across and along the veins, suggesting open system precipitation (Touzain et al., 2010).

Across the regimes of high-temperature metamorphism and

partial melting of graphite-bearing rocks graphite dissolves to form COH fluids, part of which, especially the lighter isotope-bearing fluids, escape the system causing a bulk  $^{13}\text{C}$  enrichment. Based on field, textural and carbon isotope evidence, from a typical example from the Kerala Khondalite Belt, southern Indian granulite terrane, during biotite dehydration melting of graphite-bearing rocks graphite dissolution is enhanced by  $\text{Fe}^{3+}$  reduction, however during melt crystallization graphite will reprecipitate, resulting in carbon remobilization and carbon isotope reorganization (Satish-Kumar et al., 2011b). Thus, carbon is recycled and retained as graphite in the continental crust during high-grade metamorphism and anatexis, though its isotopic composition can be considerably modified.

A comprehensive review of carbon isotopic composition of graphite (Fig. 1b) and carbonate rocks in continental collision zone revealed the role of recycling in continental crust during orogenesis. A detailed review on the movement of carbon from a carbon isotope perspective will be presented to understand the role of carbonate and graphite as "long-term sinks" of carbon during orogenesis.

#### References:

- Farquhar, J., Chacko, T., 1991. Isotopic evidence for involvement of  $\text{CO}_2$ -bearing magmas in granulite formation. *Nature*, 354, 60–63.
- Muller, R.D., Mather, B., Dutkiewicz, A., Keller, T., Merdith, A., Gonzalez, C.M., Gorczyk, W., Zahirovic, S., 2022. Evolution of Earth's tectonic carbon conveyor belt. *Nature*, 605, 629–639.
- Okamoto, A., Oyanagi, R., Yoshida, K., Uno, M., Satish-Kumar, M., 2021. Rupture of wet mantle wedge by self-promoting carbonation. *Comm. Earth Environ.*, 2, 151, DOI: 10.1038/s43247-021-00224-5
- Satish-Kumar, M., 2005. Graphite-bearing  $\text{CO}_2$ -fluid inclusions in granulites: Insights on graphite precipitation and carbon isotope evolution *Geochim. Cosmochim. Acta*, 69, 3841–3856.
- Satish-Kumar, M., 2000. Ultrahigh-temperature metamorphism in Madurai granulites, Southern India: Evidence from carbon isotope thermometry. *J. Geol.*, 108, 479–486.
- Satish-Kumar, M., Wada, H., 2000. Carbon isotopic equilibrium between calcite and graphite in Skallen marbles, East Antarctica: Evidence for preservation of peak metamorphic temperatures. *Chem. Geol.*, 166, 172–183.
- Satish-Kumar, M., Hermann, J., Miyamoto, T., Osanai, Y., 2010. Fingerprinting a multistage metamorphic fluid–rock history: Evidence from grain scale Sr, O and C isotopic and trace element variations in high-grade marbles from East Antarctica. *Lithos*, 114, 217–228.
- Satish-Kumar, M., Hokada, T., Owada, M., Osanai, Y., Shiraishi, K., 2013. Neoproterozoic orogens amalgamating East Gondwana: Did they cross each other? *Precambrian Res.*, 234, 1–7.
- Satish-Kumar, M., Jaszczak, J.A., Hamamatsu, T., Wada, H., 2011b. Relationship between structure, morphology and carbon isotopic composition of graphite in marbles: Implications for calcite-graphite carbon isotope thermometry.

- Amer. Mineral., 96, 470–485.
- Satish-Kumar, M., Santosh, M., 1998. A petrological and fluid inclusion study of calc-silicate – charnockite associations from southern Kerala, India: implications for CO<sub>2</sub> influx. *Geol. Mag.*, 135, 27–45.
- Satish-Kumar, M., Shirakawa, M., Imura, A., Otsuji-Makino, N., Imanaka-Nohara, R., Malaviarachchi, S.P.K., Fitzsimons, I.C.W., Sajeev, K., Grantham, G.H., Windley, B.F., Hokada, T., Takahashi, T., Shimoda, G., Goto, K.T., 2021. A geochemical and isotopic perspective on tectonic setting and depositional environment of Precambrian meta-carbonate rocks in collisional orogenic belts. *Gondwana Res.*, DOI: 10.1016/j.gr.2021.03.013
- Satish-Kumar, M., Wada, H., Santosh, M., 2002. Constraints on the application of carbon isotope thermometry in high- to ultrahigh-temperature metamorphic terranes. *J. Metamorph. Geol.*, 20, 335–350.
- Satish-Kumar, M., Wada, H., Santosh, M., Yoshida, M., 2001. Fluid-rock history of granulite facies humite-marbles from Ambasamudram, southern India. *J. Metamorph. Geol.*, 19, 395–410.
- Satish-Kumar, M., Yoshida, M., Wada, H., Niitsuma, N., Santosh, M., 1998. Fluid flow along microfractures in calcite from a marble from East Antarctica: Evidence from gigantic (21 per mil) oxygen isotopic zonation. *Geology*, 26, 251–254.
- Satish-Kumar, M., Yurimoto, H., Itoh, S., Cesare B., 2011a. Carbon isotope anatomy of a single graphite crystal in a metapelitic migmatite revealed by high-spatial resolution SIMS analysis *Contrib. Mineral. Petrol.*, 162, 821–834.
- Touret, J.L.R., Huizenga, J.M., Kehelpannala, K.V.W., Piccoli, F., 2019. Vein-type graphite deposits in Sri Lanka: The ultimate fate of granulite fluids. *Chem. Geol.*, 508, 167–181.
- Touzain, P., Balasooriya, N., Bandaranayake, K., Descolas-Gros, C., 2010. Vein graphite from the Bogala and Kahatagaha-Kolongaha mines, Sri Lanka: A possible origin. *The Can. Mineral.*, 48, 1373–1384.

# Ultrahigh-temperature granulites from southern India: multi-stage metamorphism during Gondwana assembly

Bing Yu<sup>1</sup>, M. Santosh<sup>1,2\*</sup>, Toshiaki Tsunogae<sup>3,4</sup>, Cheng-Xue Yang<sup>1</sup>, Sung Won Kim<sup>5</sup>

<sup>1</sup>School of Earth Sciences and Resources, China University of Geosciences Beijing, No. 29 Xueyuan Road, Haidian District, Beijing 100083, China

<sup>2</sup>Department of Earth Science, University of Adelaide, Adelaide SA 5005, Australia

<sup>3</sup>Graduate School of Life and Environmental Sciences (Earth Evolution Sciences), University of Tsukuba, Ibaraki 305-8572, Japan

<sup>4</sup>Department of Geology, University of Johannesburg, Auckland Park 2006, South Africa

<sup>5</sup>Geological Research Division, Korea Institute of Geoscience and Mineral Resources, Daejeon 34132, Republic of Korea

\*E-mail:santosh@cugb.edu.cn

The Southern Granulite Terrane (SGT) in India is well known for granulite facies rocks metamorphosed at ultra-high temperature (UHT) conditions in the various crustal blocks as well as within the Palghat-Cauvery Suture Zone (PCSZ) which is considered as a trace of the Late Neoproterozoic - Cambrian Gondwana suture. A suite of Mg-Al-rich UHT granulites from the northern margin of the Madurai Block adjacent to the PCSZ records unique mineral assemblage and multi-stage metamorphism. Deformed Mg-Al-rich layers, lenses, and boudins of various dimensions occur within the regional gneisses, detailed petrological and mineralogical studies as well as zircon and monazite U-Pb geochronology show two distinct tectono-thermal cycles. Early-stage metamorphism was identified to be represented by sodic gedrite + kyanite indicating high-pressure prograde stage assemblage, followed by sillimanite-garnet-orthopyroxene that formed during pressure decrease and temperature increase. The rare remnant gedrite is also stable at the near-peak UHT metamorphism until it was replaced by sapphirine. The rocks subsequently underwent decompression that formed sapphirine + cordierite and sapphirine + plagioclase symplectite around sillimanite. Dehydration during decompression generated orthopyroxene-sillimanite-quartz assemblage with the appearance of

sapphirine, defining the diagnostic mineral assemblage indicative of peak UHT metamorphism ( $T > 900$  °C) at relatively high-pressure ( $P > 9$  kbar). The UHT peak metamorphism in this region is consistent with the results of P-T calculations using conventional geothermometers and phase equilibrium modeling ( $T$  up to 1050 °C,  $P$  over 12 kbar). Abundant gedrite and plagioclase megacrysts formed during the influx of hydrous fluids that overprinted part of the early metamorphic features. Detrital zircon grains in the metasediments indicate protolith ages of ca. 2.5 Ga and the metamorphic overgrowths yield  $^{206}\text{Pb}/^{238}\text{U}$  mean ages concentrated at ca. 550-520 Ma. Monazite ages define another younger group  $^{206}\text{Pb}/^{238}\text{U}$  mean ages at ca. 450 Ma. The prograde high-pressure granulite-facies metamorphism and the following UHT event correlate with the subduction-collision tectonics at 550-500 Ma associated with the final stage of amalgamation of the Gondwana supercontinent, while the 420-460 Ma monazite age might represent hydration at the post-orogenic stage, possibly associated with deep shearing and fluid influx.

**Keywords:** Mg-Al granulite; Ultrahigh-temperature metamorphism; Zircon and monazite Geochronology; Gondwana supercontinent.

# Generation of crystal-rich erupted products by fluid-driven crystal-mush remobilization: Perspective from the Nageng (sub-)volcanic complex, East Kunlun Orogen, NW China

Xiao-Dong Chen <sup>1\*</sup>, Bin Li <sup>2</sup>

<sup>1</sup> Department of Earth and Space Sciences, Southern University of Science and Technology, Shenzhen 518055, Guangdong, China  
<sup>2</sup> Key Laboratory of Metallogenic Prediction of Nonferrous Metals and Geological Environment Monitoring (Ministry of Education), School of Geosciences and Info-Physics, Central South University, Changsha, Hunan 410083, China

Corresponding author email: [wskjatatjiily@gmail.com](mailto:wskjatatjiily@gmail.com)

Remobilization of upper crustal crystal-rich magma reservoirs (“crystal mush”) following melt extraction has been widely invoked in the formation of crystal-rich erupted products. However, the melt storage duration and conditions, and the pre-eruptive magma chamber processes remain poorly understood. Here, we present new whole-rock elemental and Sr-Nd-Pb isotope data, and zircon U-Pb-Hf isotope and trace element data of the Nageng (sub-)volcanic complex in the East Kunlun Orogen of NW China. This complex consists of the highly-evolved (high SiO<sub>2</sub>, Rb/Sr) crystal-poor rhyolite and less-evolved crystal-rich rhyodacite and dacite porphyry. These rock types are genetically linked, based on their similar chondrite-normalized REE patterns and Nd-Hf isotopes, and their linear trends of <sup>208</sup>Pb/<sup>204</sup>Pb and <sup>207</sup>Pb/<sup>204</sup>Pb vs. <sup>206</sup>Pb/<sup>204</sup>Pb. Their depleted whole-rock ε<sub>Nd</sub>(t) (-9.74 to -7.37) and zircon ε<sub>Hf</sub>(t) (-7.16 to -3.48) values, together with their Proterozoic two-stage Hf model ages (1707–1474 Ma), are indicative of an ancient lower crustal magma source. The overlapping zircon ages but distinct composition (74–80 vs. 60–66 wt.% SiO<sub>2</sub>) and crystallinity (~5 vs. 30–40 vol.%) between crystal-poor rhyolite and dacite porphyry can be explained by melt

extraction from the crystal mush zone. The lack of resorption textures and large age interval (~8 Myr) between zircon cores (ca. 228 Ma) and rims (ca. 220 Ma) indicate that the crystal mush remained partially molten for protracted duration. The melt storage condition was constrained by Ti-in-zircon thermometry to low-temperature, around the granitic solidus (650–700°C). The crystal-rich nature but negative Eu anomalies suggest that the dacite porphyry was formed in the roof zone (solidification front) of the crystal mush. The occurrence of resorbed zircon cores (ca. 220 Ma) overgrown by much younger rims (ca. 213 Ma) for crystal-rich rhyodacite demonstrates the long-term rejuvenation of a semi-solidified crystal mush. The similar zircon core-rim Ti contents and Th/U, Yb/Gd, Zr/Hf ratios preclude that the crystal mush was rejuvenated by hotter, more mafic magmas. However, the widespread fluorite-rich magmatic-hydrothermal veining, combined with the reduced nature (indicated by the zircon Ce<sup>4+</sup>/Ce<sup>3+</sup> drop from core to rim) of the crystal-rich rhyodacite, imply that the volatile-rich fluid influx may have been important in reactivating the crystal-mush for later crystal-rich rhyodacite eruption.

# Reconstructing the Lancang Terrane (SW Yunnan) and implications for early Paleozoic Proto-Tethys evolution at the northern margin of Gondwana

Yuehua Wei<sup>a</sup>, Jian-Wei Zi<sup>a,d\*</sup>, Guichun Liu<sup>b,c</sup>

<sup>a</sup> State Key Laboratory of Geological Processes and Mineral Resources, China University of Geosciences, Wuhan 430074, China

<sup>b</sup> Faculty of Land Resource Engineering, Kunming University of Science and Technology, Kunming 650093, China

<sup>c</sup> Yunnan Institute of Geological Survey, Kunming 650216, China

<sup>d</sup> John de Laeter Centre, Curtin University, Kent Street, Bentley, WA 6102, Australia

The Lancang Group in SW Yunnan constitutes a pivotal component of the continental margin bounding the Proto- and Paleo-Tethys oceans, yet its formation timing, composition and tectonic affinity remain illdefined. In this contribution, we present new zircon U-Pb age and whole-rock geochemistry data from volcanic and sedimentary rock units, which are compiled with published data, to refine the depositional age, provenance and nature of the group and its host terrane. The Lancang Group consists of five formations, two of which (Manlai and Huimin) contain abundant metavolcanic rocks. The metavolcanic rocks show a secular change in geochemistry, from EMORB-like calc-alkaline series of the ca. 495 Ma Manlai Formation, to arc-like high-K series of the Huimin Formation. Five metavolcanic samples from the Huimin Formation yielded zircon U-Pb ages between  $478 \pm 5$  Ma and  $442 \pm 5$  Ma. The late Cambrian-Ordovician arc magmatism is related to an active continental margin setting associated with subduction of the Proto-Tethys Ocean. The time-integrated geochemical variation shown by the volcanic rocks likely reflects evolving maturity of the arc system. The youngest detrital zircon ages of the five formations, in conjunction with age constraints from the interbedded volcanic rocks, suggest that the Lancang Group was largely accumulated during the early Paleozoic. The Lancang Terrane is reconstructed as a continental block, which formed part of the magmatically-active margin of the Proto-Tethys during the early Paleozoic. Provenance analysis based on detrital zircon age spectra and Hf isotope data indicates Gondwana affinities

of the terrane. Furthermore, xenocrystic zircon ages and zircon Hf and whole-rock Nd model ages from igneous rocks support presence of Neoproterozoic-Mesoproterozoic basement underlying the terrane. The reconstructed Lancang Terrane bears important implications for understanding the configuration of the northern margin of Eastern Gondwana and the relationship between the Proto- and Paleo-Tethys oceans (Fig.1).

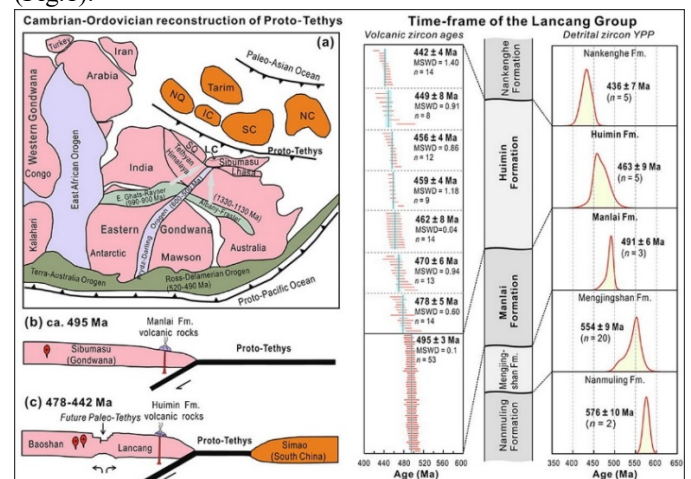


Fig. 1. The Time-frame of the Lancang Group and Cambrian-Ordovician reconstruction of Proto-Tethys

**Keywords:** Lancang Group; Lancang Terrane; Huimin volcanics; early Paleozoic; Proto-Tethys; Gondwana margin.

# Origin of fertile lithospheric mantle beneath eastern North China Craton: Combined effects from melt impregnation and asthenospheric cooling

Lei-Tao Cao<sup>a</sup>, Jian-Ping Zheng<sup>a,b\*</sup>, Hong-Kun Dai<sup>b\*</sup>

<sup>a</sup> School of Earth Sciences, China University of Geosciences, Wuhan 430074, China

<sup>b</sup> State Key Laboratory of Geological Processes and Mineral Resources, China University of Geosciences, Wuhan 430074, China

\* Corresponding authors: Dr. Jianping Zheng ([jpzheng@cug.edu.cn](mailto:jpzheng@cug.edu.cn)), Dr. Hongkun Dai ([hkdai@cug.edu.cn](mailto:hkdai@cug.edu.cn))

The eastern North China Craton (NCC) is known for replacement of refractory lithospheric mantle by fertile ones relevant to the (Paleo-) Pacific subduction, yet origin of the fertile domains remains enigmatic, leaving behind incomplete picture on the complex lithosphere-asthenosphere interaction. To explore these dynamic processes, we present petrology, mineral major-, trace-element and in-situ Sr isotopic data on spinel peridotite xenoliths entrained by the Qingyuan Cenozoic basalt in the eastern NCC.

The xenoliths are of two groups based on textural characteristics and mineral compositions. Group A consist of amphibole-bearing lherzolites with melt pockets. They have low olivine Fo ( $\leq 89$ ) and mineral major-element compositions deviating from residual mantle. The clinopyroxenes and coexisting amphibole outside the melt pockets have light rare earth element (LREE)-enriched patterns and comparable  $^{87}\text{Sr}/^{86}\text{Sr}$  ratios (0.7035-0.7039 and 0.7029-0.7033, respectively). The melt pocket-hosted clinopyroxenes also exhibit LREE-enriched patterns but elevated  $^{87}\text{Sr}/^{86}\text{Sr}$  ratios (0.7040-0.7062). These characteristics suggest that Group A peridotites are fragments of a refertilized lithospheric mantle

recording strong asthenospheric melt impregnation with subducted components. In contrast, Group B xenoliths, typically lherzolites, harzburgites and minor dunites, contain no amphibole and melt pockets. They have high Fo ( $\sim 90-91$ ) and their mineral major-element compositions resemble those of melting residua. The clinopyroxenes, displaying variably enriched LREE patterns with  $^{87}\text{Sr}/^{86}\text{Sr}$  ratios of 0.7020-0.7044, may be the result from cryptic metasomatism in post-Late Cretaceous according to modeling results on Th diffusion. These collectively suggest the presence of fertile mantle accretion with weak metasomatism. The related melting is shown to occur at potential temperatures of 1400-1450 °C typically related to small-scale asthenospheric upwelling.

Together with studies on Cenozoic basalt-borne peridotite xenoliths and tectonic setting in eastern NCC, we can conclude that the fertile lithospheric mantle records combined effects from melt impregnation and asthenospheric cooling. We also propose that the subduction-related small-scale upwelling produces not only refertilized lithospheric mantle with strong metasomatism, but also leaves behind melting residuals with weak metasomatism.

# Long-lived Paleoproterozoic collision process over 150 Myr in the Trans-North China Orogen: insights from metamorphic records in the Fuping Complex

Li Tang <sup>1\*</sup>, M. Santosh <sup>1,2</sup>, Richard M. Palin <sup>3</sup>, Li-Hui Jia <sup>4</sup>, Yuan-Ming Sheng <sup>1</sup>

<sup>1</sup> School of Earth Sciences and Resources, China University of Geosciences Beijing, 29 Xueyuan Road, Beijing 100083, China

<sup>2</sup> Centre for Tectonics, Exploration and Research, University of Adelaide, Adelaide SA 5005, Australia

<sup>3</sup> Department of Earth Sciences, University of Oxford, Oxford OX1 3AN, United Kingdom

<sup>4</sup> State Key Laboratory of Lithospheric Evolution, Institute of Geology and Geophysics, Chinese Academy of Sciences, Beijing 100029, China

Corresponding author email: ltang@cugb.edu.cn

Long-lived collisional orogens that formed over tens to hundreds of millions of years are common in the geological record (Palin et al., 2020). The Trans-North China Orogen (TNCO) marks the collision between the Eastern and Western Blocks of the North China Craton, and preserves metamorphic rocks with ages between 1.98 Ga and 1.80 Ga (Tang et al., 2017; Tang and Santosh, 2018). These units allow detailed assessment of the timescale and duration of crustal thickening, exhumation and cooling associated with a major Proterozoic orogeny (e.g. Zhao and Zhai, 2013; Wei et al., 2014). We present integrated petrography, mineral chemistry, phase equilibria modeling and texturally controlled in situ LA-ICP-MS monazite U-Th-Pb and trace element analyses performed on a suite of orthopyroxene-bearing pelitic granulites and garnet-biotite gneisses from the Fuping Complex within the TNCO. These rocks record clockwise pressure-temperature (P-T) paths involving granulite-facies peak conditions of 9.9-11.0 kbar and 850-880 °C for pelitic granulites, and 10.9-11.6 kbar and 860-880 °C for garnet-biotite gneisses, followed by post-peak decompression to ca. 8-9 kbar and later cooling, with final solidification of melt at <840 °C. Four monazite populations are identified in these samples. Group I grains are irregular and elongated, and occur in contact with or embay garnet. They have high REE and Y contents and metamorphic ages of 1.90-1.86 Ga, which correspond to the breakdown of garnet during post-peak decompression. Most monazite grains crystallized from melt are represented by Groups II+III+IV, and are associated with orthopyroxene, biotite, plagioclase and quartz in the matrix. They have crystallization ages between

1.86 Ga and 1.76 Ga, and have relatively low REE and Y concentrations. These data imply a long-lived (>100 Myr) post-collisional exhumation and cooling involving decompression from 10-12 kbar to ca. 9 kbar during 1.90-1.86 Ga, followed by retrograde cooling from 1.86 to 1.76 Ga under prolonged residence in the middle to lower crust. Initial collision and peak metamorphism occurred before 1.90 Ga, ultimately leading to the final cratonization of the North China Craton and its incorporation into the Columbia supercontinent.

## References:

- Tang, L., Santosh, M., Tsunogae, T., Koizumi, T., Hu, X.K., Teng, X.M., 2017. Petrology, phase equilibria modelling and zircon U-Pb geochronology of Paleoproterozoic mafic granulites from the Fuping Complex, North China Craton. *Journal of Metamorphic Geology* 35, 517-540.
- Tang, L., Santosh, M., 2018. Neoproterozoic-Paleoproterozoic terrane assembly and Wilson cycle in the North China Craton: an overview from the central segment of the Trans-North China Orogen. *Earth-Science Reviews* 182, 1-27.
- Palin, R.M., Santosh, M., Cao, W., Li, S.S., Hernández-Urbe, D., Parsons, A., 2020. Secular metamorphic change and the onset of plate tectonics. *Earth-Science Reviews* 207, 103172.
- Wei, C.J., Qian, J.H., Zhou, X.W., 2014. Paleoproterozoic crustal evolution of the Hengshan-Wutai-Fuping region, North China Craton. *Geoscience Frontiers* 5, 485-497.
- Zhao, G.C., Zhai, M.G., 2013. Lithotectonic elements of Precambrian basement in the North China Craton: review and tectonic implications. *Gondwana Research* 23, 1207-1240.

# Geochronology and geochemistry of the Algoma-type banded iron formation in the Fuping Complex, North China Craton: Implications for Paleoproterozoic metallogeny and tectonic setting

Tao Zeng<sup>1</sup>, Li Tang<sup>1\*</sup>, M. Santosh<sup>1,2</sup>

<sup>1</sup> School of Earth Sciences and Resources, China University of Geosciences Beijing, 29 Xueyuan Road, Beijing 100083, China

<sup>2</sup> Centre for Tectonics, Exploration and Research, University of Adelaide, Adelaide SA 5005, Australia

Corresponding author email: ltang@cugb.edu.cn

Banded iron formations (BIFs) are significant for deciphering the chemical composition of ancient seawater, as well as the Precambrian tectonic setting. Precambrian BIFs deposits are widely distributed in the Archean-Paleoproterozoic greenstone belts of the North China Craton and composed predominantly of Neoproterozoic Algoma-type (ca. 2.55Ga) including those in the Anshan-Benxi and eastern Hebei areas of the northern Eastern Block (Zhai and Santosh, 2011; Li et al., 2020), together with minor Paleoproterozoic Superior-type represented by the Yuanjiacun BIFs in the Lüliang Complex of the Trans-North China orogen (Liu and Yang, 2015; Hou et al., 2017; Lan et al., 2019). The Zhaigou BIF deposit is associated with Paleoproterozoic Wanzi supracrustal sequence in the Fuping Complex, central North China Craton. Here, we present systematic mineralogical, petrological, geochronological and geochemical data of the meta-sedimentary rocks, BIF ores and meta-mafic rocks from the Zhaigou BIF deposit for the first time to constrain the depositional age, origin and tectonic setting of the Paleoproterozoic BIF deposit. The banded iron ores in the Zhaigou deposit are hosted in the Wanzi supracrustal sequence and show close association with amphibolites. Whole-rock geochemical data show the iron ores are enriched in HREE with low  $(La/Yb)_{PAAS}$  values (0.037-0.073), and exhibit positive La (0.898–1.14), Eu (3.34-6.21) and Pr (1.05–1.10) anomalies. The PAAS-normalized REY patterns resemble that of the 1:100 mixture of high-temperature hydrothermal fluid and seawater, indicating the ore-forming materials were derived from the mixture of the two end members. The absence of negative Ce anomaly ( $Ce/Ce^* = 0.81\sim 0.90$ )

indicates an anoxic condition. Most BIF samples have high contents of  $SiO_2$  and  $Fe_2O_3^T$ , relatively low contents of  $Al_2O_3$ ,  $TiO_2$ , and high-field strength elements (e.g., Zr, Hf, Th, U), indicating the less contribution of continental detrital materials to the BIF mineralization. The chondrite-normalized REE patterns of amphibolites are flat with no significant Ce and Eu anomalies, indicating that the protolith of amphibolites was probably basaltic rocks formed in island arc setting. Detrital zircons in biotite gneiss samples show similar age distributions and have dominantly Neoproterozoic ages (ca. 2.76–2.55Ga), suggesting the provenance from the Fuping TTG gneisses. Zircon U-Pb results of BIF ores yield weighted mean  $^{207}Pb/^{206}Pb$  ages of  $2028 \pm 33$  Ma and  $1874 \pm 52$  Ma, which are interpreted to represent the formation age of Zhaigou BIF and the subsequent metamorphic event, respectively. To sum up, the Zhaigou BIF deposit belongs to the Algoma-type which shows close association with the Paleoproterozoic sedimentary sequence and basaltic magmatism in island arc setting during the terrane assembly process in the Trans-North China Orogen.

## References:

- Zhai, M.G., Santosh, M., 2011. The early Precambrian odyssey of the North China Craton: a synoptic overview. *Gondwana Research* 20, 6–25.
- Li, L. X., Zi, J.W., Meng, J., Li, H.M., Birger, R., Stephen, S., Simon, A.W., Li, Y.H., 2020. Using in situ monazite and xenotime U-Pb geochronology to resolve the fate of the “missing” banded iron formation-hosted high-grade hematite ores of the North China Craton. *Economic Geology* 15, 189–204.
- Liu, L., Yang, X.Y., 2015. Temporal, environmental and tectonic

significance of the Huoqiu BIF, southeastern North China Craton: Geochemical and geochronological constraints. *Precambrian Research* 261, 217-233.  
Hou, K.J., Ma, X.D., Li, Y.H., Liu, F., Han, D., 2017. Chronology,

geochemical, Si and Fe isotopic constraints on the origin of Huoqiu banded iron formation (BIF), southeastern margin of the North China Craton. *Precambrian Research* 298, 351-364.

# Distal gold mineralization associated with porphyry system: The case of Hongzhuang and Yuanling deposits, East Qinling, China

Yuan-Ming Sheng<sup>1</sup>, Li Tang<sup>1, 2\*</sup>, Shou-Ting Zhang<sup>1\*</sup>, Yu Zhao<sup>3</sup>, M. Santosh<sup>1, 4</sup>

<sup>1</sup> School of Earth Sciences and Resources & State Key Laboratory of Geological Processes and Mineral Resources, China University of Geosciences Beijing, 29 Xueyuan Road, Beijing 100083, China

<sup>2</sup> Key Laboratory of Tectonic Controlled Mineralization and Oil Reservoir of Ministry of Natural Resources, Chengdu University of Technology, China

<sup>3</sup> China Electronic Information Industry Development Research Institute, Beijing 100081, China

<sup>4</sup> Department of Earth Science, University of Adelaide, Adelaide SA 5005, Australia

Corresponding author: Li Tang (ltang@cugb.edu.cn); Shou-Ting Zhang (zst@cugb.edu.cn)

The East Qinling Metallogenic Belt (EQMB) is a significant mineral resource repository of Au, Mo, W, Pb, Zn and Ag in China, with at least 600t gold reserves (Deng and Wang, 2016; Dong and Santosh, 2016). The Hongzhuang and Yuanling gold deposits are located in the Shiyagou ore field within the Xiong'er shan area, East Qinling, China, where the ore bodies are hosted in Xiong'er Group and mainly controlled by EW-trending and NE-trending faults. The gold mineralization mechanism and the possible genetic link with the porphyry magmatism and hydrothermal events remain unclear. Here we present results from systematic field investigation, petrographic observation, in situ trace elements and sulfur isotope of pyrite to elucidate the genesis of gold mineralization in these deposits. Based on the occurrences of pyrite in different hydrothermal veins, three types of pyrite are identified from each deposit, including: i) coarse-grained cubic pyrite (HZ-Py1 and YL-Py1) in stage I milky quartz vein; ii) medium- to fine-grained pyrite (HZ-Py2 and YL-Py2) in stage II polymetallic sulfides veins; iii) coarse-grained pyrite (HZ-Py3 and YL-Py3) symbiotic with calcite in stage III quartz-calcite vein. The LA-ICP-MS trace element analyses of pyrite show that Au occurs as invisible nanoparticles or nano-sized inclusions in pyrite through absorption-chemisorption during the growth of pyrite or as nano-sized Au-bearing mineral inclusions. The  $\delta^{34}\text{S}$  values of different generations of pyrite in the Hongzhuang and Yuanling gold deposits range from 3.92‰ to 6.43‰ and 2.82‰ to 4.46‰, respectively, indicating that the ore-forming materials were mainly derived from

mantle-related source with affinity to the Late Mesozoic granitic magmatism. The Hongzhuang and Yuanling gold deposits are spatially and temporally correlated with the Shiyagou pluton and they show consistent material sources. We propose that the hydrothermal Au mineralization in these deposits were the distal products generated from the post-magmatic fluids of the Shiyagou porphyry system (Fig. 1). The stretching and thinning of the early Cretaceous lithosphere led to the upwelling of magma and migration of fluid, forming the Au mineralization in fault structures in the shallow crust.

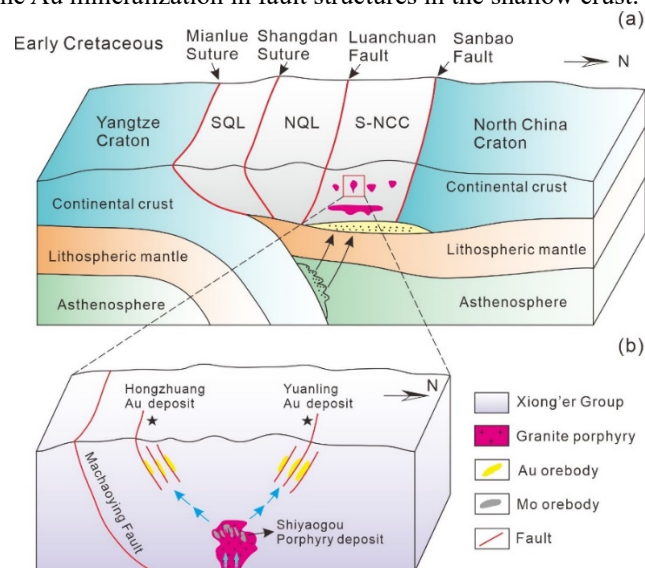


Fig. 1 (a) Schematic tectonic model for the Early Cretaceous

---

of the Qinling orogen; (b) Cartoon showing the Shiyaogou porphyry system and the formation of the Hongzhuang and Yuanling gold deposits.

**References:**

Deng, J., Wang, Q.F., 2016. Gold mineralization in China: Metallogenic provinces, deposit types and tectonic framework.

Gondwana Res. 36, 219-274.

Dong, Y.P., Santosh, M., 2016. Tectonic architecture and multiple orogeny of the Qinling Orogenic Belt, Central China. Gondwana Res. 29, 1-40.

## Origin and evolution of magma and tectonic implication of mafic dykes: The Permian diabases in Santanghu Basin, NW China

Minru Zhao <sup>a</sup>, Xin Jiao <sup>a\*</sup>, Yiqun Liu <sup>a</sup>, Dingwu Zhou <sup>b</sup>, Ziyuan Meng <sup>a</sup>, Yiyao Yang <sup>a</sup>

<sup>a</sup> State Key Laboratory of Continental Dynamics, Department of Geology, Northwest University, Xi'an, Shaanxi, China;

<sup>b</sup> College of Geological Science and Engineering, Shandong University of Science and Technology, Qingdao, Shandong, China

The Permian mafic dykes of Santanghu Basin offer an opportunity to study the nature of mantle source and tectonic setting of basin, as well as to provide the theoretical basis for structural transformation of East Junggar region. In this study, zircon U–Pb geochronology, mineral composition analysis, whole-rock elemental and Sr–Nd isotopic geochemistry were conducted to explore the origin and evolution of the primitive magma. LA-ICPMS zircon U–Pb dating yields ages at 269 Ma. The elemental geochemistry results suggest enrichments in Ba, Pb and Sr but depletions in Nb, Ta, Zr and Hf, which indicate that the magma source was influenced by fluid metasomatism. All samples show moderate initial Sr–Nd isotope results

( $^{87}\text{Sr}/^{86}\text{Sr}$ )<sub>i</sub>=0.704299 to 0.704490 and  $\epsilon_{\text{Nd}}(t) = +6.16$  to  $+6.83$ ) and have high Sm/Yb ratios, which suggest that the diabases were derived from partial melting of 5%–7% spinel-garnet herzolite lithospheric mantle. Combined with petrological, geochronological data and the regional tectonic background, it is interpreted that the diabases from Santanghu Basin originated from lithospheric mantle metasomatized by subduction fluids under the background of intracontinental extension.

**Keywords:** Permian diabases, Santanghu Basin, origin, fluid metasomatism, intracontinental extension

# Neoproterozoic Vertical Tectonism in eastern North China: Structure, Metamorphism and Numerical Modeling

Jian Zhang<sup>1,2</sup>, Chen Zhao<sup>1,2</sup>, Chenying Yu<sup>1,2</sup>, Ting Yang<sup>2</sup>, Guochun Zhao<sup>3</sup>, Peter A. Cawood<sup>4</sup>, Changqing Yin<sup>1,2</sup>, Jiahui Qian<sup>1,2</sup>, Peng Gao<sup>1,2</sup>

<sup>1</sup> School of Earth Sciences and Engineering, Sun Yat-Sen University, China

<sup>2</sup> Southern Marine Science and Engineering Guangdong Laboratory (Zhuhai), China

<sup>3</sup> Department of Earth and Space Sciences, Southern University of Science and Technology, China

<sup>4</sup> Department of Earth Sciences, University of Hong Kong, Hong Kong SAR

<sup>5</sup> School of Earth, Atmosphere and Environment, Monash University, Clayton, Australia

The debate on the role of Vertical versus Horizontal Tectonism in Archean cratons is intimately linked to the initiation time and mechanism of plate tectonics. The dome-and-keel architecture preserved in some Mesoproterozoic and older cratons, such as the Kaapvaal and Pilbara cratons, has an intrinsic relationship with the Vertical Tectonism. Whether such a structural pattern also occurs widely in Neoproterozoic cratons remains poorly constrained. Determining the kinematics, geometry, structural evolution, and the timing of these structures is crucial to understanding the tectonic regime of the early Earth. Our detailed mapping and structural analysis revealed that the eastern North China Craton preserves Neoproterozoic greenstone-granite rock association with typical dome-and-keel structures. Metamorphic data for these rock assemblages record both anticlockwise P–T paths involving near-isobaric cooling (IBC) and clockwise paths with nearly isothermal decompression (ITD) from nearby locations leading to controversial and contradictory interpretations. To resolve the geodynamic process of such a dome-and-keel architecture and the presence of coexisting diverse P–T paths and to place them within a viable geodynamic regime, we conducted 2D thermomechanical numerical models with the initial and boundary conditions similar to that of the Neoproterozoic eastern North China Craton. Our model results reveal that heat transferred from the high-temperature lower boundary and crustal density inversion leads to crustal-scale sagduction that generates the observed

dome-and-keel architecture and results in four major types of P–T–t paths: (1) an anticlockwise IBC-type P–T–t path in which the supracrustal rocks progressively sink to a deep crustal level through sagduction, and experience a long-lived residence followed by ambient mantle cooling without significant exhumation; (2) an clockwise ITD-type P–T–t path where the supracrustal rocks sink to the deep crust and are partly captured by upwelling felsic magmas, resulting in rapid exhumation to a middle crustal level; (3) a newly identified crescent-type P–T–t path that reveals an integrated burial-exhumation cycle characterized by an initial high dT/dP<sub>burial</sub> stage, followed by the rapid exhumation to the upper crust and extensive low dT/dP<sub>cooling</sub>; (4) a hairpin-type P–T–t path in which deeply buried supracrustal rocks experience a slow exhumation rate. The dome-and-keel architecture and P–T–t paths produced by the numerical model conform to the structural, metamorphic and geochronological data of the Eastern Block. We propose that the geological complexity of eastern China and temporally coexisting diverse P–T–t paths most likely developed under a mantle plume-related crustal-scale sagduction geodynamic regime in Neoproterozoic.

## Acknowledgment

This study was financially supported by the National Natural Science Foundation of China (42025204, 41890831), The University of Hong Kong Seed Fund for Basic Research (201811159089), and the Australian Research Council (FL160100168).

# The Triassic lower crust in West Qinling and the strict dichotomy of the Qinling–Dabie Orogen

Thomas Bader<sup>1,2,\*</sup>, Lifei Zhang<sup>1</sup>, Xiaowei Li<sup>2</sup>

<sup>1</sup> Key Laboratory of Orogenic Belts and Crustal Evolution, MOE, School of Earth and Space Science, Peking University, Beijing 100871, P. R. China, thomas.bader@pku.edu.cn

<sup>2</sup> State Key Laboratory of Geological Processes and Mineral Resources and School of Earth Sciences and Resources, China University of Geosciences, Beijing 100083, P. R. China

Immanent to the east–west stretching Qinling–Tongbai–Hong’an–Dabie–Sulu Orogen welding North and South China is a strict lateral dichotomy: voluminous granitoids (255–195 Ma; Hu et al., 2020) crop out almost exclusively in West Qinling, while the exhumation of (ultra)high-pressure [(U)HP] eclogites (254–220 Ma; Zhang et al., 2009) is restricted to Hong’an–Dabie–Sulu in the east. Based on paleomagnetic data, igneous petrogenesis, sedimentology, and structural analysis, the literature discusses manifold reasons for the dichotomy: the rotation of North with respect to South China, oblique continental convergence with scissor-like closure of the Mianlüe Ocean, west-ward propagation of the slab break-off to shallower levels, and orogen-parallel rheological differences.

The metamorphism in the hanging-wall plate is an excellent recorder of orogenic processes but it could hitherto hardly be utilized for explaining the dichotomy due to paucity of data. To close this knowledge gap, we designed a regional survey and determine the extension and conditions of metamorphism through zircon petrochronology, phase equilibrium modeling, and Raman spectroscopy of carbonaceous matter. Foci herein are three north–south profiles located at *c.* 107° E (Baohé Valley east of Guangtoushan), *c.* 108° E (Foping Dome), and *c.* 108°40′ (Xunyang Basin), respectively.

A field metamorphic gradient leads northward along the Baohé Valley, from the greenschist facies Mianlüe Suture to the upper amphibolite facies, less than 10 km wide high-grade core of West Qinling; to the north of this core the metamorphic gradient reverses. The southernmost analyzed sample, a chloritoid quartzite, testifies to <450–500 °C, >0.3 GPa. Located 2.5 km north of it, a metapelitic mylonite and a garnet staurolite gneiss experienced peak metamorphism at 550 °C, 0.8–0.9 GPa and 570 °C, 0.7 GPa, respectively. Diffusion modeling for garnet from the garnet staurolite gneiss implies a

clockwise metamorphic evolution at a heating–cooling rate of 10 °C/Ma (corresponding to a time span of 25 Ma between the onset of garnet growth and cooling through 400 °C). An association of migmatitic sillimanite garnet gneiss (750 °C, 0.6–0.7 GPa) and garnet amphibolite (*c.* 700 °C, 0.7 GPa) represents the highest metamorphic grade of the profile. The association is crosscut by undeformed intermediate and felsic veins; in one of which, magmatic amphiboles crystallized at 725 °C, 0.7 GPa. A garnet staurolite schist and a garnet amphibole gneiss taken further north yielded 580–620 °C, 0.6 GPa and 620 °C, 0.7 GPa, respectively.

The Foping Dome profile crosses a migmatite–amphibolite–granulite association on a length of *c.* 40 km. The granulites are stratiform, typically decimeter-thick layers in leucosomes with a peak mineral assemblage of diopside–plagioclase–quartz–ilmenite±biotite, calcic amphibole. Peak metamorphic conditions in the core of the dome are 830 °C, 1.0 GPa. Decompression began in the upper amphibolite to granulite facies given the replacement of kyanite by sillimanite in rare Al-rich rocks and the occasional growth of orthopyroxene in granulites. To the south, peak metamorphic conditions decrease to 770 °C, 0.7 GPa (migmatitic garnet gneiss) and eventually 595 °C, 0.5 GPa (metagreywacke); at the eastern margin of the Foping Dome, the peak temperatures reached 510 °C. At its western margin, a diorite younger than the dome-forming structures but older than the penetrative regional schistosity intruded at 780 °C, 0.3 GPa. The oldest metamorphic single zircon from the Foping Dome is *c.* 215 Ma old. Almost all the metamorphic zircon ages of two garnet gneisses span 205–190 Ma; Ti-in-zircon temperatures (630–700 °C) broadly correlate with age; the youngest zircons (<192 Ma) show HREE enrichment indicative of garnet resorption. We interpret the zircons as dating cooling of the

Foping Dome, from the crystallization of the anatectic melt to garnet resorption at subsolidus conditions.

In the Xunyang Basin, a sequence of siliciclastic sediments and tuffites shows uniformly 450–520 °C, 0.4–0.6 GPa, conditions comparable to the western margin of the Foping Dome. We recognize regional Barrovian medium-*P* metamorphism until about 109 °E; at c. 110 °E, the outcrop area of Triassic *HP* metamorphism begins in Wudang Shan.

The Foping Dome constitutes the eastern section of the high-grade metamorphic core of West Qinling, which extends for roughly 160 km east–west, beyond the Baohe valley and Guangtoushan. The restriction of the outcrop area of Triassic–Early Jurassic HT metamorphic rocks to West Qinling adds to the unique dichotomy of the orogen. In terms of timing, our geochronology correlates the migmatization and granulite formation in West Qinling with the exhumation of the (U)*HP* metamorphic rocks of Hong’an–Dabie–Sulu to middle–lower crustal levels (Zhang et al., 2009) and with the gravitational collapse in West Qinling proposed on the basis of igneous petrogenesis (Hu et al., 2020). The new data concur with the

notion that the Qinling–Tongbai–Hong’an–Dabie–Sulu Orogen owes its unique dichotomy from oblique convergence.

#### **Acknowledgment**

The National Natural Science Foundation of China (41350110224) and the Open Research Project of the State Key Laboratory of Geological Processes and Mineral Resources, China University of Geosciences (GPMR201820) supported this study.

#### **References:**

- Hu, F., Liu, S., Ducea, M.N., Chapman, J.B., Wu, F., Kusky, T., 2020. Early Mesozoic magmatism and tectonic evolution of the Qinling Orogen: Implications for oblique continental collision. *Gondwana Research* 88, 296–332. <https://doi.org/10.1016/j.gr.2020.07.006>
- Zhang, R.Y., Liou, J.G., Ernst, W.G., 2009. The Dabie–Sulu continental collision zone: A comprehensive review. *Gondwana Research* 16, 1–26. <https://doi.org/10.1016/j.gr.2009.03.008>

## Geological control of the eastern Great Wall: Mountain-basin relationships in the eastern North China Craton

Boran Liu<sup>1,2</sup>, Sanzhong Li<sup>1,2</sup>, Franz Neubauer<sup>3</sup>, Junlai Liu<sup>4</sup>

<sup>1</sup> Frontiers Science Center for Deep Ocean Multispheres and Earth System, Key Lab of Submarine Geoscience and Prospecting Techniques, College of Marine Geosciences, Ocean University of China, Qingdao 266100, China

<sup>2</sup> Laboratory for Marine Mineral Resources, Qingdao National Laboratory for Marine Science and Technology, Qingdao 266237, China

<sup>3</sup> Department of Geology and Geography, Paris-Lodron-University Salzburg, Salzburg A-5020, Austria

<sup>4</sup> State Key Laboratory of Geological Processes and Mineral Resources, China University of Geosciences, Beijing 100083, China

The E–W trending Yanshan belt, an intraplate fold-thrust belt located in the northern North China Craton, has experienced several episodes of Mesozoic deformation, which resulted in the widely distributed magmatism and mountain-basin tectonics that completely re-shaped the topography of the eastern North China Craton. The eastern part of the famous Chinese Great Wall was built on the high range of the southeastern Yanshan mountain belt juxtaposed to the plain, which directly relates to the Bohai Bay basin. Our study focuses on which tectonic processes created such mountain-basin couple in Mid-Late Mesozoic times. The U-Pb LA-ICP-MS dating of zircons yield ages of 114 to 201 Ma for various granites and 115 to 116 Ma for volcanic rocks from Yixian and Jiufotang Fms. The detrital zircons from the Lower Cretaceous sandstones yield four age groups of 2587 to 2460 Ma, 2222 to 1828 Ma, 297 to 190 Ma and 187 to 100 Ma, which are all sourced from the Qinglong and surrounding areas and indicating that the Qinglong area started to uplift after the Middle Jurassic. The Qinglong area underwent multiple deformation by NE–SW compression in the Middle-Late Jurassic times, WNW–ESE compression in the Late Jurassic to Early Cretaceous, ENE–WSW extension in the Early Cretaceous and NNW–SSE compression in the Late Cretaceous during the final stage of Yanshanian orogeny. Meanwhile, widely distributed granite intrusions and emplacement of the Upper Jurassic-Lower Cretaceous volcanic rocks indicate a large amount of magma input into the area. The Qinglong area with the Great Wall along its southern margin close to adjacent plain to the south was uplifted to form the Qinglong highland and surrounding related basins by

combination of the following three processes: the multiple tectonic Late Jurassic and Late Cretaceous shortening processes related to Yanshanian orogeny, Early Cretaceous regional extension triggered by slab-retreat of the Paleopacific ocean and inflation of large amount magma at depth during Jurassic and Early Cretaceous.

**Funding:** this work was funded by National Natural Science Foundation of China (Grant no. 41230206, 41430211).

# Orocline in the Eastern Central Asian Orogenic Belt

Yongjiang Liu<sup>1,2</sup>, Qingbin Guan<sup>1,2</sup>, Sanzhong Li<sup>1,2</sup>, Zhaoxu Chen<sup>1,2</sup>, Tong Zhou<sup>1,2</sup>

<sup>1</sup> Frontiers Science Center for Deep Ocean Multispheres and Earth System, Key Lab of Submarine Geoscience and Prospecting Techniques, College of Marine Geosciences, Ocean University of China, Qingdao 266100, China

<sup>2</sup> Laboratory for Marine Mineral Resources, Qingdao National Laboratory for Marine Science and Technology, Qingdao 266237, China

The Central Asian Orogenic Belt (CAOB) is the largest accretionary orogen in the world with considerable Phanerozoic juvenile crustal growth. The eastern segment of the CAOB is occupied by NE China and its adjacent areas, which locate in a triangle area surrounded by Siberian Craton to the northwest, North China Craton (NCC) to the south and Pacific oceanic plate to the east. Therefore, the NE China is a key area to study the geological evolution of multiple tectonic systems and the overprinting, which has become a hot research topic. In the past five decades, especially the last two decades, there have been many detailed geological investigations carried out and a lot of new data reported in NE China. A progress has been achieved in tectonic evolution, however, there are still many open questions and arguments dealing with tectonic model, correlation of tectonic units, amalgamation of different blocks and their tectonic affinity. In this study, we did a detailed review of the tectonic evolution of NE China and regional comparison and correlation of different tectonic units in the eastern segment of CAOB. We re-subdivided NE China in the eastern CAOB into two old blocks of Erguna block (EB) and Jiamusi block (JB) with Precambrian basement, Xing'an accretionary terrane (XAT), Songliao accretionary terrane (SAT) and Zhangguangcai accretionary terrane (ZGCAT), which are separated from each other by the Xinlin-Xiguitu suture (XXS), Hegenshan-Heihe suture (HHS), Longfengshan suture (LFS) and Mudanjiang-Yilan suture (MYS). The ZGCAT is dominantly composed of early Paleozoic magmatic arc materials and minor late Paleozoic igneous rocks with an old Yichun mini-block, while the SAT consists dominantly of

the late Paleozoic magmatic rocks with two small old blocks of the Xilinhot and Longjiang mini-blocks. According to the tectonic correlation and comparison of different tectonic units, we established a new orocline tectonic model for the eastern CAOB: 1) the XAT and ZGCAT accreted to the southern margin of Ereendavaa-Erguna-Mamyn block (EEMB) and Bureya-Jiamusi-Khanka block (BJKB) with the closure of Xinlin-Xiguitu-Heilongjiang ocean during the early Paleozoic; 2) Subsequently, the SAT accreted to the southern margin of integrated XAT-ZGCAT terrane with the closure of Hegenshan-Nenjiang-Longfengshan ocean during the late Paleozoic. These initially W-E linear shape of accretionary orogenic belts was ultimately bent southward through Paleozoic time and constituted a huge Paleozoic orocline, NE China Orocline, which collided with NCC by a scissor-like style closure of Paleo-Asian Ocean (PAO) from west to east along the Solonker-Xar Moron-Changchun-Yanji suture (SXCYS) during the late Permian-middle Triassic. The NE China orocline, together with Tuva-Mongol Orocline and Kazakhstan Orocline in the western CAOB, constituted a huge multiple orocline tectonic system in the CAOB. Our study will contribute to the understanding on tectonic evolutions of CAOB and the NE Asian and suggests that the orocline should be a common tectonic model for accretionary orogeny.

**Funding:** this work was funded by National Natural Science Foundation of China (42130305), Taishan Scholars (ts20190918) and Qingdao Leading innovation talents (19-3-2-19-zhc).

# Traversing the Himalayan Orogen 2022-Report of the 10th Student Himalayan Field Exercise Tour

M. Yoshida<sup>a\*</sup>, K. Arita<sup>b</sup>, T. Sakai<sup>c</sup>, B.N. Upreti<sup>d</sup>

<sup>a</sup> Gondwana Institute for Geology and Environment, Hashimoto, Japan

<sup>b</sup> Hokkaido University Museum, Sapporo, Japan

<sup>c</sup> Faculty of Science and Technology, Shimane University, Matsue, Japan

<sup>d</sup> Nepal Academy of Science and Technology, Kathmandu, Nepal

\* Corresponding author at the Gondwana Institute for Geology and Environment, Hashimoto and also at the Department of Geology, Tri-Chandra Campus, Tribhuvan University, Kathmandu (Em. Professor). E-mail: [gondwana@oregano.ocn.ne.jp](mailto:gondwana@oregano.ocn.ne.jp)

The Cenozoic Himalayan Orogeny includes geological processes of the dispersion of Gondwana and growth of Asia/Amasia. The orogen thus shows us the realistic view of the global crustal movement. The Student Himalayan Field Exercise Tour (SHET) aimed to show students the full N-S section of the Himalayan Orogen (Fig. 1) started in 2012 to let students feel the dynamic crustal processes in the field and have interest in geology. Since then, the SHET was conducted every year (except in 2021 due to the Covid-19 pandemic). The details of the SHET program are given on the SHET home page (SHET-HP, 2022).

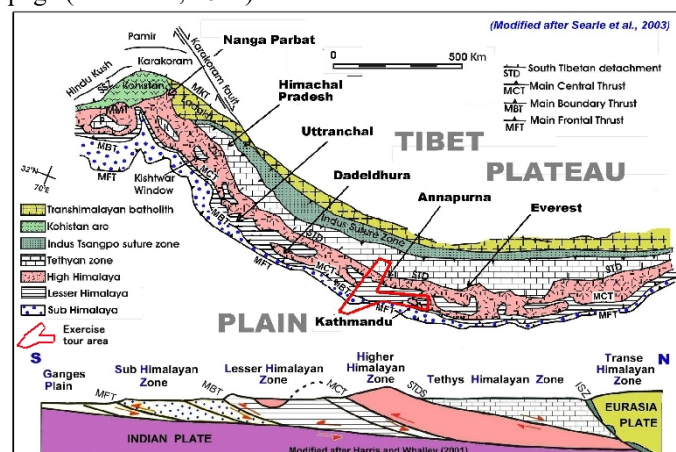


Fig. 1 Geologic outline of the Himalayan Orogen and the study area

The 10th SHET was successfully carried out in March 2022 as follows, the details are given by Yoshida (2022). The advertisement of the SHET-10 started in May 2021 and 11 students including a Chinese student funded by the IAGR

registered January 2022, however, 5 among them cancelled in February due to the pandemic problem.

On the 6<sup>th</sup> March 2022, the SHET-10 team including 5 Japanese and a Nepali and a Japanese leaders/teachers of the tour departed Kathmandu by a chartered bus for the field excursion. The tour course included a full N-S traverse of the Himalayan Orogen in the west-central Nepal from Mustang north of Annapurna to Terai through Kali Gandaki and Tinau Khola, the course having been same as that during the SHET-1 to SHET-9.

The weather was fine and participants met no health problems throughout the tour and thus could enjoy the full fascination of the Himalayan geology in the field. Before and after the field tour, the team had pre- and post- field tour seminars and city tours in Kathmandu inviting many Nepali students. On the 18<sup>th</sup> March the Japanese team left Kathmandu for Japan. The SHET-10 thus completed successfully. The only problems were to clear regulations and rules related to the Covid-19 pandemic at immigration of and return to countries, although they were anyway of no fundamental problem. An outline of the SHET-10 including highlight views of the field observation will be displayed at the presentation.

## Reference cited:

- SHET-HP, 2022, Student Himalayan Field Exercise site, in the GIGE homepage, [http://www.gondwanainst.org/geotours/Studentfieldex\\_index.htm](http://www.gondwanainst.org/geotours/Studentfieldex_index.htm)
- Yoshida, M., 2022 (ed.), Traversing the Himalayan Orogen 2022--A Record of the 10th Student Himalayan Field Exercise Tour in March 2022 (in Japanese and English). Field Science Publishers, Hashimoto, 191 pages.

# Geochemical characteristics and tectonic significance of the Marzheng diorites on the southern margin of the East Kunlun Orogenic Belt

Bin Zhang<sup>a</sup>, Yunpeng Dong<sup>a,b,\*</sup>, Shengsi Sun<sup>a</sup>, Dengfeng He<sup>a</sup>, Bo Hui<sup>a</sup>, Yuangang Yue<sup>a</sup>, Xiang Ren<sup>a</sup>, Weidong He<sup>a</sup>

<sup>a</sup> State Key Laboratory of Continental Dynamics, Department of Geology, Northwest University, Xi'an, China

<sup>b</sup> Department of Earth Science, Western University, London, Ontario, Canada

The East Kunlun Orogenic Belt (E-KOB) of the northern Tibetan Plateau is an accretionary orogenic belt, which has experienced complicated tectonic evolutionary processes of the Proto- to Paleo-Tethys Ocean. The Muztagh-Buqingshan-Anemaqen ophiolitic mélangé zone is an accretionary complex related to the northward subduction of the Tethyan Ocean. Numerous intrusions outcropped in MBAM have witnessed the long-term subduction-accretionary process and thus site the key to comprehending the tectonic evolution of the E-KOB, as well as the Tethyan Ocean. In this study, petrological, geochronological, and geochemical studies of the Marzheng diorites in the MBAM were carried out to explore the Early Paleozoic tectonic evolution of the E-KOB. Zircon U–Pb dating analysis suggests that the diorites were formed in the

Early Ordovician at ca. 470 Ma. Furthermore, the  $\epsilon_{\text{Hf}}(t)$  values (5.3–14.1), Mg# values (39.7–51.2), and Nb/Ta (12.8–14.8), Zr/Hf (33.8–44.8), and Lu/Yb (0.15–0.16) ratios are generally close to those of depleted mantle-derived rocks and the diorites were originated from a depleted asthenosphere mantle source. In addition, these diorites are characterized by enriched light rare earth elements and depleted high-field-strength elements (i.e., Nb, Ta, P, and Ti), similar to the fingerprints of arc-related gabbroic-dioritic rocks. This is also consistent with their high H<sub>2</sub>O melt (6.0–8.3%) and oxygen fugacity ( $\log f_{\text{O}_2} = -14.3$  to  $-13.5$ ) features, indicating that they were formed in a subduction-related setting. Our new investigations suggest that the Proto-Tethys Ocean in the East Kunlun was still actively subducting northward during the Early Ordovician.

## Calc-alkaline plutons in intra-oceanic arc of Proto-Tethys Ocean (Qilian Orogen, NW China) and construction of arc upper crust

Chao Wang<sup>a\*</sup>, Shuguang Song<sup>b</sup>, Guochun Zhao<sup>a,c</sup>, Mark B. Allen<sup>d</sup>, Li Su<sup>e</sup>, Tianyu Gao<sup>f</sup>, Tao Wen<sup>b</sup>, Di Feng<sup>b</sup>

<sup>a</sup> Department of Earth Sciences, The University of Hong Kong, Pokfulam Road, Hong Kong, China

<sup>b</sup> MOE Key Laboratory of Orogenic Belts and Crustal Evolution, School of Earth and Space Sciences, Peking University, Beijing 100871, China

<sup>c</sup> State Key Laboratory of Continental Dynamics, Department of Geology, Northwest University, Northern Taibai Street 229, Xi'an 710069, China

<sup>d</sup> Department of Earth Sciences, Durham University, Durham DH1 3LE, UK

<sup>e</sup> Institute of Earth Sciences, State Key Laboratory of Geological Processes and Mineral Resources, China University of Geosciences, Beijing 100083, China

<sup>f</sup> School of Earth Sciences and Resources, China University of Geosciences, Beijing 100083, China

Intra-oceanic arcs are one of the major building blocks of continents, and the rarely exposed calc-alkaline plutons in intra-oceanic arcs constitute as a critical arc crustal section. These calc-alkaline plutons are compositionally similar to continental crust, and thus their petrogenesis bears important implication for the formation of continental crust. Here we present results of an integrated study, involving field investigation, petrology, geochronology and geochemistry, on calc-alkaline intermediate–felsic plutons within a Proto-Tethyan intra-oceanic arc in the Lajishan terrane of the Qilian Orogen at the northern margin of Tibetan Plateau. These calc-alkaline intermediate–felsic plutons range from gabbroic diorites, through diorites, to granodiorites, with mafic magmatic enclaves (MMEs) hosted in diorites and granodiorites. In situ zircon U-Pb dating demonstrates that these plutons were emplaced in the Early Paleozoic (474–460 Ma), almost coeval with previously identified volcanics (boninites, ankaramites, high-Mg basaltic andesites, high-Al andesites, sanukites). Geochemistry of these plutons indicates

that they were differentiation products of subduction-metasomatized arc mantle-derived melts, and isotope modelling constrains that their mantle source was metasomatized by less than 10% addition of slab-derived fluids/melts. Their parental melts experienced polybaric medium- to high-pressure fractional crystallization to generate the compositional variation of these plutons. There are two types of MMEs according to their different geochemistry (high- and low-MgO MMEs) and both of them are early crystallized arc mantle-derived melts captured by evolving magmas. High-MgO MMEs represent near-primitive melts, while low-MgO MMEs stand for relatively evolved melts. The Lajishan calc-alkaline intermediate–felsic plutons and arc volcanics constructed the upper section of a Proto-Tethyan intra-oceanic arc, and the composition of this intra-oceanic arc was still juvenile and primitive, which was further refined towards maturity through arc-continent collision in response to the closure of the Proto-Tethys ocean.

# Quantifying the extent of the Paleo-Asian Ocean during the Late Carboniferous to Early Permian

Donghai Zhang<sup>1,2,\*</sup>, Baochun Huang<sup>2,\*</sup>, Guochun Zhao<sup>3,1</sup>, Joseph G. Meert<sup>4</sup>

<sup>1</sup> State Key Laboratory of Continental Dynamics, Department of Geology, Northwest University, Northern Taibai Str. 229, Xi'an 710069, China

<sup>2</sup> Key Laboratory of Orogenic Belt and Crust Evolution, Ministry of Education, School of Earth and Space Sciences, Peking University, Beijing 100871, China

<sup>3</sup> Department of Earth Sciences, The University of Hong Kong, Pokfulam Road, Hong Kong

<sup>4</sup> Department of Geological Sciences, 241 Williamson Hall, University of Florida, Gainesville, FL 32611, USA

\*Corresponding author:

Baochun Huang

School of Earth and Space Sciences, Peking University, Yiheyuan Road No. 5, Haidian District, Beijing 100871

E-mail: [bchuang@pku.edu.cn](mailto:bchuang@pku.edu.cn)

Donghai Zhang

Department of Geology, Northwest University, Northern Taibai Str. 229, Xi'an 710069

E-mail: [dhzhang@nwu.edu.cn](mailto:dhzhang@nwu.edu.cn)

The Paleo-Asian Ocean (PAO) separated North China and Tarim from Mongolia and Siberia. Dating the closure of the PAO is critical to our understanding of East Asian tectonics during the formation of Pangea, yet existing estimates differ by up to 130 Myr (380 Ma to 250 Ma). In this study, we report two robust paleomagnetic results from 320-280 Ma volcanic-sedimentary strata in the South Mongolia-Xing'an Belt. Stable characteristic remanences of both results are likely primary and characterized by positive fold tests, consistent polarity with the Kiaman Superchron (~318-262 Ma) and average

paleosecular variation. The new results indicate that the northward motion of North China and Mongolia paralleled Laurussia from the Late Carboniferous to Early Permian. The N-S width of the PAO in the east-central segment (reference site: 43°N/114°E) was ca. 2700 km during the Late Carboniferous to Early Permian. The existence of this wide oceanic basin impeded floral and faunal interchange between North China and Mongolia. The PAO finally closed and formed a unified North China-Amuria block at ca. 250 Ma.

# A Tarim-North India connection in northern Gondwana associated with final closure of the Proto-Tethys Ocean: Constraints from provenance of early Paleozoic sedimentary rocks in the Altyn Tagh orogen

Qian Liu <sup>a\*</sup>, Guochun Zhao <sup>b, a</sup>, Jianhua Li <sup>c</sup>, Jinlong Yao <sup>a</sup>, Yigui Han <sup>a</sup>, Peng Wang <sup>d</sup>, Toshiaki Tsunogae <sup>e, f</sup>

<sup>a</sup> State Key Laboratory of Continental Dynamics, Department of Geology, Northwest University, Xi'an 710069, China

<sup>b</sup> Department of Earth Sciences, The University of Hong Kong, Pokfulam Road, Hong Kong, China

<sup>c</sup> China Institute of Geomechanics, Chinese Academy of Geological Sciences, Beijing 100081, China

<sup>d</sup> School of Earth and Environmental Sciences, University of Queensland, Brisbane, QLD, Australia

<sup>e</sup> Graduate School of Life and Environmental Sciences, The University of Tsukuba, Ibaraki 305-8572, Japan

<sup>f</sup> Department of Geology, University of Johannesburg, Auckland Park 2006, South Africa

\* Corresponding Author e-mail: [liuqian@nwu.edu.cn](mailto:liuqian@nwu.edu.cn)

The final assembly of the main body of Gondwana have been generally accepted to had completed by the early Paleozoic. However, the evolution of the northern margin of Gondwana, which involved many present-day East Asian blocks associated with final closure of the Proto-Tethys Ocean, is still enigmatic. Due to the paucity of reliable early Paleozoic paleomagnetic and paleobiogeographic data, much controversy remains as to where the Tarim craton was located in northern Gondwana in response to final closure of the North and South Altyn Oceans (two branches of the Proto-Tethys Ocean between southeastern Tarim and northern Gondwana).

Provenance reconstruction of sedimentary rocks has been widely applied to constrain paleogeographic relationships among tectonic units. This study focused on early Paleozoic sedimentary rocks in the Altyn Tagh orogen, southeastern Tarim, and carried out detrital zircon U-Pb dating and Hf isotopic analyses. New results indicate that the studied sedimentary rocks were probably deposited from ca. 494 to 426 Ma. Based on provenance tracing, a local Altyn Tagh source region to the south of the North Altyn Ocean is suggested for the ca. 494-477 Ma sedimentary rocks, whereas an increase detrital supply from the Tarim craton to the north of the North Altyn Ocean characterizes the ca. 465-449 Ma

sedimentary rocks. This provenance shift constrained the timing of final closure of the North Altyn Ocean between ca. 477 and 465 Ma. The ca. 444-426 Ma sedimentary rocks have comparable U-Pb-Hf isotopes of detrital zircons to the ca. 465-449 Ma ones, implying sediment recycling after final closure of the North Altyn Ocean. Together with suprasubduction zone-type ophiolitic, (ultra)high-pressure metamorphic, magmatic, and structural records in the Altyn Tagh orogen, final closure of the North Altyn Ocean probably occurred in the Middle Ordovician, postdating final closure of the South Altyn Ocean in the latest Cambrian-Early Ordovician. Considered the other branches of the Proto-Tethys Ocean within East Asian, a progressive closure process in the period of ca. 500-420 Ma is inferred for the entire Proto-Tethys Ocean, leading to amalgamation of many East Asian blocks in northern Gondwana. In comparison with the potential Gondwana blocks, the Tarim craton was most likely linked with North India as well as some East Asian blocks (e.g., North Qilian, North Qinling, South China, Indochina, South Qiangtang, etc.), rather than with Arabia-Iran or other East Asian blocks (e.g., Lhasa and Sibumasu) adjacent to western Australia in northern Gondwana (Fig. 1).

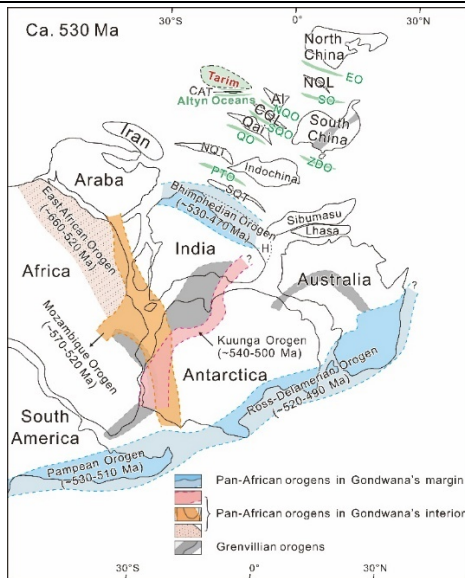


Fig.1 Reconstruction of Gondwana at ca. 530 Ma showing location and timing of major orogens (modified after Boger and Miller, 2004; Veevers, 2004; Cawood et al., 2007; Gray et al., 2008; Horton et al., 2008; Zhu et al., 2011; Zhao et al., 2018). Al—Alxa; CAT—Central Altyn Tagh; CQL—Central Qilian; NQL—North Qilian; NQT—North Qiangtang; SQT—South Qiangtang; H—Himalaya; Qai—Qaidam; NQO—North Qilian Ocean; SQO—South Qilian Ocean; QO—Qimantagh Ocean; EO—Erlangping Ocean; SO—Shangdan Ocean; ZDO—Zhenghe-Dapu Ocean; PTO—branch of the Proto-Tethys Ocean between North and South Qiangtang.

This study was financially supported by a National Natural Science Foundation of China Project (grant 41730213), a Hong Kong Research Grants Council General Research Fund (grant 17307918), and Grant-in-Aids for Scientific Research

from Japan Society for the Promotion of Science to Prof. Toshiaki Tsunogae (18H01300) and to Prof. Qian Liu (No. 19F19020).

## References:

- Boger, S.D., Miller, J.M., 2004. Terminal suturing of Gondwana and the onset of the Ross–Delamerian Orogeny: The cause and effect of an Early Cambrian reconfiguration of plate motions. *Earth Planet. Sci. Lett.* 219(1-2), 35-48.
- Cawood, P. A., Johnson, M.R., Nemchin, A.A., 2007. Early Palaeozoic orogenesis along the Indian margin of Gondwana: Tectonic response to Gondwana assembly. *Earth Planet. Sci. Lett.* 255(1-2), 70-84.
- Gray, D.R., Foster, D.A., Meert, J.G., Goscombe, B.D., Armstrong, R., Trouw, R.A.J., Passchier, C.W., 2008. A Damara orogen perspective on the assembly of southwestern Gondwana. *Geol. Soc. Spec. Publ.* 294(1), 257-278.
- Horton, B.K., Hassanzadeh, J., Stockli, D.F., Axen, G.J., Gillis, R.J., Guest, B., Amini, A., Fakhari, M.D., Zamanzadeh, S.M., Grove, M., 2008. Detrital zircon provenance of Neoproterozoic to Cenozoic deposits in Iran: Implications for chronostratigraphy and collisional tectonics. *Tectonophysics*, 451(1-4), 97-122.
- Veevers, J.J., 2004. Gondwanaland from 650–500 Ma assembly through 320 Ma merger in Pangea to 185–100 Ma breakup: supercontinental tectonics via stratigraphy and radiometric dating. *Earth Sci. Rev.* 68(1-2), 1-132.
- Zhao, G.C., Wang, Y.J., Huang, B.C., Dong, Y.P., Li, S.Z., Zhang, G.W., Yu, S., 2018. Geological reconstructions of the East Asian blocks: From the breakup of Rodinia to the assembly of Pangea. *Earth Sci. Rev.* 186, 262-286.
- Zhu, D.C., Zhao, Z.D., Niu, Y.L., Dilek, Y., Mo, X.X., 2011. Lhasa terrane in southern Tibet came from Australia. *Geology*, 39(8), 727-730.

## Eruptive tempo of Emeishan large igneous province: relations to biotic crises and paleoclimate changes around the Guadalupian-Lopingian boundary

Hu Huang<sup>a,\*</sup>, Magdalena H. Huyskens<sup>b</sup>, Qing-Zhu Yin<sup>b</sup>, Peter A. Cawood<sup>c</sup>, Mingcai Hou<sup>a</sup>, Jianghai Yang<sup>d</sup>, Fuhao Xiong<sup>a</sup>, Yuansheng Du<sup>d</sup>, Chenchen Yang<sup>a</sup>

<sup>a</sup> State Key Laboratory of Oil and Gas Reservoir Geology and Exploitation, Institute of Sedimentary Geology, Chengdu University of Technology, Chengdu 610059, China

<sup>b</sup> Department of Earth and Planetary Sciences, University of California at Davis, Davis, California 95616-8605, USA

<sup>c</sup> School of Earth, Atmosphere & Environment, Monash University, Melbourne, VIC 3800, Australia

<sup>d</sup> State Key Laboratory of Biogeology and Environmental Geology, China University of Geosciences, Wuhan 430074, China

The Emeishan large igneous province (ELIP) is thought to be a potential driver for the biotic crises and paleoclimate changes around the Guadalupian-Lopingian boundary (GLB), but the lack of high-precision radiometric dates to constrain the duration and eruption rates of the volcanism has limited the assessment of their relationship. Here, we present new chemical abrasion-isotope dilution-isotope ratio mass spectrometry U-Pb zircon geochronology of three samples from the lowermost and uppermost parts of the volcanic succession in the central portion of the ELIP. The results

demonstrate that Emeishan volcanism began by  $260.55 \pm 0.07$  Ma and persisted until at least  $257.22 \pm 0.37$  Ma. Combined with a previously published age of  $259.1 \pm 0.5$  Ma for silicic ignimbrites, we estimate that  $\sim 85\%$  of ELIP volume erupted within  $1.45 \pm 0.50$  Ma. Our new results confirm that the Emeishan volcanism began slightly prior to the initiation of the associated mass extinction event and is contemporaneous with the associated warming interval. The new data support the hypothesis that the ELIP likely triggered the biotic crises and paleoclimate changes around the GLB.

# New Carboniferous paleomagnetic data from Mongolia and their implications for the paleogeographic evolution of the Central Asian Orogenic Belt

Qiang Ren<sup>a,\*</sup>

<sup>a</sup> *Institute of Sedimentary Geology, Chengdu University of Technology, Chengdu 610059, China*

The eastern Central Asian Orogenic Belt (CAOB) is composed of two important collage systems, the Khazakstan collage system in west and the Tuva-Mongolia collage system in east. The paleogeographic evolution of the eastern CAOB during the Carboniferous period is very controversial. Paleomagnetism remains the most useful tool for studying plate kinematics and provides independent evidence for paleogeographic reconstruction. However, reliable paleomagnetic constraints have not been available previously to address this issue. Here we report newly obtained combined paleomagnetic and geochronological results from the Upper Mississippian Gunbayan Formation in the Amuria Block (AMB) and the Lower Pennsylvanian Altan-Ovoo Formation in the Tuva-Mongol Block (TMB). Zircon U–Pb dating of tuff beds from the Gunbayan and Altan-Ovoo formations yield ages of  $331.0 \pm 2.7$  and  $315.5 \pm 2.4$  Ma, respectively. A total of 263 paleomagnetic specimens underwent stepwise thermal demagnetization. After removing the viscous remanent magnetizations of the recent geomagnetic field, stable high-temperature components (HTCs), carried by magnetite, were

successfully acquired from 240 specimens. The HTCs of the Gunbayan Formation passed a fold test and a reversal test, and those of the Altan-Ovoo Formation passed a fold test, suggesting that they represent primary remanence magnetizations. We used the elongation/inclination method to test and correct for all the HTC directions of the clastic rocks of the studied formations. Their corresponding paleomagnetic poles are  $46.0^\circ\text{N}/320.0^\circ\text{E}$  ( $A_{95}=2.0^\circ$ ) at ca. 330 Ma for the AMB and  $43.5^\circ\text{N}/355.9^\circ\text{E}$  ( $A_{95}=2.9^\circ$ ) at ca. 315 Ma for the TMB. The updated paleomagnetic database indicates with certainty that both the TMB and the AMB were located in northern hemisphere low-latitude regions and close to the equator at ca. 330 Ma, suggesting that the Boreal Realm might have extended into the equatorial region at the onset of the large ice age of the Carboniferous. The paleobiogeographic characteristics and distribution of climate-sensitive lithologies indicate that this realm occupied a wide northern temperate belt during 330–315Ma.

**Keywords:** Central Asian Orogenic Belt; Amuria Block; Tuva-Mongol Block; Carboniferous; Paleomagnetism; Low latitudes; Boreal Realm.

# Online databases of the geologic formations of the Indian Plate, China and Indochina, with display onto plate reconstructions of East Asia

OGG, James<sup>1,2</sup>, DU, Wen<sup>3</sup>, CHANG, Sabrina<sup>4</sup>, MISHRA, Suyash<sup>4</sup>, ZAHIROVIC, Sabin<sup>3</sup>, AULT, Aaron<sup>4</sup>, HOU, Hongfei<sup>5</sup>, MAMALLAPALLI, O'Neil<sup>6</sup>, LI, Haipeng<sup>2</sup>, HOU, Mingcai<sup>1</sup>, DONG, Bui<sup>7</sup>, OGG, Gabi<sup>8</sup>

<sup>1</sup> Institute of Sedimentary Geology, Chengdu University of Technology, Chengdu, Sichuan, 610059, China

<sup>2</sup> Deep-time Digital Earth Research Center of Excellence (Suzhou), International Union of Geological Sciences, 1699 Zu Chongzhi South Road, Kunshan (Jiangsu), China

<sup>3</sup> EarthByte Group, School of Geosciences, The University of Sydney, Sydney, NSW 2006, Australia

<sup>4</sup> Electrical and Computer Engineering, Purdue University, West Lafayette, IN 47907

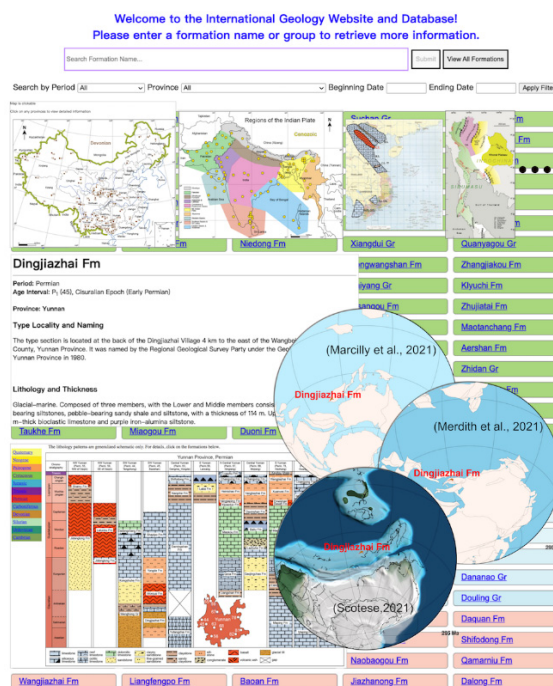
<sup>5</sup> Institute of Geology, Chinese Academy of Geological Sciences, Beijing, 100037, China

<sup>6</sup> Oil and Natural Gas Corporation (ONGC), Chennai, India

<sup>7</sup> Faculty of Geology, Vietnam National University of Science, Hanoi, Viet Nam

<sup>8</sup> Geologic TimeScale Foundation, 1224 N Salisbury St., West Lafayette, IN 47906

Building paleogeographic maps onto tectonic plate reconstruction models requires team efforts to compile databases of regional sedimentary and volcanic facies, data sharing standards, and computer projection methods. Two goals of the Deep-Time Digital Earth (DDE) program of the International Union of Geological Sciences (IUGS) Paleogeography Working Group are: (1) to interconnect online national databases for all geologic formations, and to compile these online "lexicons" for countries that currently lack these; (2) to project the combined paleogeographic output of these distributed databases for any time interval onto appropriate plate tectonic reconstructions.



Therefore, we have worked with regional experts to compile new cloud-based lexicons for East Asia regions that are enhanced by graphic user-interfaces and interactive visualization techniques. Online lexicons with map-based and stratigraphic-column navigation are currently completed for the Proterozoic through Phanerozoic of the Indian Plate (ca. 800 formations), China (ca. 2500 as of Sept 2022), Vietnam (over 200) and Thailand (ca. 200 formations). A multi-database search system (age, region, lithology keywords, etc.) enables all returned entries be displayed by-age or in alphabetical order. Then, if a geologic age had been specified,

a user with a single click can plot the original extent of the corresponding regional formations (filled with their appropriate lithologic facies patterns) onto any of three different proposed plate reconstruction models. Essentially, the goal is to create a view of the sediments and volcanics that were accumulating onto the Earth's surface at any past time. Our team is currently working with the Macrostrat and eODP teams at Univ. Wisconsin (Madison) to interlink to their regional facies-time compilations for the Americas and the ocean basins

# Doushantuo Formation phosphorite succession (SW China) records the Ediacaran Phosphogenesis Event: New evidence from Danzhai phosphorite deposit

Li-Ming Yu<sup>1</sup>, Hao Zou<sup>1,2\*</sup>, Bin Xiao<sup>1</sup>, Jiang-Han Wu<sup>1</sup>, Jin-Xiang Sheng<sup>1</sup>, Hui-Dong Yu<sup>1</sup>, Hai-Feng Cheng<sup>1</sup>, Chang-Cheng Huang<sup>1</sup>

<sup>1</sup> State Key Laboratory of Oil and Gas Reservoir Geology and Exploitation, Chengdu University of Technology, Chengdu 610059, China

<sup>2</sup> Key Laboratory of Tectonic Controls on Mineralisation and Hydrocarbon Accumulation of Ministry of Land and Resources, Chengdu University of Technology, Chengdu 610059, China

\*E-mail: zouhao21@gmail.com

The Ediacaran-early Cambrian period is not only the key period of global climate and life evolution, but also recorded the occurrence of the second large-scale phosphogenesis event in history of the Earth (Caird et al., 2017; Ye et al., 2020). Phosphorite of the Ediacaran Doushantuo Formation accumulated in the South China during the period, producing the first true phosphorite giant in Earth history (Zhang et al., 2019). At present, there is no consensus on the origin of the metallogenic materials and the mode of formation of this phosphorite mineralization in the Doushantuo phosphorite deposits in South China (Yang et al., 2019). Therefore, the study on the formation of phosphorite in the Ediacaran Doushantuo Formation, South China will help in our better understanding of the role of the phosphorus-forming event in that period.

Here, we present a detailed study of geology, petrology, and geochemistry and C-O isotopes of the Doushantuo phosphorite, shale and dolomite samples at Danzhai, southwest Guizhou. Our field, petrologic, geochemical and isotopic data suggest that:

(1) The ore-forming materials of the Doushantuo phosphorite deposit may have an input of marine hydrothermal and the organic-rich water brought by up-welling;

(2) The phosphogenesis of the late Doushantuo phosphate deposit is mainly the result of growth and mineralization of microorganisms, accompanied by the mechanical dynamic

action of seawater.

**Keywords:** Ediacaran; Doushantuo Formation; Danzhai phosphate deposit.

## References

- Caird, R.A., Pufahl, P.K., Hiatt, E.E., Abram, M.B., Rocha, A.J.D., Kyser, T.K., 2017. Ediacaran stromatolites and intertidal phosphorite of the Salitre Formation, Brazil: Phosphogenesis during the Neoproterozoic Oxygenation Event. *Sedimentary Geology*. 350, 55-71.
- Yang, H.Y., Xiao, J.F., Xia, Y., Xie, Z.J., Tan, Q.P., Xu, J.B., Guo, H.Y., He, S., Wu, S.W., 2019. Origin of the Ediacaran Weng'an and Kaiyang phosphorite deposits in the Nanhua basin, SW China. *Journal of Asian Earth Sciences*. 182, 103931.
- Ye, Y.T., Wang, H.J., Wang, X.M., Zhai, L.N., Wu, C.D., Zhang, S.C., 2020. Elemental geochemistry of lower Cambrian phosphate nodules in Guizhou Province, South China: An integrated study by LA-ICP-MS mapping and solution ICP-MS. *Palaeogeography, Palaeoclimatology, Palaeoecology*. 538, 109459.
- Zhang, Y.G., Pufahl, P.K., Du, Y.S., Chen, G.Y., Liu, J.Z., Chen, Q.G., Wang, Z.P., Yu, W.C., 2019. Economic phosphorite from the Ediacaran Doushantuo Formation, South China, and the Neoproterozoic-Cambrian Phosphogenic Event. *Sedimentary Geology*. 388, 1-19.

# The last Neoproterozoic rift magmatism on the margin of western Yangtze

Chang-Cheng Huang<sup>1</sup>, Hao Zou<sup>1,2\*</sup>, Hai-Feng Chen<sup>1</sup>, Hui-Dong Yu<sup>1</sup>, Bin Xiao<sup>1</sup>, Chun-Mei Liu<sup>1</sup>

<sup>1</sup> State Key Laboratory of Oil and Gas Reservoir Geology and Exploitation, Chengdu University of Technology, Chengdu, Sichuan 610059, China

<sup>2</sup> Key Laboratory of Tectonic Controls on Mineralisation and Hydrocarbon Accumulation of Ministry of Land and Resources, Chengdu University of Technology, Chengdu 610059, China

\*E-mail: zouhao21@gmail.com

The geological record preserves evidence of “snowball Earth” glaciations during the Cryogenian Period, the Sturtian onset at ca. 717 Ma and the Marinoan onset at ca. 651 Ma (Hoffman et al., 2021). Compared to the Sturtian, the trigger for the Marinoan is still unclear due to the absence of large igneous provinces (LIPs). This study first discovered magmatic rock (LLBZ granite) during “snowball Earth” at the western margin of the Yangtze Block in China. LLBZ granite with Low  $\delta^{18}\text{O}$  emplaced at the onset of the Marinoan and derived from partial melting of the mafic rocks in a continental rift. We systematically compiled data and found interglacial period, which occurred after the Sturtian glaciation, absent magma activity. Rifting magma activity similar to the LLBZ granite started at 651 Ma. This time overlapped the onset of the Marinoan. This temporal rule also existed in rifting magma activity of other parts of the world (e.g., Siberian, Tarim, and Altun-Qilian-Kunlun; Lan et al., 2022; Peng et al., 2019; Yarmolyuk et al., 2005; Zhu et al., 2008). After combining that increased CIA data across South China, Congo (Zhou et al., 2021), and Australia before the Marinoan, and palaeomagnetic results of the breakup of major continental blocks of the Rodinia occurred at ca. 650 Ma (Li & Evans, 2011). We suggest the last breakup of Rodinia caused newly rifted margins, increased planetary weather ability, and played an important role in the onset of the Marinoan.

In combining with previous research and the results of this research, we draw the following conclusions:

The LLBZ granite formed at  $651.2 \pm 2.1$  Ma and derived from low-degree partial melting of mafic rocks. The zircons of LLBZ granite have low  $\delta^{18}\text{O}$  values between +2.74 to +5.34 ‰ and indicate LLBZ granite formed in a continental rift. The rift-related magmatic rocks similar to LLBZ granite were all

emplaced after ca. 651 Ma in South China, Siberian, Tarim, and Altun-Qilian-Kunlun. This time overlapped the onset of the Marinoan. After combining that increased CIA data across South China, Congo, and Australia before the Marinoan, and palaeomagnetic results of the breakup of major continental blocks of the Rodinia occurred at ca. 650 Ma. We propose the last breakup of the Rodinia caused the increased area of rifted margins and precipitation in regions inside the supercontinent. Eventually promoting silicate weathering that significantly enhanced and the onset of the Marinoan.

**Keyword:** Snowball Earth; Marinoan; Rodinia Supercontinent; Yangtze Block; U-Pb zircon age; Hf-O isotopes

## References

- Hoffman, P. F., Halverson, G. P., Schrag, D. P., Higgins, J. A., Domack, E. W., Macdonald, F. A., Pruss, S. B., Blättler, C. L., Crockford, P. W., Hodgkin, E. B., Bellefroid, E. J., Johnson, B. W., Hodgskiss, M. S. W., Lamothe, K. G., LoBianco, S. J. C., Busch, J. F., Howes, B. J., Greenman, J. W., & Nelson, L. L. (2021), Snowballs in Africa: sectioning a long-lived Neoproterozoic carbonate platform and its bathyal foreslope (NW Namibia). *Earth-Science Reviews*, 219, 103616.
- Lan, Z. W., Huyskens, M. H., Le Hir, G., Mitchell, R. N., Yin, Q. Z., Zhang, G. Y., & Li, X. H. (2022), Massive Volcanism May Have Foreshortened the Marinoan Snowball Earth. *Geophysical Research Letters*, 49(6).
- Li, Z. X., & Evans, D. A. D. (2011), Late Neoproterozoic 40° intraplate rotation within Australia allows for a tighter-fitting and longer-lasting Rodinia. *Geology*, 39(1).
- Peng, Y. B., Yu, S. Y., Li, S. Z., Zhang, J. X., Liu, Y. J., Li, Y. S., & Santosh, M. (2019), Early Neoproterozoic magmatic

- 
- imprints in the Altun-Qilian-Kunlun region of the Qinghai-Tibet Plateau: Response to the assembly and breakup of Rodinia supercontinent. *Earth-Science Reviews*, 199, 102954.
- Yarmolyuk, V. V., Kovalenko, V. I., Sal'Nikova, E. B., Nikiforov, A. V., Kotov, A. B., & Vladykin, N. V. (2005), Late Riphean rifting and breakup of Laurasia; data on geochronological studies of ultramafic alkaline complexes in the southern framing of the Siberian Craton. *Doklady earth sciences*, 404(7), 1031-1036.
- Zhou, T., Pan, X., Sun, R., Deng, C., Shen, J., Kwon, S. Y., Grasby, S. E., Xiao, J., & Yin, R. (2021), Cryogenian interglacial greenhouse driven by enhanced volcanism: Evidence from mercury records. *Earth and Planetary Science Letters*, 564, 116902.
- Zhu, W. B., Zhang, Z. Y., Shu, L. S., Lu, H. F., Su, J. B., & Yang, W. (2008), SHRIMP U-Pb zircon geochronology of Neoproterozoic Korla mafic dykes in the northern Tarim Block, NW China: implications for the long-lasting breakup process of Rodinia. *Journal of the Geological Society*, 165.

# Study on the origin and enrichment of sedimentary rare earth elements: A case of REE deposits in the adjacent areas of Yunnan and Guizhou

Bin Xiao<sup>1</sup>, Hao Zou<sup>1,2\*</sup>, Enyuan Tian<sup>1,3</sup>, Liming Yu<sup>1</sup>, Changcheng Huang<sup>1</sup>, Chenghui Hu<sup>1</sup>, Daxing Gong<sup>3</sup>

<sup>1</sup> State Key Laboratory of Oil and Gas Reservoir Geology and Exploitation, Chengdu University of Technology, 610059, China

<sup>2</sup> Key Laboratory of Tectonic Controls on Mineralization and Hydrocarbon Accumulation of Ministry of Land and Resources, Chengdu University of Technology, Chengdu, Sichuan 610059, China

<sup>3</sup> Institute of Multipurpose Utilization of Mineral Resources, China Academy of Geological Sciences, Chengdu, Sichuan, 610041, China

\*E-mail: zouhao21@gmail.com

At the bottom of the Late Permian Xuanwei Formation in southwestern China, widely distributed clay rocks directly overlie the top of the Emeishan flood basalt, and are strongly enriched in rare earth elements (REE) with the total rare earth oxide (TREO) average content of 1500 ppm (Tian et al., 2021), which can be used as potential rare earth resources. This new type of REE resource is different from the existing REE types. It is formed in continental sedimentary environment and closely related to sedimentation (Gong et al., 2020).

This study revealed the material source of the REE rich rock system and the surface migration of rare earth elements through deposit geology, major and trace elements, detrital zircon U-Pb and Lu-Hf isotopes of REE deposits in the Adjacent Areas of Yunnan and Guizhou.

In combining with previous research and the results of this research, we draw the following conclusions:

1. The REE-rich claystone was deposited at 257.22-254.62Ma (2.6Myr). The average deposition rate is very slow (0.076-0.61 cm/ka).

2. The source area of the REE-rich clay rock is the denudation zone in the inner zone of Emeishan LIP, and the material source is mainly the syenite, followed by the high-Ti basalt and felsic igneous rocks. The siltstone at the bottom of

the Xuanwei Formation is mainly originated from felsic volcanic rocks, followed by basalt, mafic rock, and limestone of Maokou Formation and Qixia Formation. The iron clay rock is formed by the weathering of the Emeishan flood basalt.

3. There is undoubtedly a surface REE migration pattern of "weathering of REE-rich matrix → fluid migration → physical or chemical precipitation → enrichment". The origin of REE-rich clay rock in this study is strong evidence for this view.

**Keywords:** Sedimentary REE; Origin and Enrichment; Western Yangtze Block; Detrital zircon;

## References

- Gong, D.X., Hui, B., Dai, Z.M., Lai, Y., Tian, E.Y., 2020. A New Type of REE Deposit Found in Clay Rock at the Top of the Permian Emeishan Basalt in the Yunnan-Guizhou Area. *Acta Geologica Sinica (English Edition)*. 94(01):204-205.
- Tian, E.Y., Gong, D.X., Lai, Y., Qiu, X.L., Xie, H., Tian, K.Z., 2021. Genesis and Enrichment of Sedimentary Rare Earth in Weining Area, Guizhou Province. *Earth Science*. 46(08):2711-2731. (in Chinese with English abstract)

# Geochemical and Hf-O isotopic evidence from the Mopanshan complex in the western margin of the Yangtze, South China: Implications for breakup of Rodinia Supercontinent

Hui-Dong Yu<sup>1</sup>, Hao Zou<sup>1,2\*</sup>, Hai-Feng Chen<sup>1</sup>, Chang-Cheng Huang<sup>1</sup>, Chun-Mei Liu<sup>1</sup>, Cheng-Hui Hu<sup>1</sup>

<sup>1</sup> State Key Laboratory of Oil and Gas Reservoir Geology and Exploitation, Chengdu University of Technology, Chengdu, Sichuan 610059, China

<sup>2</sup> Key Laboratory of Tectonic Controls on Mineralisation and Hydrocarbon Accumulation of Ministry of Land and Resources, Chengdu University of Technology, Chengdu 610059, China

\*E-mail: zouhao21@gmail.com

A large number of Neoproterozoic magmatic rock assemblages exposed in the western margin of the Yangtze Block are of great significance for determining the tectonic evolution history of South China in the Neoproterozoic, and then determining the mechanism of the breakup of the Rodinia supercontinent and the position of South China in the supercontinent. However, a series of scientific issues concerning the genesis and tectonic properties of magmatic rocks are still very controversial, which has caused great uncertainty about the fragmentation mechanism of the Rodinia supercontinent and the position of South China in Rodinia. At present, the main theories of Neoproterozoic magmatic activity tectonics related to breakup in the western margin of Yangtze Block are as follows: (1) The origin of super mantle plume activity. It is considered that the magmatic rocks in the western margin of the Yangtze were formed in a continental rift environment, and that the western margin of the Yangtze was located at the core of the Rodinia supercontinent in the Neoproterozoic, connecting Australia and North America. (Li, 1999; Ling et al., 2003; Wang and Li, 2003; Li et al., 2002, Wang et al., 2007, 2008); (2) The origin of oceanic crust subduction. It is considered that the magmatic rocks in the western margin of the Yangtze were formed in a volcanic arc environment, and that the western margin of the Yangtze was closer to the northwest of Australia in the Neoproterozoic, that is, at the edge of the Rodinia supercontinent (Zhao et al., 2002; Zhou et al., 2002; Zhao and Zhou, 2007).

This paper carried out petrological, geochemical, zircon U-Pb chronology and Hf-O isotopic studies of the Mopanshan (MPS) Neoproterozoic granitoids in the western margin of the Yangtze Block, we draw the following conclusions:

(1) MPS syenogranite and granodiorite are calc-alkaline weakly peraluminous I-type granites formed by partial melting of mafic young lower crust due to underplating of mantle-derived magmatic melts.

(2) Mature crustal material and mantle-derived components were involved in the formation of MPS granodiorite. Shimian mafic rocks may be a potential source of MPS syenogranite and MPS granodiorite.

(3) MPS syenogranite and granodiorite are located in the continental rifting setting caused by mantle plume activities, and the high temperature water-rock reaction occurred during the magma crystallization process, and there was low  $\delta^{18}\text{O}$  magmatism.

We considered that South China was located at the core of the Rodinia supercontinent in the Neoproterozoic before the breakup of the Rodinia supercontinent, rather than a continental margin model that places South China northwest of Australia, nor does it support South China as an isolated landmass model outside the Rodinia supercontinent.

**Keyword:** Rodinia Supercontinent; Yangtze Block; Mopanshan Complex; U-Pb zircon age; Hf-O isotopes ca.750-720 Ma

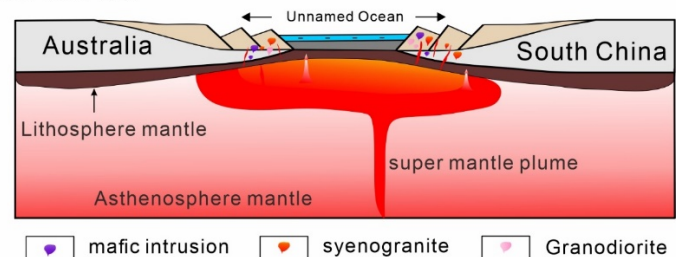


Fig. 1. Neoproterozoic tectonic evolution model of the South China Block (after Peng et al., 2012; Zou et al., 2020).

## References

- Li, X.H., 1999. U-Pb zircon ages of granites from the southern margin of the Yangtze Block: timing of Neoproterozoic Jinning Orogeny in SE China and implications for Rodinia Assembly. *Precambrian Res.* 97, 43–57.
- Ling, W.L., Gao, S., Zhang, B.R., Li, H.M., Liu, Y., Cheng, J.P., 2003. Neoproterozoic tectonic evolution of the northwestern Yangtze craton, South China: Implications for amalgamation and break-up of the Rodinia Supercontinent. *Precambrian Res.* 122, 111–140.
- Wang, J., Li, Z.X., 2003. History of Neoproterozoic rift basins in South China: Implications for Rodinia break-up. *Precambrian Res.* 122, 141–158.
- Li, X.H., Li, Z.X., Zhou, H., Liu, Y., Kinny, P.D., 2002. U-Pb zircon geochronology, geochemistry and Nd isotopic study of Neoproterozoic bimodal volcanic rocks in the Kangdian Rift of South China: implications for the initial rifting of Rodinia. *Precambrian Res.* 113, 135–154.
- Wang, X.C., Li, X.H., Li, W.X., Li, Z.X., 2007. Ca. 825 Ma komatiitic basalts in South China: First evidence for >1500 °C mantle melts by a Rodinian mantle plume. *Geology* 35, 1103–1106.
- Wang, X.C., Li, X.H., Li, W.X., Li, Z.X., Liu, Y., Yang, Y.H., Liang, X.R., Tu, X.L., 2008. The Bikou basalts in the northwestern Yangtze block, South China: Remnants of 820–810 Ma continental flood basalts. *Geol. Soc. Am. Bull.* 120, 1478–1492.
- Zhao, G.C., Cawood, P.A., Wilde, S.A., Sun, M., 2002. Review of global 2.1–1.8 Ga orogens: implications for a pre-Rodinia supercontinent. *Earth-Sci. Rev.* 59, 125–162.
- Zhou, M.F., Kennedy, A.K., Sun, M., Malpas, J., Leshneret, C.M., 2002. Neoproterozoic Arc-Related Mafic Intrusions along the Northern Margin of South China: Implications for the Accretion of Rodinia. *J. Geol.* 110, 611–618.
- Zhao, J.H., Zhou, M.F., 2007. Geochemistry of Neoproterozoic mafic intrusions in the Panzhihua district (Sichuan Province, SW China): Implications for subduction-related metasomatism in the upper mantle. *Precambrian Res.* 152, 27–47.
- Peng, S.B., Kusky, T.M., Jiang, X.F., Wang, L., Wang, J.P., Deng, H., 2012. Geology, geochemistry, and geochronology of the Miaowan ophiolite, Yangtze craton: Implications for South China's amalgamation history with the Rodinian supercontinent. *Gondwana Res.* 21, 577–594.
- Zou, H., Li, Q. L., Bagas, L., Wang, X. C., Chen, A. Q., Li, X. H., 2021. A Neoproterozoic low- $\delta^{18}\text{O}$  magmatic ring around South China: Implications for configuration and breakup of Rodinia supercontinent. *Earth Planet. Sci. Lett.* 575, 117196.

# Metallogenic characteristics and ore-controlling factors of clay-type lithium deposit in Guizhou

Daxing Gong<sup>1</sup>, Bin Xiao<sup>2</sup>

<sup>1</sup> Institute of Multipurpose Utilization of Mineral Resources, China Academy of Geological Sciences, Chengdu, Sichuan, 610041, China

<sup>2</sup> State Key Laboratory of Oil and Gas Reservoir Geology and Exploitation, Chengdu University of Technology, 610059, China

E-mail: [gongdaxing@gmail.com](mailto:gongdaxing@gmail.com)

Lithium (Li), as a strategic key mineral resource, is widely used in industries such as new energy, medicine, nuclear industry and optoelectronics (Bibienne et al., 2020). At present, the global lithium resource types can be divided into brine type, pegmatite type and clay type, of which brine type accounts for about 64%, pegmatite type accounts for about 29%, and clay type accounts for about 7% (Kesler et al., 2012). In recent years, it has been found that there are supernormal enrichment of Li in clay rocks in many places in Guizhou, including Liuzhi in western Guizhou (Zou et al., 2022), Xiuwen-Qingzhen in central Guizhou (eg., Du et al., 2021), Wuchuan-Zhengan-Daozhen in northern Guizhou (Jin et al., 2022), etc. The thickness of the stratum containing lithium is between 0 ~ 46m, and the lithium content varies greatly (about 0.55 ~ 7400 ppm), indicating great resource potential.

In this study, the ore-forming characteristics and ore-controlling factors of clay-type lithium deposit in Guizhou Province are revealed through the study of ore body morphology, ore texture structure and mineral assemblage.

In combining with previous research and the results of this research, we draw the following conclusions:

1. The enrichment of lithium occurs in specific strata, but the ore-bearing strata of clay-type lithium deposits in different regions are different. Lithium is enriched in the carbonaceous mudstone at the bottom of the Early Permian Longyin Formation in western Guizhou, the bauxite of the Early Carboniferous Jiujialu Formation in central Guizhou and the bauxite of Shuyuan Formation in northern Guizhou.

2. As far as the occurrence state of lithium is concerned, it mainly exists in cookeite and is an independent mineral. In addition, a small amount of lithium ions are adsorbed on the surface of clay minerals (such as kaolinite and montmorillonite).

3. It is a common view that mineralization occurs in the tropics and subtropics of the tropics between the tropic of Cancer. The source of lithium may come mainly from the underlying strata. In addition, the weathering and deposition of mafic magmatic rocks may also be the source of lithium.

**Keywords:** Metallogenic characteristics; Ore-controlling factors; Clay-type lithium deposit.

## References

- Bibienne, T., Magnan, J.F., Rupp, A., Laroche, N., 2020. From Mine to Mind and Mobiles: Society's Increasing Dependence on Lithium. *Elements*. 16, 265-270.
- Du, L., Tang, Y.Y., Zhang, S.F., Li, Y., Gong, X., Xiang, M.K., Wen, Y.Y., 2021. Critical Metal Enrichments in the Aluminiferous Rock Series in the Bauxite Deposits of Guizhou Province, and their Resource Potential. *Acta Sedimentologica Sinica*. 1-19. (in Chinese with English abstract).
- Jin, Z.G., Zheng, M.H., Liu, L., Huang, Z.L., Ye, L., Wu, S., Zeng, D.G., Gu, J., 2021. Distribution characteristics and enrichment mechanism of lithium in bauxite series in Guizhou Province. *Acta Geologica Sinica*. 1-13. (in Chinese with English abstract).
- Kesler, S.E., Gruber, P.W., Medina, P.A., Keoleian, G.A., Everson, M.P., Wallington, T.J., 2012. Global lithium resources: Relative importance of pegmatite, brine and other deposits. *Ore Geology Reviews*. 48, 55-69.
- Zou, H., Xiao, B., Gong, D.X., Huang, C.C., Li, M., Yu, L.M., Tian, E.Y., Liu, C.M., Chen, H.F., Hu, C.H., 2022. Origin and tectonic setting of Pingqiao fluorite-lithium deposit in the Guizhou, southwest Yangtze Block, China. *Ore Geology Reviews*. 143, 104755.

# Cenozoic tectonic activity characteristics of Qingshuihe Basin based on fluvial geomorphology And tectonic analysis

Yang Wang<sup>1</sup>

<sup>1</sup> Department of geology, Northwest University, Xi'an, Shanxi 710000

## Abstract:

Since the late Cenozoic, a series of extensional subbasins and tectonic belts have been formed in the northeastern margin of the Qinghai-Tibet Plateau due to the impact of the Indo-Eurasian plate and the northeast direction extrusion. Basin geomorphology plays an important role in the study of the formation process of rock uplift and river erosion, and records the geomorphic characteristics of the basin and the surface evidence of geomorphic evolution. The surface tectonic activity of Qingshuihe River basin is obvious, and the geomorphic features have a good response to the tectonic activity. In this paper, based on 30M resolution DEM data, the geomorphic parameters of Qingshuihe River basin in South Ningxia were extracted by ArcGIS10.2, and the Stream-length gradient (SL), Hypsometric integral (HI), Elongation ratio (RE) and Asymmetry Factor (AF) of 22 large rivers were accurately calculated. The geomorphologic and morphological characteristics of Qingshui River basin were obtained quantitatively, and the regional differentiation of the above indexes was discussed. At the same time, the state of tectonic activity of the basin was comprehensively evaluated by combining the relevant geological data and field survey data. The results show that : (1) The average SL of the study area is 169, indicating that the overall active deformation degree of the area is high. (2) The river channel in the west is longer than that in the east, and the grades of AF and RE are larger than those in the east, indicating that the uplift rate in the east is higher than that in the west. (3) HI indicate that the Qinghai-Tibet Plateau plate and the Ordos plate have been uplifted differently since the Quaternary, resulting in different geomorphic evolution stages in the two sides of the Qingshui River.

**Keywords:** Fault structure, Fluvial landform, Northeastern margin of Qinghai-Tibet Plateau, Qingshui River Basin, Geomorphological parameters

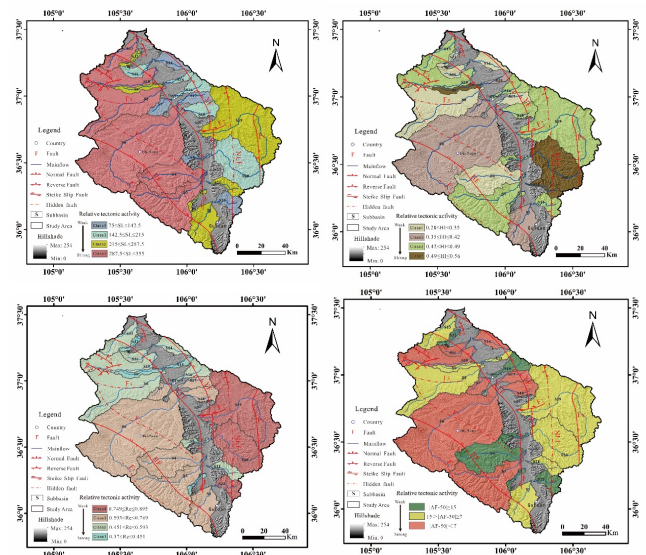


Figure 1. Geomorphologic factor map of Qingshuihe River Basin.

Table 1.22 Parameters of sub-watershed

| No  | Length  | Head | Outlet | Dispersion | Area            | SI      | Hi    | Re    | Af     |
|-----|---------|------|--------|------------|-----------------|---------|-------|-------|--------|
|     | Km      | m    | m      | m          | km <sup>2</sup> |         |       |       |        |
| S1  | 39.057  | 2006 | 1536   | 470        | 502.583         | 157.472 | 0.333 | 0.640 | 10.174 |
| S2  | 19.735  | 1923 | 1507   | 416        | 50.626          | 147.147 | 0.412 | 0.370 | 0.474  |
| S3  | 68.821  | 2124 | 1461   | 663        | 1116.274        | 249.386 | 0.463 | 0.679 | 26.120 |
| S4  | 57.858  | 2244 | 1458   | 786        | 770.831         | 245.791 | 0.305 | 0.657 | 2.621  |
| S5  | 18.665  | 1648 | 1422   | 226        | 69.211          | 85.519  | 0.453 | 0.484 | 2.403  |
| S6  | 116.330 | 2189 | 1332   | 857        | 3108.066        | 353.851 | 0.345 | 0.749 | 15.085 |
| S7  | 22.358  | 1453 | 1316   | 137        | 141.044         | 87.182  | 0.365 | 0.662 | 18.296 |
| S8  | 81.202  | 2001 | 1280   | 721        | 1111.073        | 295.714 | 0.307 | 0.527 | 13.472 |
| S9  | 34.173  | 1565 | 1283   | 282        | 130.641         | 145.612 | 0.541 | 0.379 | 12.709 |
| S10 | 70.508  | 1943 | 1264   | 679        | 592.100         | 279.591 | 0.410 | 0.531 | 34.446 |
| S11 | 30.653  | 1662 | 1267   | 395        | 136.352         | 138.101 | 0.323 | 0.593 | 19.347 |
| S12 | 19.194  | 1771 | 1251   | 520        | 60.466          | 145.778 | 0.296 | 0.445 | 2.828  |
| S13 | 45.072  | 1794 | 1189   | 605        | 292.938         | 249.449 | 0.420 | 0.529 | 14.035 |
| S14 | 25.424  | 1592 | 1268   | 324        | 175.324         | 107.223 | 0.282 | 0.558 | 19.392 |
| S15 | 17.786  | 1610 | 1278   | 332        | 67.492          | 133.766 | 0.372 | 0.451 | 13.972 |
| S16 | 29.007  | 1635 | 1303   | 332        | 200.550         | 142.506 | 0.405 | 0.585 | 5.079  |
| S17 | 24.439  | 1599 | 1323   | 276        | 164.756         | 102.138 | 0.319 | 0.617 | 20.592 |
| S18 | 24.687  | 1668 | 1328   | 340        | 214.125         | 127.711 | 0.394 | 0.683 | 28.557 |
| S19 | 96.865  | 1807 | 1392   | 415        | 1868.228        | 171.363 | 0.448 | 0.855 | 13.987 |
| S20 | 52.309  | 1798 | 1423   | 375        | 946.157         | 135.572 | 0.483 | 0.895 | 9.231  |
| S21 | 27.163  | 1830 | 1489   | 341        | 162.140         | 146.084 | 0.551 | 0.535 | 9.396  |
| S22 | 21.841  | 1745 | 1543   | 202        | 204.875         | 70.011  | 0.411 | 0.810 | 4.302  |

# Subduction-related mafic to felsic magmatism in the Xiangpishan concentric calc-alkaline arc complex, NE Tibetan Plateau

Feng-Hui Zou<sup>a, b</sup>, Cai-Lai Wu<sup>a, \*</sup>, Li-Huan Deng<sup>c</sup>, Dong Gao<sup>a, b</sup>, Yuan-Hong Gao<sup>a</sup>

<sup>a</sup> Institute of Geology, Chinese Academy of Geological Sciences, Beijing 100037, China;

<sup>b</sup> School of Earth Sciences, China University of Geosciences, Wuhan 430074, China;

<sup>c</sup> School of Geography and Tourism, Huanggang Normal University, Huanggang 43800, China

## 1 Introduction

Voluminous granitic rocks are intrusive in the West Qinling Orogen, especially in the westernmost tip along the Zongwulong-Qinghai-nanshan Tectonic Belt (hereinafter termed 'ZQTB'). The ZQTB situated in the northern margin of the Gonghe basin, NE Tibetan Plateau, is embedded in the Proto-Tethys realm and the Late Paleozoic to Early Mesozoic igneous rocks relative to the evolution of Paleo-Tethys Ocean are developed in the belt, which is a key window for deciphering the transition from Proto- to Paleo-Tethys.

## 2 Geological and petrological features of the Xiangpishan complex

The Xiangpishan arc complex (ca. 510 km<sup>2</sup>) is located in the middle part of the ZQTB, NE Tibetan Plateau. Along the marginal and interior regions of the complex, several acidic and lamprophyric dykes are scatteredly exposed. The complex consists of a felsic core (granodiorite) surrounded by quartz diorite in the middle to diorite and minor gabbro at the margin with locally less volume of monzogranite.

## 3 Analytical methods

All analytical methods in this work cover *in-situ* LA-ICP-MS U-Pb dating, Lu-Hf isotope analyses of zircon, and whole-rock chemical analyses.

## 4 Analytical results

Twenty-four zircon grains of dioritic MMEs yielded variable Th/U ratios (0.57-2.64), giving a weighted mean age of 257±3 Ma. Their corresponding  $\epsilon_{\text{Hf}}(t)$  values are from -1.62 to +1.82. Thirty concordant zircon crystals of diorite gave a <sup>206</sup>Pb/<sup>238</sup>U concordia age of 254±3 Ma and their  $\epsilon_{\text{Hf}}(t)$  values ranged from -2.67 to 0.34. Thirty analyzed zircon spots of quartz diorite produced low Th/U ratios of 0.27-0.86 and had a mean age of 255±2 Ma. All grains presented significant negative  $\epsilon_{\text{Hf}}(t)$  (-3.14 to -0.39). Thirty zircon crystals of medium-grained granodiorite gave a <sup>206</sup>Pb/<sup>238</sup>U concordia age

of 262±2 Ma and displayed variable  $\epsilon_{\text{Hf}}(t)$  between -2.64 and 1.16. For the studied samples, they cover an extensive scope of compositions about their variable silica contents (46.14-73.61 wt.%). They reveal an evident chemical variation with respect to TiO<sub>2</sub>, MgO, FeO<sub>tot</sub>, Al<sub>2</sub>O<sub>3</sub>, and CaO; whereas the other major elements display a restricted scope. The concentration ranges of compatible elements like Co, Ni, Cr and V are 2.32-50.2 ppm, 1.98-66.4 ppm, 6.84-365.2 ppm and 12.5-310.0 ppm, respectively.

## 5 Discussion

### 5.1. Petrogenesis

We have obtained a zircon U-Pb age of 249±2 Ma for gabbro, 254±3 Ma for diorite, 255±2 Ma for quartz diorite, 262±2 Ma for medium-grained granodiorite, 257±4 Ma for fine-grained granodiorite dyke and 257±3 Ma for associated MMEs. Thus, we conclude that the gabbroic to dioritic to acidic magmatism in the Xiangpishan district was emplaced at the time of 249-262 Ma, *i.e.*, the Late Permian to Early Triassic.

Magma mixing process within the studied complex could be evidenced through field features, macroscopic and microscopic textures, petrographic observations and geochemical data. Mafic, felsic, and hybrid members were elaborated in favor of the magma-mixing hypothesis as a formation mechanism for rocks in the complex. In this scenario, diorite and quartz diorite are regarded as resultant hybridized products of magma mixing between gabbro (mafic end-member) and granodiorite (felsic end-member) in varying proportions. Further, the quantitative calculation from Mass Balances Modelling manifests that the mass of mafic magmas (ca. 67-79%) is involved to achieve the hybridization. Based on the geochemical data, we regard the gabbro in the Xiangpishan area as the derivative of a lithospheric mantle source which was metasomatized by the slab-derived fluid during subduction,

---

and crystal fractionation (like clinopyroxene, hornblende, and Fe-Ti oxides) has taken place during the magmatic evolution. While granodiorites were derivatives from the partial melting of the Late Paleoproterozoic to Middle Mesoproterozoic medium- to high-K basaltic lower crust under the initial condition of water-undersaturation (2.3-2.5 wt% H<sub>2</sub>O) and moderate pressure (ca. 7-10 kbar), with involvement of minor volumes of depleted mantle compositions.

## 5.2. Tectonic implications

The gabbro and dioritic MMEs are enrichment in LREEs and LILEs (e.g., Rb and K), depletion in HREEs and HFSEs (e.g., Nb, Ta, Zr, Hf and Ti), and dominantly calc-alkaline in compositions. In tandem with low Ti/V ratios ranging from 24 to 30, these features demonstrate their ubiquitous 'arc signature' (Pearce, 1982), indicative of a subduction-related environment. Combined with regional setting, the Xiangpishan concentric calc-alkaline arc complex was emplaced in an active continental arc margin setting relative to the southward subduction of the Paleo-Zongwulong Ocean. Finally, an evolutionary model has been proposed that the asthenosphere-lithosphere interaction played an important role during emplacement of the concentric complex, where the limited volume of mantle-derived melts act as the supplier of heat and mass (mainly volatile components) to induce partial melting of the juvenile mafic lower crust and mixed (or mingled) with the produced crust-derived magma during the oceanic subduction, which led to the generation of diorites as well as mafic microgranular enclaves (MMEs).

## 6 Conclusions

Felsic magma similar to mafic magma, both have consistent crystallized ages, *i.e.*, 249-262 Ma; as the hybrid derivatives from mixing between felsic and mafic magmas, diorites have analogous ages to felsic rocks and MMEs. The mass (ca. 67-79%) of mafic magmas is involved to achieve the hybridization. The Xiangpishan complex was emplaced in an active continental arc margin setting relative to the southward subduction of the Paleo-Zongwulong Ocean.

## Acknowledgments

This work was jointly funded by National Natural Science Foundation of China (Nos. 41872071, 40672049, 42101073) and China Geological Survey Project (Nos. DD20190006).

## References

Pearce, J.A., 1982. Trace element characteristics of lavas from destructive plate boundaries, In: Thorpe, R.S. (Ed.), *Orogenic Andesites and Related Rocks*. John Wiley and Sons, Chichester, England, pp. 528-548.

---

## Tracing archives of intra-oceanic arcs and tracking periods of subduction erosion: evidence from greywacke sandstones of central and eastern Kazakhstan

Inna Safonova<sup>a-c</sup>, Alina Perfilova<sup>a,b</sup>

<sup>a</sup> Novosibirsk State University, Pirogova St. 1, Novosibirsk, 630090, Russia

<sup>b</sup> Sobolev Institute of Geology and Mineralogy, SB RAS, Koptyuga ave. 3, Novosibirsk 630090, Russia

<sup>c</sup> South-West Jiaotong University, FGEE, Chengdu 610031, Sichuan, China

---

Proportions of juvenile and recycled crust in intra-continental orogenic belts formed in place of paleo-oceans as a key issue of tectonic and metallogenic paleo-reconstructions. Major sites of the growth of juvenile continental crust are intra-oceanic arcs at Pacific-type convergent margins. However, island-arc igneous complexes can disappear from the geological record because of tectonic erosion. Erosion of magmatic arc leaves either clastic rocks, typically greywacke sandstones, often parts of trench/fore-arc/back-arc turbidite associations.

For reconstructing ancient Pacific-type convergent margins, we must know which types of arcs existed that time: intra-oceanic or continental. Fossil Pacific-type orogenic belts typically exhibit very complicated relationships between different lithologies, often with few, if any, outcrops of arc igneous rocks. We reconstructed fossil intra-oceanic arcs in central and eastern Kazakhstan, which existed at Pacific-type convergent margins of the Paleo-Asian Ocean (PAO) in Paleozoic time. Our reconstructions are based on published and new U-Pb detrital zircon ages, petrographic, geochemical and isotope (Sm-Nd, Lu-Hf) data from greywacke sandstones hosted by accretionary complexes of central and eastern Kazakhstan in comparison with data from arc igneous rocks, in particular, with those occurring as fragments in serpentinite mélange.

Four orogenic belts of the western Central Asian Orogenic belt are under consideration: Itmurundy and Tekturmas in central Kazakhstan (early Paleozoic) and Zharma and Char in eastern Kazakhstan (middle-late Paleozoic). All orogenic belts formed at active margins of the PAO. Study of greywacke sandstones represent a valuable instrument for reconstructing survived and disappeared magmatic arcs taking into account

episodes of subduction erosion. In addition, the role of serpentinite is also very important for the reconstruction of episodes of tectonic erosion. We argue that (1) all sandstones hosted by accretionary complexes are greywackes deposited close to their igneous sources and buried rapidly; (2) their provenances are dominated by mafic to andesitic igneous rocks; (3) the parental melts of their igneous protoliths were derived from juvenile mantle sources; (4) the igneous protoliths are typically emplaced in intra-oceanic arc settings; (5) the sandstones get deposited in fore-arc/trench basins or, to a lesser degree, in back-arc basins.

The data from sandstones and serpentinite mélange allowed us to reconstruct middle-late Cambrian and Ordovician arcs in the Itmurundy and Tekturmas belts and late Devonian and Carboniferous arcs in the Zharma and Char belts. The obtained results clearly show signatures of subduction erosion in both early and late Paleozoic times. Evidence for this comes from (1) disappearance of certain peaks of U-Pb ages in younger sandstones compared to older ones (Tekturmas, Char, Zharma); (2) scarce/small outcrops of arc igneous complexes (Itmurundy, Char); (3) presence of pieces of arc rocks in serpentinite mélange (Itmurundy, Tekturmas, Char); (4) magmatic lulls. The middle-late Cambrian arcs (Itmurundy, Tekturmas) were fully destroyed by subduction erosion. The Ordovician arc survived better, but that of the Itmurundy belt was stronger destroyed compared with the coeval arc of the Tekturmas belt. The late Devonian arc of the Zharma belt better survived than that of the Char belt. Both, the early and late Paleozoic active margins of the PAO were characterized by alternating periods of accretionary growth and subduction erosion.

The work was supported to the Russian Science Foundation, project 21-77-20022.